Author's response:

We thank the reviewers for a careful reading and correction of our manuscript. Their suggestions have strongly helped improving the quality of the manuscript.

Following the suggestions of the anonymous referees 2, 3 and 4 we have added in the revised manuscript the description of the meteorological conditions during the measurement periods in both cities. A figure with the time series of wind direction and speed, temperature and precipitation has been added in the supplementary information (Fig. S2) and is described in the methodology section. Moreover, the average wind directions and speed during each measurement loop are now reported in a wind rose plot in Fig. 4 and 5 (spatial distributions for Tartu and Tallinn, respectively) and are fully discussed in the manuscript.

As suggested by anonymous referees 2 and 4, a detailed analysis of the source apportionment diagnostics has been added in the revised manuscript. A figure including (a) Q/Q_{exp} as a function of the number of factors, (b) correlations between OA sources with external factors as a function of the number of factors and the decrease in Q/Q_{exp} time series (c) and profiles (d) for increasing number of factors has been added in the supplementary information (Fig S5). Moreover, a table reporting the correlations between the OA sources from our four-factor solution and literature profiles has been added in the main text.

Moreover, following the suggestion of anonymous referee 4, we have added the correlation coefficients (R^2) between the spatial distributions of all sources and compounds in Tartu in the revised manuscript (Table S1).

Lastly, in order to give an overview of the major local PM sources, we have added emission maps in the revised manuscript (Fig. S1). The wood combustion and industrial sources and the traffic emission rates of the main streets are reported in these maps.

Anonymous Referee #1

Received and published: 29 February 2016

This paper uses mobile measurements to spatially map aerosols and trace gases in two Estonian cities. The use of high time resolution instruments means that good spatial resolution is obtainable and the results are systematically analysed to present statistics on the urban increments. The use of source apportionment techniques on the AMS and Aethalometer data adds extra depth to the results. Overall, the analysis appears solid and the results are well presented. I recommend publication subject to minor (mostly technical) revisions.

Page 1, line 1: *Please be more specific when referring to 'polluted continental areas'.*

Changes in text:
Page 1, Line 30: A strong increase in the secondary organic and inorganic components was observed during periods with transport of air masses from northern Germany~~polluted continental areas~~, while the primary local emissions accumulated during periods with temperature inversions.

Page 2, line 18: *PM2.5 has been the major focus for over 20 years now, so can hardly be described as 'recent'.*

Author's response: We fully agree with the reviewer's comment and have removed "recently" in the revised manuscript.

Changes in text:
Page 2, Line 21: ~~Recently, m~~Major attention has been devoted to the study of the $PM_{2.5}$ fraction (particulate matter with an aerodynamic equivalent diameter $d_{aero} \leq 2.5$ μm), which has been linked…

Page 6, line 20: *Remove the word 'highly'.*

Author's response: Removed in the revised manuscript.

Page 11: *More explanation and justification of the P05 method should be given. Why was the 5th percentile chosen? What specific effect was the subtraction expected to achieve? Given that the base of the sigmoid fits was allowed to vary, why is this even necessary?*

Author's response: This is a good point raised by the reviewer that needs additional explanation. The subtraction of P05 is needed in order to decrease the background variability of each single loop before averaging. This step could be skipped if the sigmoid fit could be applied to single loops, but this is not possible due to the high variability in the signal within each single loop. We tested the sensitivity of the method by subtracting P10 instead of P05, and no major changes were observed in the results. This information has been added in the revised manuscript.

Changes in text:
Page 14 Line 7: In most ~~of the~~ cases the base of the sigmoid function~~s~~ is slightly above zero. This indicates that the ~~P05 previously~~ subtracted P05 didn't represent the full regional background, which is therefore given by the sum of the average P05 and the base of the sigmoid function. Note that the initial subtraction of P05 would not be necessary if the longitudinal profile of each single loop could be fitted. ~~However,~~ this is not possible due to the high concentration variability within each single loop. A sensitivity analysis was performed by using P10 instead of P05 and no major changes were observed in the final results.

Page 12, line 13: *The use of the median does not completely rule out the influence of the kerbside increment because street canyon effects (e.g. when the local wind is perpendicular to a road) can cause on-road emissions to persist is this microenvironment and the increment to no longer manifest itself as discrete spikes in the data. This would cause the median to increase over what would be expected of the urban background. Because these measurements are taken on-road, it is perhaps inevitable that estimates of the urban background will be biased slightly high because of the influence of traffic sources, so this should be added as a caveat. It may be possible to exclude this by selectively averaging the less-busy roads.*

Author's response: This has been discussed further in the revised manuscript.

Changes in text:
Page 13, Line 27: While the averaged profiles take into account the effects of the measured point sources in the urban area (mostly traffic and residential emissions), the use of the median profiles is expected to represent more selectively ~~exclude these effects, making the results more representative of~~ the urban background concentrations. We note that the influence of curbside increments may not be completely removed when using median increments (e.g. accumulation of traffic emissions due to street canyon effects), and therefore these increments might be biased high and should be regarded as our highest estimates of urban background concentrations.

Page 12, line 3: *Replace 'component' with 'components'.*

Author's response: Replaced in the revised manuscript

Page 15: *How was the temperature difference between 0 and 22m measured?*

Author's response: The temperature is measured at different heights in a meteorological tower at the Tallinn Zoo monitoring station.

Anonymous Referee #2

Received and published: 26 February 2016

General Comments:

Elser et al. describe gas and aerosol measurements conducted in two Estonian cities. The authors use a mobile platform to investigate the extent to which pollution concentrations within the city limits exceed regional background levels. Via source apportionment, the authors attribute the observed organic aerosol loadings to four primary sources: traffic emissions, biomass burning, primary residential emissions, and secondary aerosol formation. The authors map the spatial distribution of each component to identify source "hot spots." In both cities, traffic-related components were most variable in the city center while biomass burning and primary residential emissions were concentrated in populated regions. Secondary components were well distributed throughout each city and had the least impact by point sources; however, increases in secondary aerosol were most strongly influenced by long-range transport of air masses originating from polluted regions west of Estonia.

The paper presents a useful and effective methodology for studying the impact of point sources on local air quality. Furthermore, these measurements are important as they assess the pollutant levels and source contributions in an understudied region of Europe. The manuscript is very well organized and many of the conclusions are well supported. I have some recommendations that would improve the quality of the manuscript. Upon addressing these comments, I recommend the manuscript for publication.

First, I believe that further details of the source apportionment should be included to strengthen the argument of a four-factor solution. Questions and comments pertaining to this aspect of the manuscript are summarized below. Second, parts of the methodology section employ sentence structure and wording that, at times, is awkward and/or difficult to follow. While I do not wish to interfere with stylistic choices, I believe that some rewording of these sections may help the manuscript read more fluently. Suggestions are provided in the Minor Comments.

Source Apportionment

The authors identify four factors that sufficiently describe the variation in the data. The authors are thorough with the comparison of factors with external tracers; however, there is little discussion and no figures demonstrating the model residuals as the PMF solution is pushed to higher factors. The authors describe their observations (Page 10, lines 12 – 24), however a figure should be included demonstrating the behavior of Q/Q_{exp} as a function of the number of factors. Furthermore, the authors present a 5-factor solution, but argue that the fifth "unknown" factor exhibits a primary emission temporal pattern (which is uncharacteristic of a LV-OOA factor) and therefore does not significantly improve the interpretation of data. While this may be true, I believe it is necessary to demonstrate that the temporal residuals are not significantly improved for a 5-factor solution. It may be that the "unknown" factor results from factor splitting or some other mathematical construct. In any case, the PMF discussion should better describe the factor residuals.

The authors invoke bootstrapping as a means of constraining the error in the PMF solution. The author's note that bootstrapping inherently varies the algorithm starting point (i.e., seed) and therefore accounts for model uncertainties; however, the PMF solution may also be strongly affected by variations in fpeak (Ulbrich et al. 2009). There is little discussion about

the rotational ambiguity of the PMF solution. I believe this discussion is necessary in order to evaluate the robustness of the PMF solution.

Finally, I believe it would be useful to compare the factor profiles to published spectra. This comparison would provide additional justification for the resolved factors. Specifically, I have some questions regarding the RIOA factor. The RIOA factor exhibits a temporal pattern that appears to be unique; however, the RIOA factor only exists in a 4 or higher factor solution and is primarily resolved from the BBOA and HOA factors (Fig S3). Consequently, the factor associated with RIOA results from the contribution of two other primary emission factors. While this may be simply due to the fact that RIOA, BBOA, and HOA are common in residential areas, this result may also be a result of factor splitting.

There are a number of ways the authors can provide additional evidence in support of the RIOA factor. The simplest option would be to compare the factor profiles to published spectra. The authors provide some comparison in the text, however a supplemental figure would be more illustrative. A more thorough analysis would be to perform PMF on subsets of the data and determine if the RIOA factor is still resolved. For example, if one were to remove time periods when the RIOA component is dominant, does PMF still resolve an RIOA factor? I believe these additional tests would strengthen the authors' PMF solution.

Author's response:
Based on the reviewer comment, we have additionally performed a thorough residual analysis as a function of the number of factors. These diagnostics are presented in the new figure Fig. S5 in the supplementary of the revised manuscript (see below). This figure includes the change in Q/Q_{exp}, in the correlation coefficients (R^2) of the resolved factors with the external markers and the change in the residuals time series and profiles for solutions with increasing number of factors. We show that the correlation coefficients (R^2) between factors and markers increase when a fourth factor is included, but are not improved when a fifth factor is added. The addition of the fourth factor, which enabled the extraction of RIOA, allows explaining additional structures in the residuals' time series and unsaturated fragments in the residuals mass spectrum. Including a fifth factor also improves the model mathematical quality, by additionally explaining $C_xH_yN_w$ and biomass burning (at *m/z* 60 and 73) related fragments. The additionally extracted factor in the five-factor solution, referred to as 'unknown', has elevated contributions from oxygenated fragments often related to SOA (*m/z* 44) and BBOA (*m/z* 60 and 73), but a time series that unambiguously relates this factor to a spatially variable primary emission source. In effect, the majority (62%) of this factor contribution arises from a split in the BBOA factor from the four-factor solution (the rest comes from the residuals and the OOA). Moreover, the sum of the contributions of the 'unknown' factor and the BBOA from the five-factor solution matches the BBOA contributions from the four-factor solution (R^2 = 0.97 and slope = 1.15 as shown in Fig. S6). This split in the BBOA is very likely a direct consequence of the variable nature of this combustion source, but the two BBOA-like factors extracted in the five-factor solution could not be related to different emission processes. The addition of this factor did not affect the spectral profiles and time series of the other factors and their correlations with their respective markers and did not aid the interpretation of the data. Therefore, we considered the four-factor solution as an optimal representation of our data. This discussion is now added in the text.

The f_{peak} approach has been used in the past to study the rotational uncertainty of the source apportionment solution. However, varying the fpeak parameter allows to trace only one dimension through the rotationally accessible domain (which is multi-dimensional), and therefore provides only a lower limit for rotational uncertainty (Paatero et al., 2014). Bootstrap is a more effective approach to explore the rotational ambiguity and provides an upper limit for the rotational uncertainty.

A table containing the correlation coefficients (R^2) between the OA profiles from the four-factor solution and literature profiles has been added in the main text of the revised manuscript (Table 2). The high correlations retrieved for the RIOA with cooking spectra from literature (R^2 of about 0.8), strengthens the use of a four-factor solution and the link between our RIOA spectra and cooking emissions.

As described in the text, within the bootstrap method 64 % of the original points are used in each replicate of the input matrices. For all one-hundred bootstrap runs the RIOA was retrieved and the solution was very stable. Moreover, we also performed some PMF runs using only the data from Tallinn, where RIOA is more homogeneous compared to Tartu, and this factor was still always resolved. Therefore, this factor will always be resolved even when performing PMF on smaller subsets of the data.

Changes in text:

Page 10, Line 31: Some important diagnostic parameters of the source apportionment (including Q/Q_{exp}, factor-marker correlation, and time-series and profiles residuals for solutions with different number of factors) are reported in Fig. S5. The correlation coefficients (R^2) between factors and markers significantly increase when a fourth factor is included, but are not improved when a fifth factor is added. The addition of the fourth factor, which enabled the extraction of RIOA, allows explaining additional structures in the residuals' time series and unsaturated fragments in the residuals mass spectrum. Including a fifth factor also improves the model mathematical quality, by additionally explaining $C_xH_yN_w$ and biomass burning (at *m/z* 60 and 73) related fragments. The additionally extracted factor in the five-factor solution, referred to as 'unknown', has elevated contributions from oxygenated fragments often related to SOA (*m/z* 44) and BBOA (*m/z* 60 and 73), but a time series that unambiguously relates this factor to a spatially variable primary emission source. In effect, the majority (62%) of this factor contribution arises from a split in the BBOA factor from the four-factor solution (the rest comes from the residuals and the OOA). Moreover, the sum of the contributions of the 'unknown' factor and the BBOA from the five-factor solution matches the BBOA contributions from the four-factor solution (R^2 = 0.97 and slope = 1.15 as shown in Fig. S6). This split in the BBOA is very likely a direct consequence of the variable nature of this combustion source, but the two BBOA-like factors extracted in the five-factor solution could not be related to different emission processes. Furthermore, the addition of this factor did not affect the spectral profiles and time series of the other factors and their correlations with their respective markers and did not aid the interpretation of the data. Therefore, we considered the four-factor solution as an optimal representation of our data. Table 2 contains the correlation coefficients (R^2) between the OA profiles from the four-factor solution and available literature profiles (Aiken et al., 2009; Mohr et al., 2012; Setyan et al., 2012; Crippa et al., 2013b). The high correlations obtained in all cases support the use of a four-factor solution and strengthen the link between the RIOA and cooking emissions (R^2 of about 0.8 between RIOA and cooking tracer).
~~If the number of factors is decreased, the RIOA factor is not resolved and the OOA time-series becomes contaminated by local spikes, which is unexpected for a regional component (see Fig. S3 and S4). In contrast, if a five-factor solution is considered an additional highly oxygenated factor is obtained ("unknown" factor in Fig. S3 and S4). The mass spectrum of this additional factor resembles a low-volatility OOA (LV-OOA), as resolved in many previous works (Jimenez et al., 2009), but its time series exhibits the typical characteristics of the primary factors, i.e. strong increases in emission areas. Therefore, this further increase in the number of factors doesn't seem to improve the interpretation of the data, as the new factor cannot be explicitly associated to distinct sources or processes. Accordingly, a four-factor solution was considered as optimal and is utilized below.~~

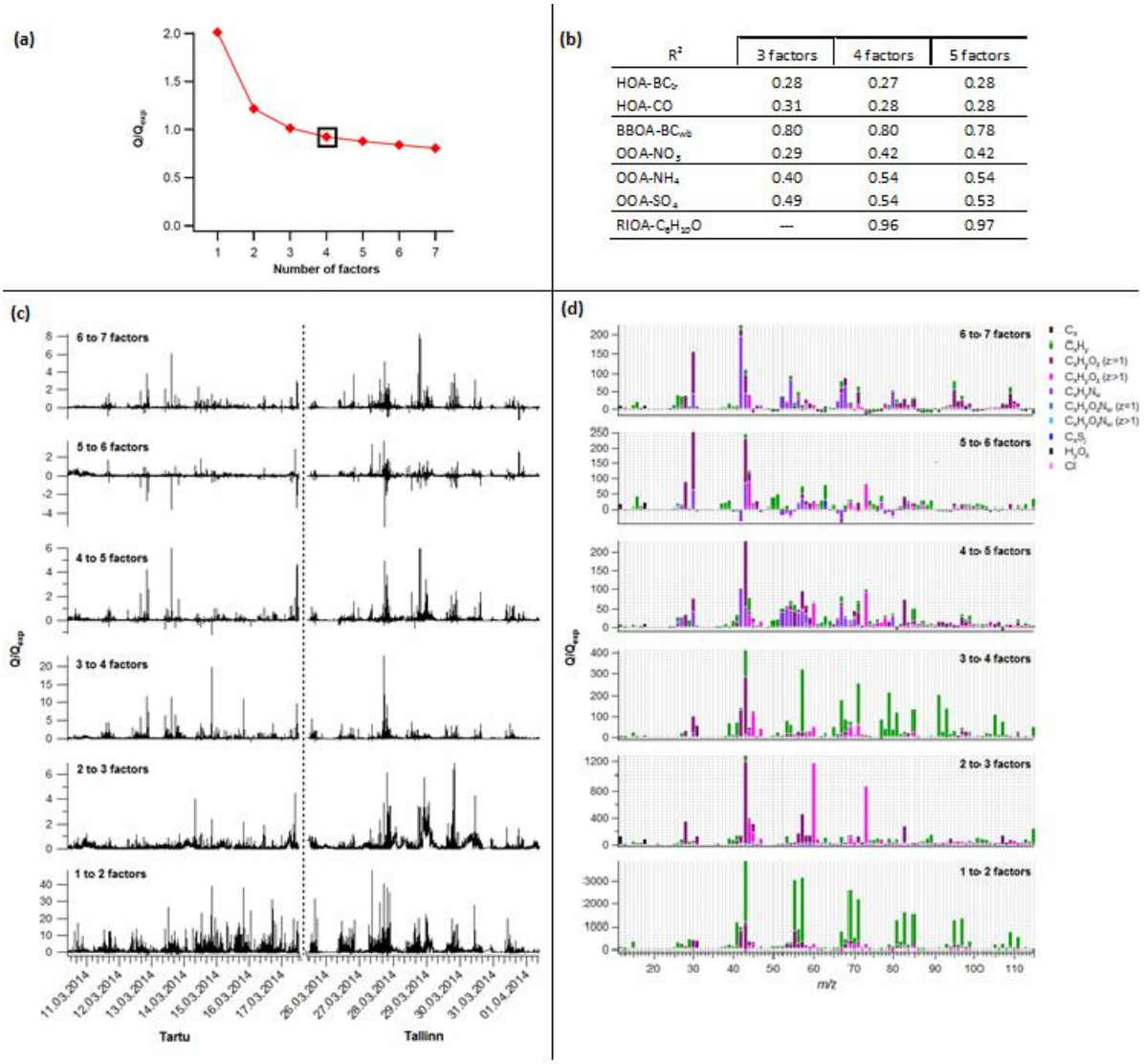

R^2	3 factors	4 factors	5 factors
HOA-BC_y	0.28	0.27	0.28
HOA-CO	0.31	0.28	0.28
BBOA-BC_{wb}	0.80	0.80	0.78
OOA-NO_3	0.29	0.42	0.42
OOA-NH_4	0.40	0.54	0.54
OOA-SO_4	0.49	0.54	0.53
RIOA-$C_8H_{20}O$	---	0.96	0.97

Figure S5 (new): Source apportionment diagnostics for increasing number of factors: (a) Q/Q_{exp}; (b) Correlation coefficient (R^2) between OA sources and markers; (c) Decrease in Q/Q_{exp} time series; (d) Decrease in Q/Q_{exp} profiles.

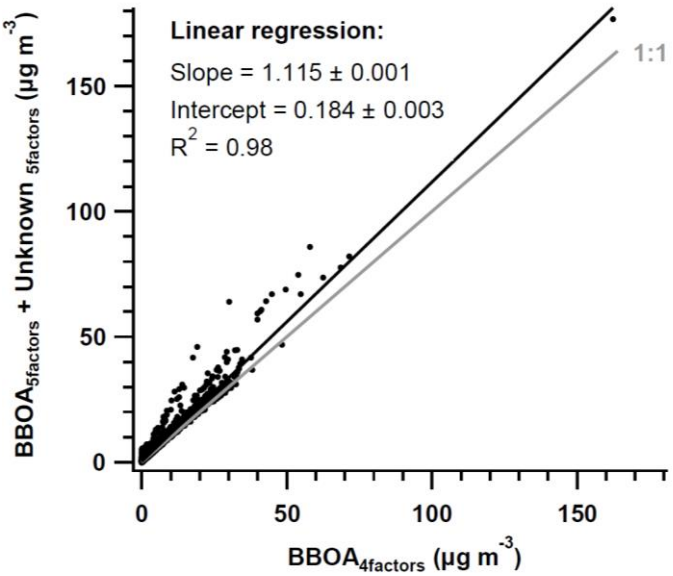

Figure S6 (new): Correlation between the BBOA time series from the four-factor solution and the sum of the BBOA and the 'unknown' time series in the five-factor solution.

Table 2: Correlation coefficients (R^2) between the OA profiles from the four-factor solution and literature profiles. Note: The different nomenclatures used in the literature for the different OOA factors have been homogenized to a semi-volatile OOA (SV-OOA) and a low-volatility OOA (LV-OOA).

R^2	Aiken et al., 2009	Mohr et al., 2012	Setyan et al., 2012	Crippa et al., 2013b
HOA-HOA	0.82	0.96	0.72	0.78
BBOA-BBOA	0.86	0.68	---	---
RIOA-COA	---	0.83	---	0.81
OOA-SVOOA	0.96	0.72	0.90	0.71
OOA-LVOOA	0.91	0.93	0.94	0.96

Specific Comments:

Page 4, Lines 29-30: *Are there any sources that outline the spatial distribution of heating systems within the city? For example, can the authors comment on why BBOA emissions are higher and more dispersed in region (2) of Tallin (Fig 1) as opposed to region (7)?*

Author's response:
To give an overview of the local PM sources, we have added emission maps of the major sources (including residential wood combustion, industry and traffic) in the revised manuscript. These maps are reported in the new Fig. S1 (see below), where residential wood combustion sources are marked with green dots, industrial sources (mainly local boiler houses) with blue markers and main streets are colored based on the traffic emission rates. It is clear that the density of sources of residential wood combustion is much higher in the southern part of the driving route in Tallinn (region 2), which is in agreement with the higher BBOA concentrations observed in this area.

Changes in text:

Page 4, Line 30: The measurements took place from 10 to 17 March 2014 in Tartu and from 25 March to 1 April 2014 in Tallinn. ~~The GPS trace of the driving routes in the two cities is shown in Fig. 1.~~ Emission maps including residential wood combustion and industrial sources and the traffic emission rates in the major streets of the two cities are reported in Fig. S1.The driving routes ~~paths~~ were chosen in order to cover heavily trafficked roads, residential areas ~~where different heating systems are used (wood/coal burning, central heating or mixed)~~ and background sites with little local emissions.

Page 14, Line 31: BBOA is ~~more~~ strongly enhanced in the residential areas, consistent with the distribution of residential wood combustion sources shown in Fig. S1. ~~and t~~The maximum BBOA enhancement is seen in the evening hours (15:00 to 21:00, LT) when domestic heating is more active.

Page 16, Line 5: BBOA (Fig. 5d~~6b~~) has higher contributions in the ~~two~~ residential areas, especially in region 2 of the driving route, where there is a very high density of residential wood combustion sources (see Fig. S1). ~~while c~~Compared to Tartu, in Tallinn the spatial distribution of RIOA (Fig. 5e~~6c~~) is more homogeneous, with only slight enhancements in the residential area and in the city center.

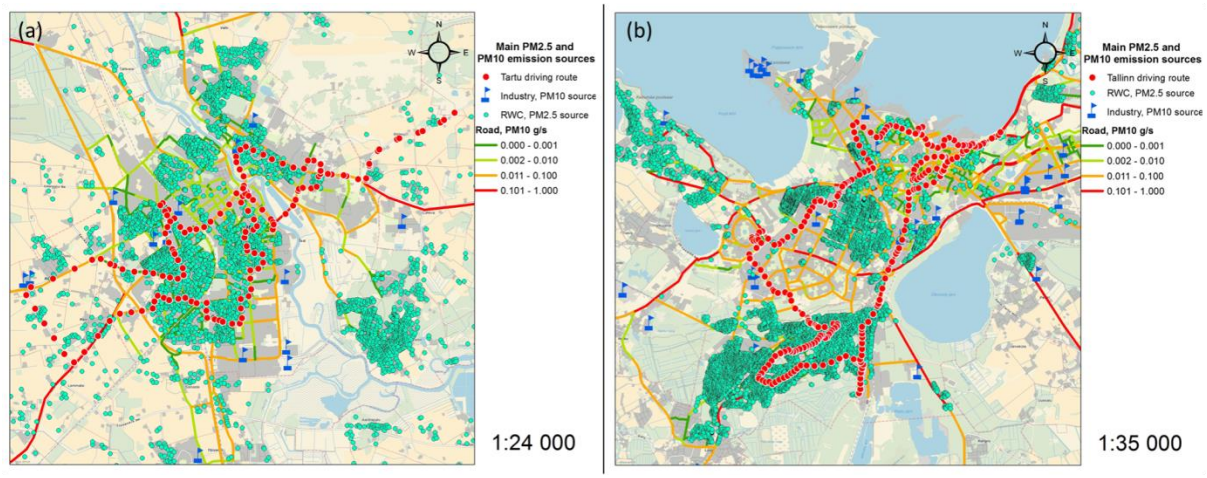

Figure S1 (new): Emission maps for (a) Tartu and (b) Tallinn. Green dots indicate residential wood combustion sources, blue markers indicate industrial sources (mainly local boiler houses) and the color of the main streets represents the traffic emission rates.

Page 8, Line 5: *What studies have used the eBC source apportionment method? Please provide references.*

Author's response: We thank the reviewer for the valuable remark. We have added the following references in the modified manuscript: Favez et al., (2010), Herich et al. (2011), Sciare et al. (2011) and Crilley et al. (2015).

Changes in text:

Page 8, Line 14: This method is described in detail in Sandradewi et al. (2008) and has been successfully applied at many locations across Europe (Favez et al., 2010; Herich et al., 2011, Sciare et al., 2011; Crilley et al., 2015).

Page 12, Lines 24-26: *From what directions do emissions in Tartu/Tallin drain? It would seem to make most sense to take the upwind concentrations as your regional background. Perhaps a discussion of the topography and typical springtime meteorological conditions would help orient the reader to understand which airspaces reflect background conditions.*

Author's response:
As mentioned in the introduction of this review, we have included detailed wind direction and wind speed analyses for the measurement periods in both cities in the revised manuscript. The time series of the wind direction, wind speed and the wind roses showing the average wind direction and speed during each loop are reported for the two measurement locations in the revised manuscript (Fig. S2, Fig. 4b and Fig. 5b). During the mobile measurements, the wind was predominantly from the west in Tartu, and from west and east in Tallinn.
The west winds observed during the drives in Tartu (with speeds between 1 and 2.6 m s^{-1}), don't seem to influence the background concentrations measured in the east side of the loop, as the base values obtained for the east side are always equal or lower than those obtained in the west (see Table 3). As the differences between the east and west base values (from the sigmoid fits) are in most cases minor, the west-east averages were used to calculate the urban increments concentrations.
In Tallinn, in order to identify possible processes influencing the spatial distributions of the measured pollutants for the two different wind patterns, the average spatial distributions were calculated for loops with west winds (7 loops) and east winds (16 loops), excluding drives during accumulation events. The results of these analyses are reported in the supplementary of the revised manuscript (Fig. S14 and S15) and show that, in general, the wind direction doesn't have a visible effect on the identified source areas and similar enhancements are found for both wind directions. A detailed analysis of the spatial distributions shows that BBOA, SO_4 and NO_3 show considerably higher enhancements for west winds, while HOA is more increased for east wind conditions. This difference is most probably related to the presence of west winds during the weekend (enhanced residential emissions) and east winds during the week-day measurements (enhanced traffic emissions).

Changes in text:
Page 5, Line 10: Meteorological data were recorded on~~in~~ a meteorological ~~-~~tower in Külitse (around 10 km south-east from Tartu) and in the Tartu and Tallinn-Zoo meteorological station~~s~~. The most relevant parameters (including wind direction and speed, temperature and precipitation) are reported in Fig. S2.

Page 14, Line 14: As shown by the wind rose in Fig. 4b, during the drives in Tartu the wind was predominantly from the west. However, the background concentrations measured at the east side of the loop don't seem to be affected by the transport of pollutants from the urban area, as the base values obtained for the east side are equal or lower than those from the west side (see Table 3). ~~Moreover, the fits on the west side of Tartu show always higher base values than those for the east, indicating the influence of local sources in the considered regional background area west of Tartu. However,~~ As the~~se~~ differences between the west and east fits are in most cases rather low, ~~and therefore~~ we use the west-east averages of the base values to calculate the urban increments concentrations in Table 2.

Page 16, Line 14: Winds from west and east were observed during the mobile measurements in Tallinn (Fig. 5b). In order to identify possible processes influencing the spatial distributions of the measured pollutants for the two different wind patterns, the

average spatial distributions were calculated for al loops with west wind (7 loops) and loops with east wind (16 loops, excluding drives during accumulation events). The results of these analyses are reported in the supplementary information (Fig. S14 and S15) and show that, in general, the wind direction didn't have an effect on the identified source areas and similar enhancements were found for both types of winds. A detailed analysis of these spatial distributions shows that BBOA, SO_4 and NO_3 are stronger enhanced during west winds, while HOA is more enhanced for east wind conditions. This difference is most probably related to the presence of west winds during the weekend (enhanced residential emissions) and east winds during the week-day measurements (enhanced traffic emissions).

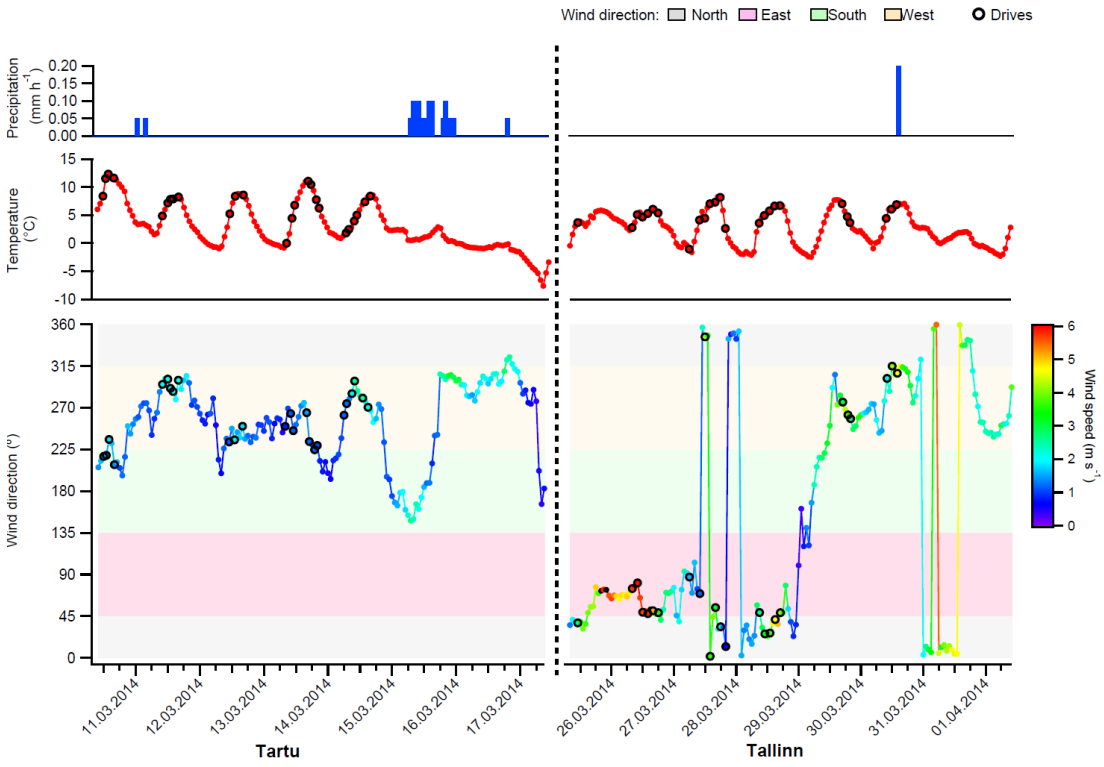

Figure S2 (New): Meteorological conditions during measurements periods in Tartu (data from the Tartu monitoring station) and Tallinn (data from the Zoo monitoring station).

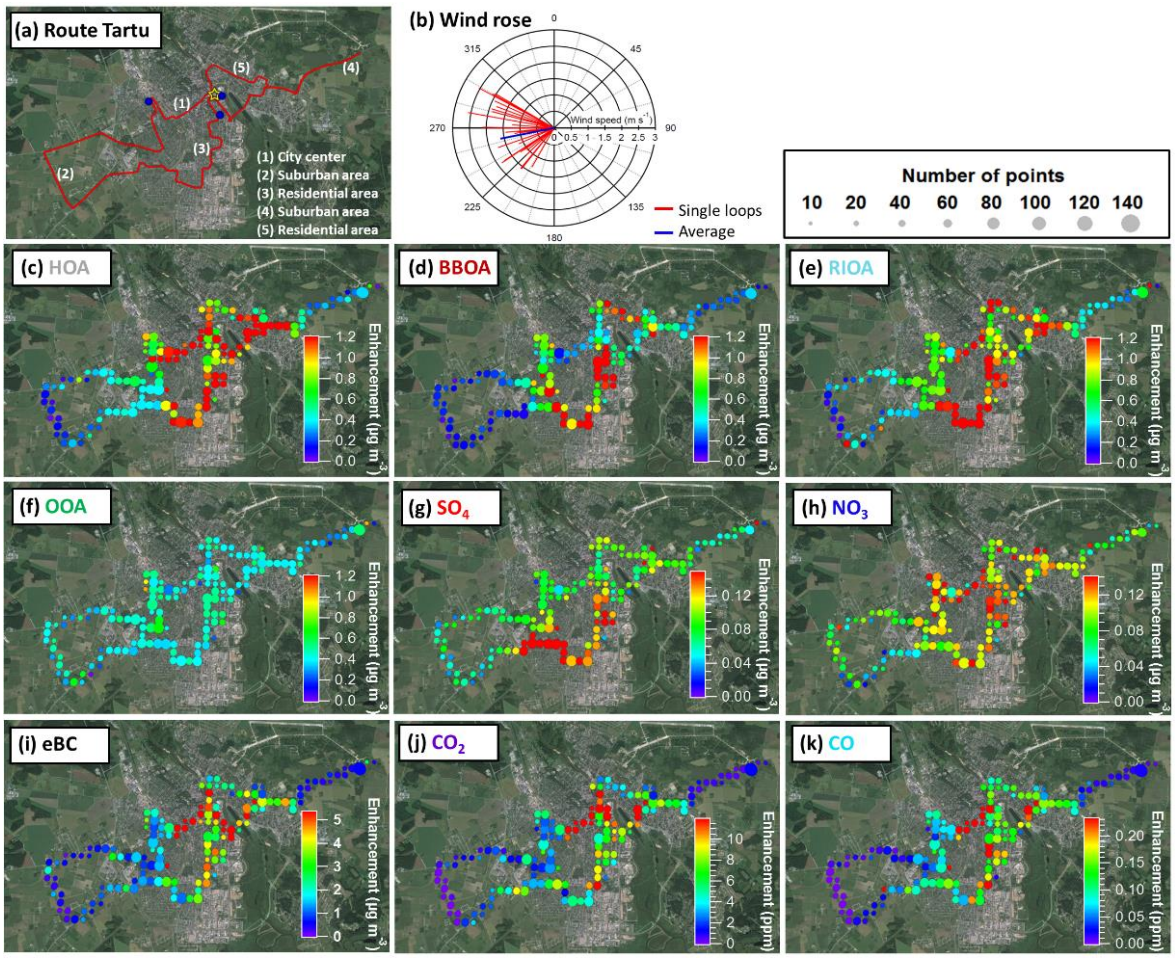

Figure 4 (Modified): (a) Driving route in Tartu: the red trace represents the GPS data, the yellow star the stationary measurements location and the blue dots the monitoring stations of the Estonian Environmental Research Institute (EERC); (b) Wind conditions during the mobile measurements in Tartu: red traces represent the wind direction and speed for the single loops and the average of all loops is represented in blue; (c to k) Average spatial distributions of all identified OA sources (panels c to f) and other measured components (panels g to k) in Tartu. The color scales represent enhancement over the background concentrations; the maximum of the color scales is fixed to the 75th percentile of the average enhancement of each component in panels g to k and to the highest 75th percentile among all OA sources in panels c to f. The sizes of the points represent the number of points that were averaged in each case.

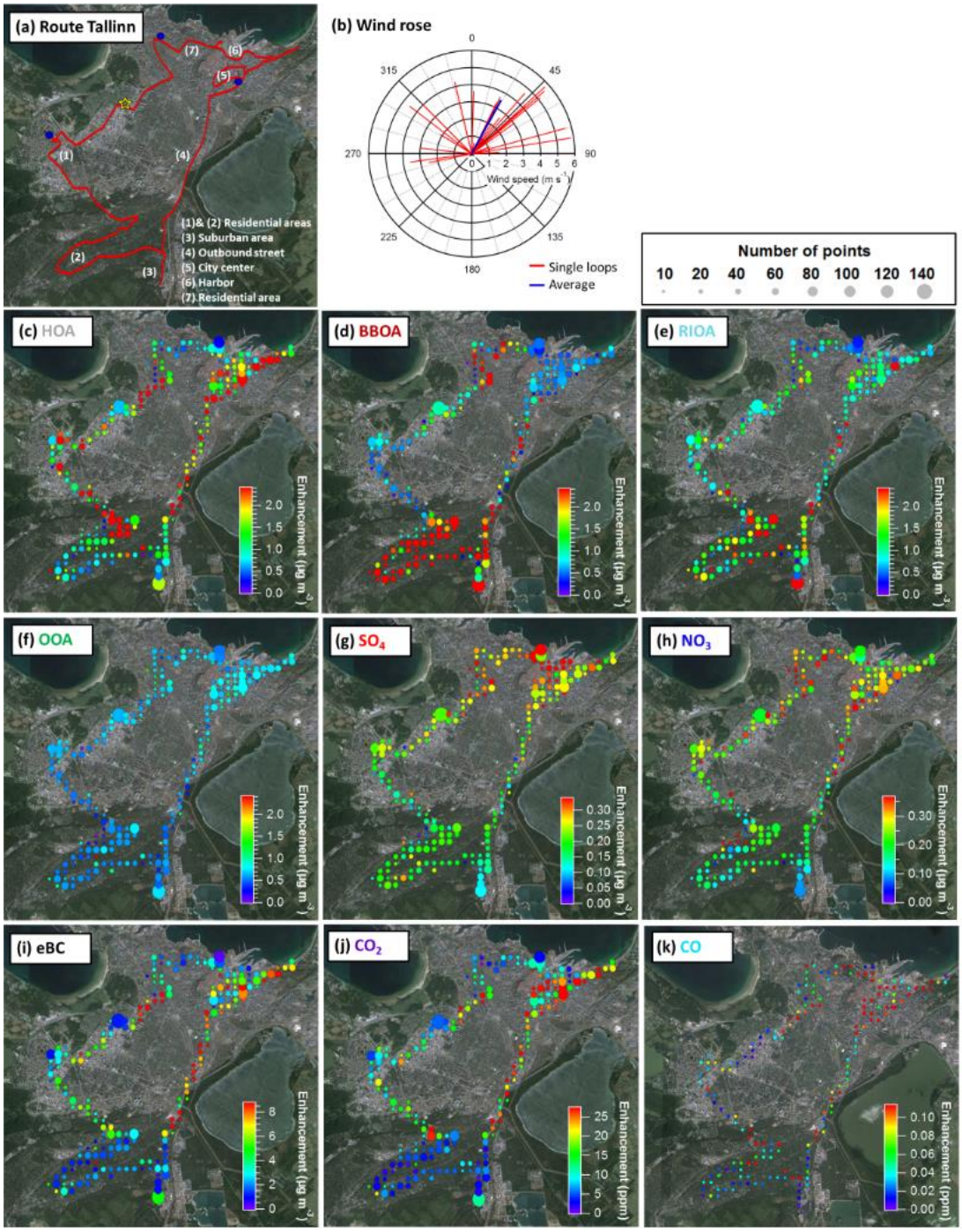

Figure 5 (Modified): (a) Driving route in Tartu: the red trace represents the GPS data, the yellow star the stationary measurements location and the blue dots the monitoring stations of the Estonian Environmental Research Institute (EERC); (b) Wind conditions during the mobile measurements in Tartu: red traces represent the wind direction and speed for the single loops and the average of all loops is represented in blue; (c to k) Average spatial distributions of all identified OA sources (panels c to f) and other measured components (panels g to k) in Tallinn. The color scales represent enhancement over the background concentrations; the maxima of the color scales have been fixed to the 75th percentile of the average enhancement of each component in panels g to k and to the highest 75th percentile among all OA sources in panels c to f. The sizes of the points represent the number of points that have been averaged in each case (Note: less data available for CO).

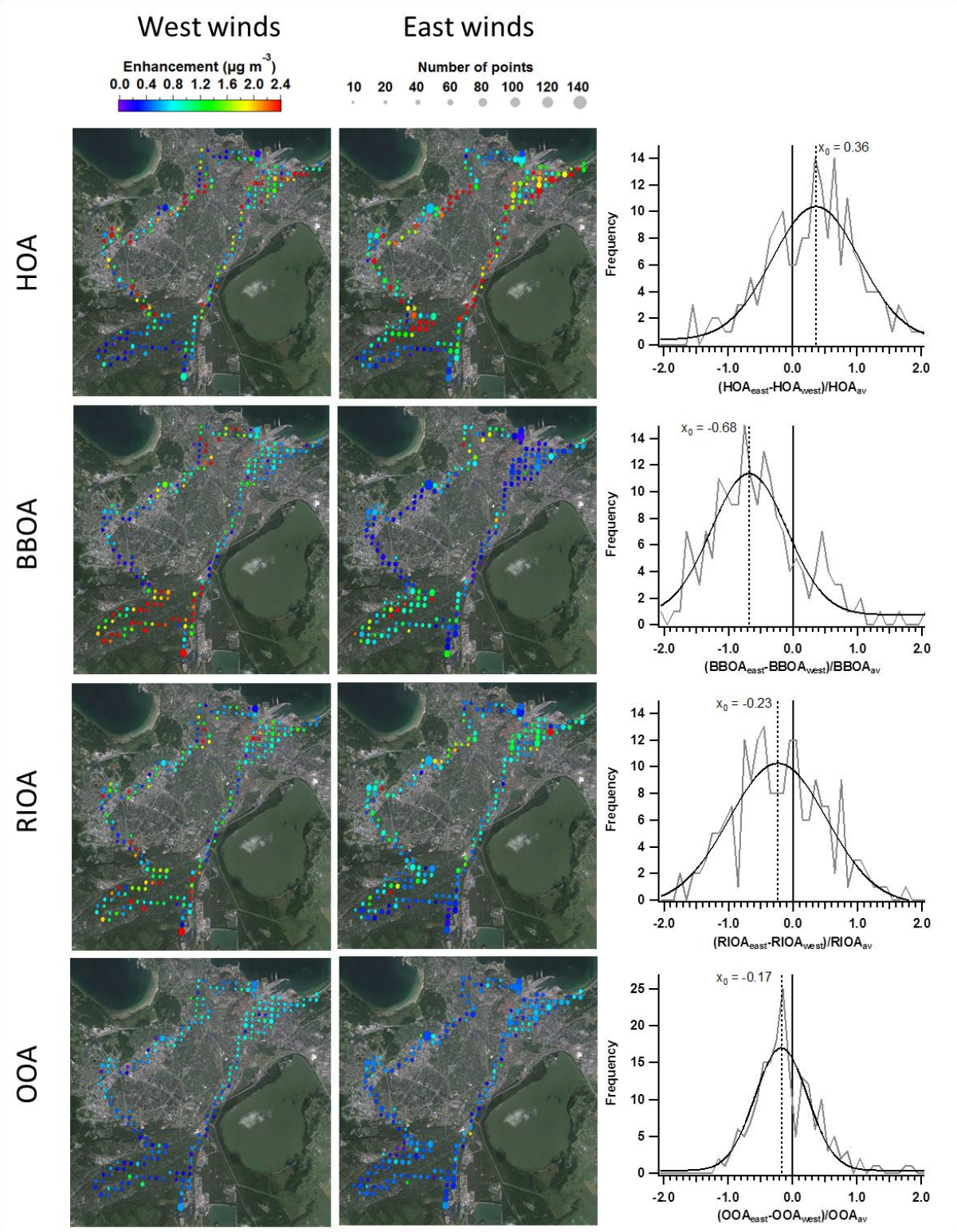

Figure S14 (New): Left: Average spatial distributions of the OA sources in Tallinn for west and east winds. The color scale represents the enhancement over the background concentrations and the size the number of points that have been averaged in each case. The data related to special events was excluded for these analyses. Right: Distribution of the normalized differences between the east- and west-related spatial distributions for each compound. X_0 indicates the center of the gauss function used to fit each distribution.

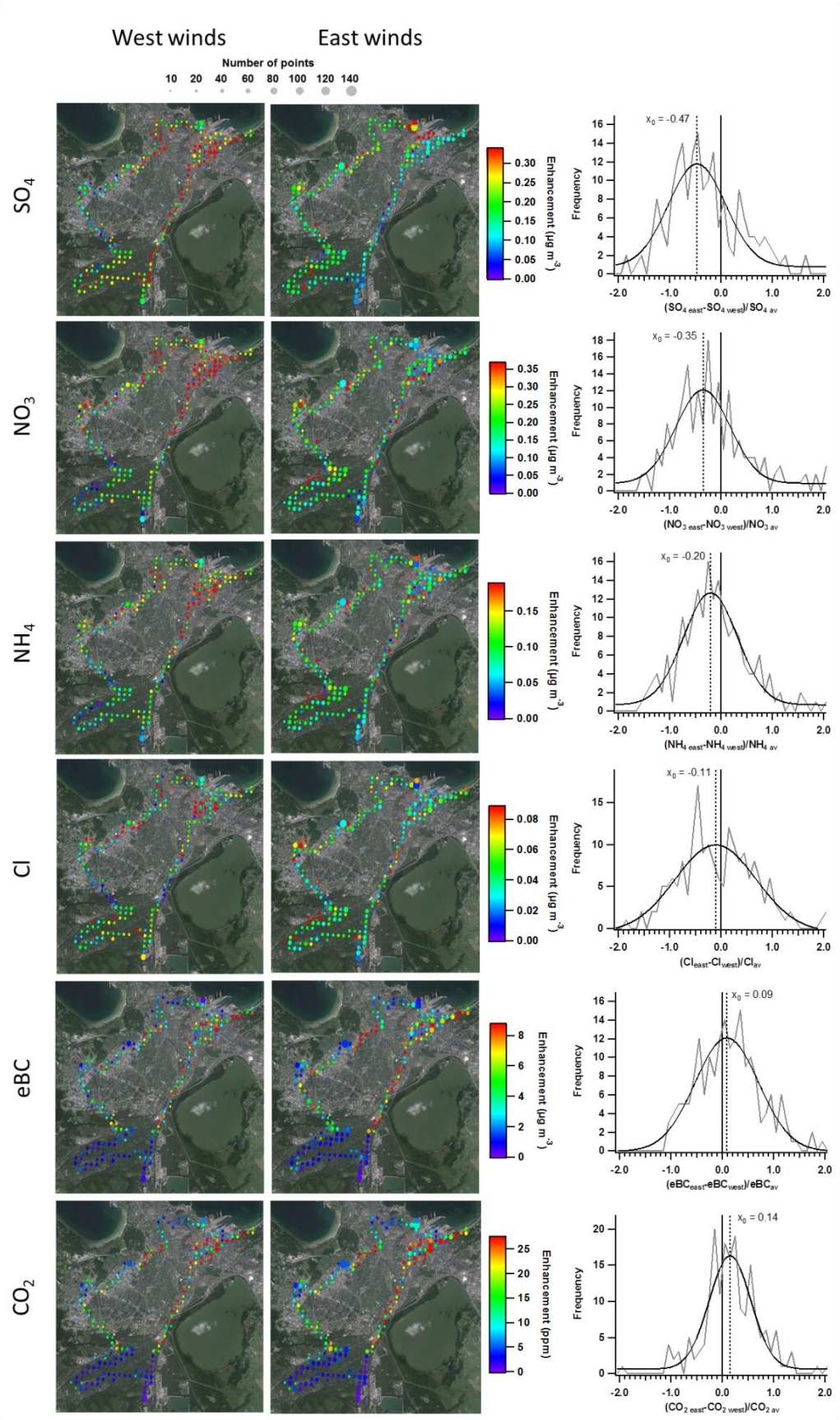

Figure S15 (New): Left: Average spatial distributions of the inorganic components (SO_4, NO_3, NH_4 and Cl), eBC and CO_2 in Tallinn for west and east wind conditions. The color scales represent the enhancement over the background concentrations and the size the

number of points that have been averaged in each case. The data related to special was excluded for these analyses. Right: Distribution of the normalized differences between the east- and west-related spatial distributions for each compound. X_0 indicates the center of the gauss function used to fit each distribution.

Page13, Lines 1-3: *Here, you state that BBOA is most enhanced during the evening hours, while on Page 11, Line 7 you state that higher loadings during the day are attributed to an increase primary sources (including BBOA). These statements tend to contradict each other. Please clarify.*

Author's response: The hours between 7:00 to 19:00, LT and 19:00 to 7:00, LT are referred to as day-time and night-time respectively, while we consider evening hours when biomass burning contribution is highest during the hours between 15:00 to 21:00, LT. So, there is an overlap between evening and day-time hours. This has been clarified in the revised manuscript.

Page 13, Lines 1-13: *Here, you discuss diurnal patterns. If possible (perhaps with the stationary measurements), it would be most illustrative if the diurnal patterns were included as a figure.*

Author's response: We agree with the reviewer that the diurnal patterns would help in our analysis. However, such analyses were not possible with our data, as stationary measurements were performed mostly overnight and mobile measurements are strongly affected by point sources. Nevertheless, similar analyses were performed using mobile conditions only, upon averaging the data over longer time periods (i.e. 2h, see Fig. S13). The discussion in Lines 1-13 in Page 13 is derived from these analyses.

Figures 5 and 6: *Consider adding the labeling from Fig 1 to these plots in order to facilitate the identification of source regions.*

Author's response: We have deleted Fig. 1 and have added the driving routes for Tartu and Tallinn in Fig. 4 and 5 of the revised manuscript.

Minor Comments

The following are wording suggestions that may help improve the fluency of the methodology section

Author's response: We thank the reviewer for the useful recommendations. The following suggestions have been introduced in the revised manuscript:

Section 2.1
Page 4, Line 13: *"… Tartu, with an area of 38.8 km2…"*
Page 4, Line 21: *"…to strongly enhance the signal of traffic emissions …"*
Page 4, Line 23: *"… with low stacks in both cities. In this regard, a detailed…."*
Section 2.2
Page 5, Line 17: *"…For this work , the AMS …"*

Page 6, Line 1: *"… measurement method automatically corrects for the loading effect …"*
Page 6, Lines 3-6: *" The concentrations of trace gases were measured by a Picarro-G2301 CO2/CH4 analyzer and a Licor-6262 CO monitor. "*
Section 2.3
Page 6, Lines 15-16: *"…collection efficiency (CE) algorithm by Middlebrook et al. (2012) was used in the calculation of ambient mass concentrations (Middlebrook et al., 2012)."*
Section 2.4
Page 4, Line 24: *"…allows the representation of a two-dimensional …"*
Page 7, line 4: *"In our case, the model input are the data and error matrices of OA…"*
Page7, Line 6: *"…contain the fits to the high-resolution data (292 ions)…"*
Page 7, Line 7: *"…agrees with the mass calculated from the unit mass resolution integration…"*
Page 7, Line 13: *"…directly calculated from the CO2+ fragment using the organic …"*
Page 7, Line 14: *"… were excluded from the PMF analysis…"*
Page 7, Line 15: *"… variability of the CO2+; these ions were reinserted post-analysis"*
Page 7, Line 18: *"… replicate datasets resulting from the perturbation of the original data…"*
Page 7, Line 20: *" … while other rows are removed (Paatero et al., 2014)…"*
Page 7, Line 23: *"Note that as each bootstrap…"*
Page 7, Line 24: *"… initialization point; thus, this methodology inherently includes the investigation of the classic seed variability…"*
Page 7, Line 25: *"…consistent, suggesting that the solution is robust."*
Section 2.4.2
Page 8, Line 8: *"… for the correlations with the external tracers, but their spatial distributions couldn't be explored…"*

Page 5, Line 20: *"…lens efficiently transmits particles with 80 nm < Dp ≤ 3 µm and has been tested in previous chamber and ambient studies (Williams et al., 2013; Wolf et al., 2015; Elser et al., 2015)"*

Author's response: As mentioned in the text and described by Williams et al. (2013), the $PM_{2.5}$ lens efficiently transmits particles between 80 nm and up to at least 3 µm. The fact that particles larger than 3 µm could also be transmitted efficiently with this system is an important detail that needs to be considered in the presence of large particles. Therefore we prefer to keep this information in the text.

Anonymous Referee #3

Received and published: 23 February 2016

The paper by Else et al. summarizes mobile springtime measurements of aerosol concentrations and several gas phase species in two Estonian cities. The measurements allowed the authors to identify 4 classes of OA in both cities. Overall, aerosol composition in both cities was similar and was dominated by higher concentration of primary types of OA during the day and by lower amount of secondary OA at night. Contribution of the secondary inorganic species was low except during a transport event.
The manuscript is very well-organized and well-written. There are two aspects that need some work in my opinion. One is related to wind direction and its variability during day and night sampling and how it might affect the interpretation of the results (see my comment below). The other aspect is that since the measurement was done in two cities, I think more can be done to compare quantitatively aerosol air quality in these two cities. Since measurements of CO are already available, I think it will be valuable to look at the enhancement ratios (not by subtracting a background) but considering scattering plots of say OA vs. CO, BC vs CO (or the PMF-resolved factors or other species vs. CO) in comparable times of the day to separate out the differences in dynamics, boundary layer heights, dilution, etc. and be able to determine a more valuable comparison of the aerosol sources in these cities. This will also allow the authors to compare the measurements with other measurements (ground based on airborne) in other cities around the world. I support publishing the paper after my comments (above and below) are addressed.

Author's response:
Indeed, ratios of different OA components to CO are generally used to take into consideration the effect of the PBL and dilution in order to investigate the evolution of a plume with photochemistry. However, here we lack measurements to estimate the photochemical lifetime of the sampled air masses (e.g NOx/NOy or VOCs).

In the figures below we display the scatter plots of different aerosol components versus CO to investigate differences between the two locations and with the time of the day. Such plots mostly reflect the profiles of combustion sources that dominate CO emissions. Similar ratios are found for the two cities (Fig. R1), which is consistent with similar sources of CO and similar emission profiles at both locations. HOA and eBC show higher ratios to CO during daytime (Fig. R2), as traffic (which dominates eBC emissions) is more enhanced during day-time compared to CO, which can be also affected by other sources (i.e. BBOA and RIOA).

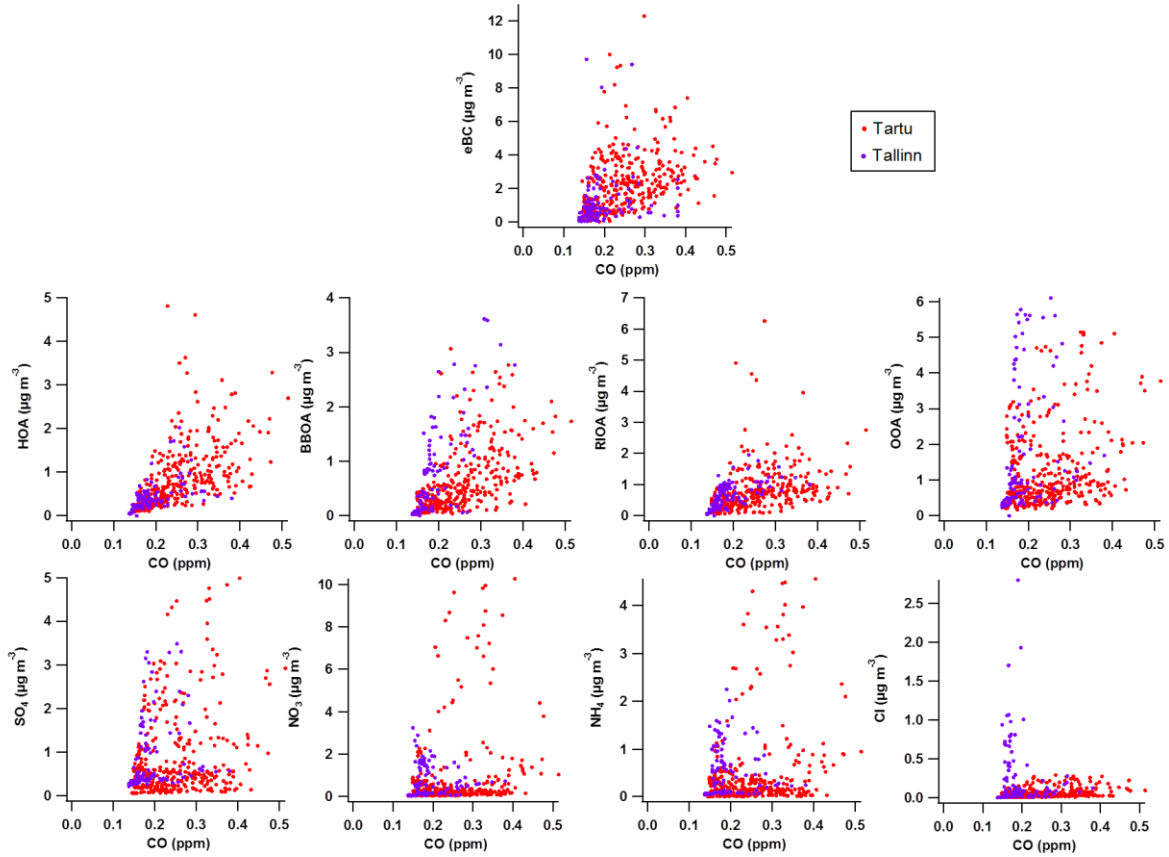

Figure R1: Scatter plots of all particle phase components versus CO, color-coded by measurement location.

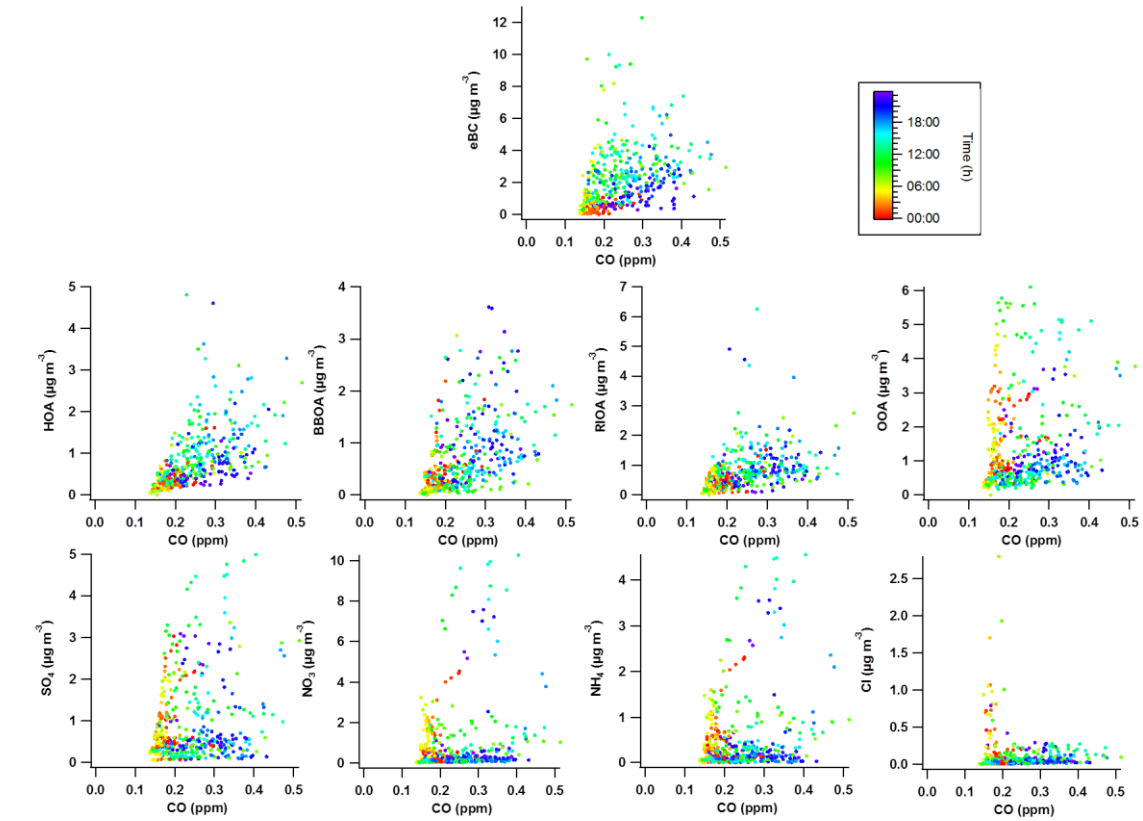

Figure R2: Scatter plots of all particle phase components versus CO, color-coded by measurement time.

Abstract: *indicate which month/season the measurements were carried out.*

Author's response: This information has been added in the abstract of the revised manuscript.

Changes in text:
Page 1, Line 14: This work presents the first spatially-resolved detailed characterization of the $PM_{2.5}$ in two major Estonian cities, ~~(~~Tallinn and Tartu~~), using mobile measurements~~. The measurements were performed in March 2014 using a mobile platform. In both cities, the non-refractory (NR)-$PM_{2.5}$ was characterized by a high-resolution time-of-flight aerosol mass spectrometer (HR-ToF-AMS) using a recently developed lens which increases the transmission of super-micron particles.

P5, L3: *It is mentioned that stationary measurements were made at night. Were there any mobile measurements also carried out at night?*

Author's response: The mobile measurements were performed between 6:00 and 23:00 LT, including only few drives during the early morning and at nighttime.

P8, L2: *Explain why A(abs)=1.7 was used for wood burning BC? And why was it that the lower wavelength of 370 nm was not used? Doesn't it make sense to use 370 nm since BrC would be stronger there?*

Author's response: The choice of the wavelengths and of the angstrom exponents used in this work are based on the findings in Zotter et al. (In prep.), where radiocarbon (^{14}C) measurements of elemental carbon (EC) are combined with Aethalometer data to determine the best Angstrom exponents for wood burning (α_{WB}) and traffic (α_{TR}). The best α values were evaluated by fitting the source apportionment results of the Aethalometer (in particular BC_{tr}/BC) against the fossil fraction of EC (EC_f/EC) derived from ^{14}C measurements. This analysis resulted in α_{tr} = 0.9 and α_{wb} = 1.68 fitting best the data when using the attenuation measured at 470 and 950 nm. Other wavelength combinations were also tested but in all cases, especially when 370 nm was used, the residuals of the fit were worse. Moreover it is known that the 370 nm channel of the Aethalometer is more sensitive to artefacts, including response to light absorbing SOA and the adsorption of VOCs on the filter. A brief description of the Aethalometer source apportionment method and the findings in Zotter et al. (In prep.) has been added in the revised manuscript.

Changes in text:
Page 8, Line 9: The Aethalometer measurements can be used to separate eBC from wood burning (eBC_{wb}) and from traffic (eBC_{tr}), by taking advantage of the spectral dependence of absorption, as described by the Ångström exponent (Ångström, 1929). Specifically, the enhanced absorption of wood burning particles in the ultraviolet and visible wavelengths region (370–520 nm) relative to that of traffic particles is used to separate the contributions of the two fractions. This method is described in detail….

Page 8, Line 19: The absorption Ångström exponent was calculated using the absorption measured at 470 and 950 nm and Ångström exponents of 0.9 and 1.7 were used for traffic and wood burning, respectively.~~,~~ These parameters were chosen following the suggestions in Zotter et al. (In prep.), where the comparison between radiocarbon (^{14}C) measurements of

elemental carbon (EC) and the Aethalometer source apportionment results allowed the identification of the best wavelengths and Ångström exponents pairs.

P8, L16-17: *Just looking at Figure 2, it seems standard deviations of the averages would be really high, and maybe that's why they're not indicated along with the average values in Panel B. I wonder if estimates of the median values (or to be more complete, box and whisker plots) of the tracers will be more valuable than the average values.*

Author's response: We decided not to report the standard deviations in Fig. 2b (now Fig. 1b) as the big variability of the data can be seen from the time series and in our case it's simply reflecting the driving conditions. Thus, we believe that the standard deviation of the time series would not provide any useful information in our case, especially because this variability can be explained by the spatial distribution of the sources. Moreover, the addition of standard deviations of the time series could introduce some confusion between the meanings of the errors in different cases, as for the source apportionment results (see Fig. 3 of the revised manuscript) we report standard deviations among the 100 bootstrap runs (which is an indication of the model uncertainty and not of the temporal variability of the sources).

P11, L15: *missing a word ": : :of ?? (data??)..."*

Author's response: We have modified this paragraph in the revised manuscript.

Changes in text:
Page 12, Line 26: RIOA is also enhanced during day-time in Tartu (27% compared to 20% during night-time), and has similar relative contributions for day- and night-time in Tallinn (20 and 22%, respectively). In contrast, BBOA shows similar relative contributions for day- and night-time in Tartu (~~explaining~~ representing about 17 % of the OA mass), and slightly lower contributions during ~~the~~ day-time in Tallinn (20 % during day-time and 25 % at night-time).

P12, L1: *replace kurbside with curbside*

Author's response: Replaced in the revised manuscript.

Figure 2: *I suggest having the inorganics on a separate axis, with max _10 ug/m3, so you can see the tracers better.*

Author's response: The plot has been modified accordingly in the revised manuscript.

Figure 5: *For some species, it appears that the conc. were very different on different sides of the loop, suggesting that the sources are towards the center of the loop (as opposed to one side, e.g., BBOA and sulfate). In other words there is gradient in the latitudinal direction as well as longitudinal direction. To further investigate the source regions, it makes sense to consider wind direction data with these distribution maps. Were wind directions consistent*

during the day and night sampling time? It seems the averages include both daytime and nighttime. Could you add average wind barbs representatives for daytime and nighttime or at least discuss the wind patterns in the text? Correct interpretation of the mean and median values in Table 2 with relation to the source regions also needs some knowledge of the wind direction.

Author's response:
As mentioned above, we have added a time series with the meteorological parameters during the measurement periods (including wind direction and speed, temperature and precipitation) in the supplementary information of the revised manuscript. No systematical difference can be observed between day and night wind conditions.
In Tartu, during the mobile measurements west winds (with speeds between 1 and 2.6 m s^{-1}) were predominant (see wind rose in Fig. 4 in the revised manuscript). However, the wind doesn't seem to influence the background concentrations measured in the east side of the loop, as the base values obtained for the this side of the loop were always equal or lower than those obtained in the west (see Table 3). Therefore, we also exclude a big influence of the transport of pollutants within the urban area and we expect that the identified source areas will not be strongly biased by this effect.

Figure 7: *Indicate in the legend that enhancement is relative to P05 values.*

Author's response: The Figure has been modified in the revised manuscript to indicate that the enhancement is relative to the P05 values. This information has also been added in the figure caption for further clarification.

Changes in text:
Figure 7 caption: Average longitude profiles of the enhancements (above P05) of all measured components and sources in Tartu.

Table 2 legend: *Indicate which city the stats refer to.*

Author's response: Added in the revised manuscript.

Changes in text:
(A) Average longitude profiles (Tartu):
(B) Median longitude profiles (Tartu):

Anonymous Referee #4

Received and published: 29 February 2016

General comments

This paper presents mobile measurements of gas- and particle-phase pollutants at two Estonian cities of Tartu and Talinn. Detail chemical composition of NR-PM2.5 as well as BC and trace gases (CO, CO2, and CH4) were observed in high time resolution and OA characteristics were found to be similar (HOA, BBOA, RIOA, and OOA) at both cities. Primary types of OA (HOA, BBOA and RIOA) were high during the day, whereas secondary OA (OOA) enhanced at night. In summary, the mobile measurements allowed the authors to observe time and spatial distribution of primary and secondary pollutants, as well as influences of long-range transport and local temperature inversion to aerosol and gases pollutants in Tartu and Talinn.

The manuscript is well structured and written. I have some comments regarding research methods, results and discussion as well as suggestions that would improve quality of the manuscript. There are also some typing errors in the text, tables and figures summarized in technical comments. Overall, I support publication of the manuscript after my comments are addressed.

Specific comments

OA source apportionment:
I believe the authors have done rigorous analysis in selecting the best PMF factor solution. I expect some of the analysis figures and/or tables are provided in the SI. PMF diagnostic plots, such as those presented by Zhang et al. (2011), are important for understanding the analysis and discussion. Residuals of time series and mass spectra for 3-, 4-, and 5-factor solutions and correlations between factors time series and external tracers (i.e., CO, eBC, SO4, NO3) are useful in understanding selection of the best factor solution. I recommend adding this information in the SI at the least.

Author's response:
As discussed above, a figure with the major source apportionment diagnostic plots has been added in the supplementary information (Fig. S5 in the revised manuscript). This figure includes the Q/Q_{exp} as a function of the number of factors, the correlation coefficients (R^2) of the resolved factors with the external markers for solutions with different number of factors and the change in the residuals time series and profiles for increasing number of factors.

Changes in text: See complete changes in text in comment below regarding the five-factor solution.

eBC source apportionment:
It is not clear why do the authors choose to calculate Angstrom exponent using absorption at 470 and 950 nm. Since Zotter et al. paper has not yet published, I could not verify how the calculation was done. I suggest adding a brief description of this calculation in the main text or SI. Also, brief description of calculation of eBCwb and eBCtr would be a useful addition in the SI.

Author's response: The choice of the wavelengths and of the angstrom exponents used in this work are based on the findings in Zotter et al. (In prep.), where radiocarbon (^{14}C) measurements of elemental carbon (EC) are combined with Aethalometer data to determine the best Angstrom exponents for wood burning (α_{WB}) and traffic (α_{TR}). The best α values were evaluated by fitting the source apportionment results of the Aethalometer (in particular BC_{tr}/BC) against the fossil fraction of EC (EC_f/EC) derived from ^{14}C measurements. This analysis resulted in α_{tr} = 0.9 and α_{wb} = 1.68 fitting best the data when using the attenuation measured at 470 and 950 nm. Other wavelength combinations were also tested but in all cases, especially when 370 nm was used, the residuals of the fit were worse. Moreover it is known that the 370 nm channel of the Aethalometer is more sensitive to artefacts, including response to light absorbing SOA and the adsorption of VOCs on the filter. A brief description of the Aethalometer source apportionment method and the findings in Zotter et al. (In prep.) has been added in the revised manuscript.

Changes in text:

Page 8, Line 9: The Aethalometer measurements can be used to separate eBC from wood burning (eBC_{wb}) and from traffic (eBC_{tr}), by taking advantage of the spectral dependence of absorption, as described by the Ångström exponent (Ångström, 1929). Specifically, the enhanced absorption of wood burning particles in the ultraviolet and visible wavelengths region (370–520 nm) relative to that of traffic particles is used to separate the contributions of the two fractions. This method is described in detail….

Page 8, Line 19: The absorption Ångström exponent was calculated using the absorption measured at 470 and 950 nm and Ångström exponents of 0.9 and 1.7 were used for traffic and wood burning, respectively.~~,~~ These parameters were chosen following the suggestions in Zotter et al. (In prep.), where the comparison between radiocarbon (^{14}C) measurements of elemental carbon (EC) and the Aethalometer source apportionment results allowed the identification of the best wavelengths and Ångström exponents pairs.

Results and discussion:

Page 10 Ln 1-2: *Could the authors provide approximate uncertainty value of ratio of BBOA and eBCwb relative to change in Angstrom exponent?*

Author's response: As mentioned in the manuscript, the BBOA to eBC_{wb} ratio is very sensitive to the chosen Ångström exponent for traffic. Zotter et al. (in prep.) recommend the use of Ångström exponents for traffic between 0.9 and 1.0, as using 1.1 leads to increased residuals in their method. Therefore, we used an Ångström exponent for traffic of 0.9 and reported the change in the BBOA to eBCwb ratio if an Ångström exponent for traffic of 1.0 had been used. This variability (ratio changed from 4 to 4.8) is an indication of the method uncertainty relative to the choice of Angstrom exponents, which is around 20%.

Page 10 Ln 2-10: *From information provided, it seems reasonable to assign RIOA as COA. The lack of diurnal variability does not mean that the factor is not a COA factor. It is possible that the lack of diurnal variability is due to homogeneous source of cooking emission, or stagnant atmosphere during measurements Have the authors look at meteorological conditions, such as wind direction and speed, when RIOA concentrations were high? I would recommend adding meteorological information in the SI.*
Identification of RIOA or COA could be further assessed by plotting the factor mass spectra side-by-side with reference mass spectra from previous studies, such as by Mohr et al.

(2012). The authors will need to provide more evidence to support identification of the RIOA factor.

Author's response:
As previously mentioned, the diagnostic plots included in the revised manuscript support the use of a four-factor solution, where the RIOA factor is resolved. In general, an increase in the correlation coefficient (R^2) is observed when going from a three- to a four-factor solution. As the correlations are not further improved when considering higher order solutions, the four-factor solution is considered the best representation of the data. Also the trend in the model residuals supports the presence of four factors, as the decrease in the residuals time series is important when increasing from three to four factors but is rather low when further increasing the number of factors.

As mentioned above, we have added a time series with the meteorological parameters during the measurement periods (including wind direction and speed, temperature and precipitation) in the supplementary information of the revised manuscript (Fig. S2). We show that in general the wind direction does not influence our measurements significantly (see Fig. 4b and Fig. S14), but the temporal variability of the factor time series, including that of RIOA, are rather driven by their spatial distribution.

A table containing the correlation coefficients (R^2) between the OA profiles from the four-factor solution and literature profiles has been added in the main text of the revised manuscript (New table 2). The high correlation between RIOA and published cooking mass spectra suggests that RIOA may be heavily influenced by cooking processes. However, we could not exclude the contribution from other residential sources (e.g. waste or coal combustion), especially also due to the lack of statistically robust diurnal patterns for cooking that are not affected by the drives. Therefore, we prefer to refer to this factor to RIOA, rather than cooking.

Changes in text: See complete changes in text in the following comment.

Page 10 Ln 16-24: *The 5th factor, LV-OOA, may not show certain process or source, but it can show whether highly oxidized OA is important in the study locations. The LV-OOA can be formed from oxidation of primary OA (e.g., BBOA) or transported into the study location. The authors can discuss this further.*

Author's response:

We now added a thorough analysis for justifying the number of factors selected. We show that the addition of a fifth factor better explains $C_xH_yN_w$ and biomass burning (at *m/z* 60 and 73) related fragments. The additionally extracted factor in the five-factor solution, referred to as 'unknown', has elevated contributions from oxygenated fragments often related to SOA (*m/z* 44) and BBOA (*m/z* 60 and 73), but a time series that unambiguously relates this factor to a spatially variable primary emission source. In effect, the majority (62%) of this factor contribution arises from a split in the BBOA of the four-factor solution (the rest comes from the residuals and the OOA). Consequently, the sum of the contributions of the 'unknown' factor and the BBOA from the five-factor solution matches the BBOA contributions from the four-factor solution (R^2 = 0.97 and slope = 1.15 as shown in Fig. S6). This split in the BBOA is very likely a direct consequence of the variable nature of this combustion source or may potentially represent its very rapid/immediate aging. That is, as the concentrations of this more oxygenated BBOA are highly variable in time and space and coincide with high BBOA concentrations, this factor cannot be transported into the study location, but rather represents an emission from another combustion regime or, less likely, an immediately

transformed primary aerosol. As this factor could not be attributed to a specific process and its addition did not significantly alter the contribution from other sources, we have considered the four-factor solution as an optimal representation of our data. This discussion is now added in the text.

Changes in text:

Page 10, Line 31: Some important diagnostic parameters of the source apportionment (including Q/Q_{exp}, factor-marker correlation, and time-series and profiles residuals for solutions with different number of factors) are reported in Fig. S5. The correlation coefficients (R^2) between factors and markers significantly increase when a fourth factor is included, but are not improved when a fifth factor is added. The addition of the fourth factor, which enabled the extraction of RIOA, allows explaining additional structures in the residuals' time series and unsaturated fragments in the residuals mass spectrum. Including a fifth factor also improves the model mathematical quality, by additionally explaining $C_xH_yN_w$ and biomass burning (at *m/z* 60 and 73) related fragments. The additionally extracted factor in the five-factor solution, referred to as 'unknown', has elevated contributions from oxygenated fragments often related to SOA (*m/z* 44) and BBOA (*m/z* 60 and 73), but a time series that unambiguously relates this factor to a spatially variable primary emission source. In effect, the majority (62%) of this factor contribution arises from a split in the BBOA factor from the four-factor solution (the rest comes from the residuals and the OOA). Moreover, the sum of the contributions of the 'unknown' factor and the BBOA from the five-factor solution matches the BBOA contributions from the four-factor solution (R^2 = 0.97 and slope = 1.15 as shown in Fig. S6). This split in the BBOA is very likely a direct consequence of the variable nature of this combustion source, but the two BBOA-like factors extracted in the five-factor solution could not be related to different emission processes. Furthermore, the addition of this factor did not affect the spectral profiles and time series of the other factors and their correlations with their respective markers and did not aid the interpretation of the data. Therefore, we considered the four-factor solution as an optimal representation of our data. Table 2 contains the correlation coefficients (R^2) between the OA profiles from the four-factor solution and available literature profiles (Aiken et al., 2009; Mohr et al., 2012; Setyan et al., 2012; Crippa et al., 2013b). The high correlations obtained in all cases support the use of a four-factor solution and strengthen the link between the RIOA and cooking emissions (R^2 of about 0.8 between RIOA and cooking tracer).
~~If the number of factors is decreased, the RIOA factor is not resolved and the OOA time-series becomes contaminated by local spikes, which is unexpected for a regional component (see Fig. S3 and S4). In contrast, if a five-factor solution is considered an additional highly oxygenated factor is obtained ("unknown" factor in Fig. S3 and S4). The mass spectrum of this additional factor resembles a low-volatility OOA (LV-OOA), as resolved in many previous works (Jimenez et al., 2009), but its time series exhibits the typical characteristics of the primary factors, i.e. strong increases in emission areas. Therefore, this further increase in the number of factors doesn't seem to improve the interpretation of the data, as the new factor cannot be explicitly associated to distinct sources or processes. Accordingly, a four-factor solution was considered as optimal and is utilized below.~~

Page 11 Ln 12-15: *Increase of RIOA in Talinn is relatively small. I think distribution of RIOA in Talinn is more homogeneous compared to Tartu. Thus, enhancement of RIOA in urban area of Talinn is not well supported.*

Author's response: We thank the reviewer for the important remark. We have accordingly modified this paragraph in the revised manuscript.

Changes in text:

Page 12, Line 19: In terms of relative contribution, OOA is dominant during night-time, explaining on average between 42 and 44 % of the OA mass in Tartu and Tallinn, respectively. ~~HOA and RIOA relative contributions to the total OA are higher during day-time (the relative contribution of HOA increases from about 20 to 32% in Tartu and from 11 to 27% in Tallinn; the relative contribution of RIOA increases from 20 to 27 % in Tartu and from 20 to 22 % in Tallinn).~~ The relative contribution of HOA to total OA mass is higher during day-time (32% in Tartu and 27% in Tallinn) than during night-time (20% in Tartu and 11% in Tallinn). RIOA is also enhanced during day-time in Tartu (27% compared to 20% during night-time), and has similar relative contributions for day- and night-time in Tallinn (20 and 22%, respectively). In contrast, BBOA shows similar relative contributions for day- and night-time in Tartu (~~explaining~~ representing about 17 % of the OA mass), and slightly lower contribution during ~~the~~ day-time in Tallinn (20 % during day-time and 25 % at night-time).

Page 13 Ln 1-3: *Spatial distribution of eBC, CO, and CO2 are consistent not only with HOA but also with BBOA. Thus, they may come from BBOA as well. It would be easier to show consistency or inconsistency by correlation coefficient (R^2) between those tracers and HOA and BBOA.*
Also, in general I disagree that CO2 is mostly traffic because it can be emitted from vegetation and other sources. The authors will need to provide more evidence to support CO2 from traffic.

Author's response: We agree that CO_2 sources other than traffic are also present in urban areas (e.g. vegetation, BBOA…). However, our results indicate that these sources don't have a visible effect on the CO_2 enhancements in the urban area, as the spatial distribution of the CO_2 enhancement corresponds best to the one of HOA. These additional sources will indeed have an effect on the CO_2 background concentrations, which are subtracted for the calculation of the enhancements.
Following the suggestion of the referee, we have added a table in the supplementary information of the revised manuscript that contains all the correlation coefficients (R^2) between the spatial distributions of all sources and components in Tartu. This table confirms that the spatial distributions of the enhancements of eBC, CO_2 and CO are in good agreement with those of HOA (R^2 of around 0.6 in all cases), but no correlation is found between these components and BBOA (R^2 of 0.1 or lower).

Changes in text:
Page 13, Line 16: Lastly, the sizes of the points represent the number of measurement points that were averaged in each case. The correlation coefficients (R^2) between the spatial distributions of all sources and components are reported in Table S1.

Page 14, Line 29: The spatial distributions of the eBC, CO_2 and CO (Fig. 4i-k ~~5g-i~~) are consistent with that of HOA (R^2 of 0.61, 0.59 and 0.58, respectively), which indicates that these species originate mostly from traffic.

Table S1: Correlation coefficient (R^2) between the spatial distributions of all sources and components.

(a) Tartu

R^2	HOA	BBOA	RIOA	OOA	SO_4	NO_3	NH_4	Cl	eBC	CO_2	CO	CH_4
HOA		0.02	0.32	0.02	0.04	0.09	0.16	0.10	**0.61**	**0.59**	**0.58**	0.06

BBOA	0.47	0.05	0.28	0.20	0.16	0.47	0.03	0.01	0.10	0.11
RIOA		0.08	0.35	0.14	0.22	0.39	0.24	0.17	0.28	0.07
OOA			0.12	0.09	0.12	0.21	0.01	<0.01	<0.01	0.01
SO_4				0.07	0.10	0.12	0.03	0.02	0.08	0.03
NO_3					**0.60**	0.28	0.08	0.08	0.11	0.11
NH_4						0.24	0.09	0.05	0.11	0.10
Cl							0.07	0.03	0.11	0.13
eBC								**0.77**	**0.75**	0.08
CO_2									**0.78**	0.08
CO										0.14
CH_4										

Technical comments

Page 4 Ln 22: *Add reference for these statements.*

Author's response: Added in the revised manuscript.

Page 5 Ln 10: *Unit for flow rate is m3 s-1 or L min-1*

Author's response: Replaced "flow" by "velocity" in the revised manuscript.

Page 5 Ln 12: *What is the size of particle in the aerosol inlet before particles are divided into different aerosol measurements.*

Author's response: There is no particle size segregation in the inlet of the mobile laboratory. Thus, the size of the measured particles depends on the instrument and inlet system cut-off. The inlet size cut-off is estimated to be at around 5 µm and the AMS lens at 2.5 µm. This information has been added in the revised manuscript.

Changes in text:
Page 5, Line 18: Two different inlet lines connected the main inlet to the aerosol and gas-phase instrumentation. The size cut-off of the inlet system was estimated to be around 5 µm.

Page 5 Ln 28: *eBC has been defined in the introduction.*

Author's response: Corrected in the revised manuscript.

Page 8 Ln 28-30: *The statement about enhancement of negative health impacts is not well supported, as it was not within the scope of this study. I suggest the authors to omit the part or revise the sentence.*

Author's response: We agree with the reviewer and have revised the sentence in the revised manuscript.

Changes in text:
Page 9, Line 11: Such intermittent pollution plumes (expected in some areas in a city) cannot be detected from stationary measurements at an urban background site, but ~~enhance~~ may be associated with negative health impacts.

Page 10 Ln 29: *Delete "secondary" or change it to "secondary source (OOA)"*

Author's response: Changed in the revised manuscript.

Page 11 Ln 24: *"the 5th percentile (P05) of"*

Author's response: Corrected in the revised manuscript.

Page 13 Ln 20: *Add space "… is 4.2 …"*

Author's response: Added in the revised manuscript.

Table 2: *Superscript for the unit µg m-3.*

Author's response: Corrected in the revised manuscript.

Figure 2:
(a) What does the different shade of purple for CO2 mean?
(b) If the average pollutant concentrations exclude those from special events, this needs to be included in the title.

Author's response: (a) The different colors used for the CO_2 time series indicate data from different analyzers. Specifically, the light purple indicates data from the Licor analyzer, which is used in the period in which the Picarro analyzer was malfunctioning. This has been clarified in the figure legend of the revised manuscript.
(b) Yes, the special events were excluded for these calculations. This has been added in the figure caption of the revised manuscript.

Figure 3: *I think mass spectra relative contribution is not in %. For comparison, relative contribution in Figure S3 is unitless.*

Author's response: We apologize for this mistake; the unit has been removed in the revised manuscript.

Figure 8: *Add in the title that the back-trajectories is from 10:00 at 10 March 2014 to 8:00 at 11 March 2014.*

Author's response: Added in the revised manuscript.

References:

Aiken, A. C., Salcedo, D., Cubison, M. J., Huffman, J. A., DeCarlo, P. F., Ulbrich, I. M., Docherty, K. S., Sueper, D., Kimmel, J. R., Worsnop, D. R., Trimborn, A., Northway, M., Stone, E. A., Schauer, J. J., Volkamer, R. M., Fortner, E., de Foy, B., Wang, J., Laskin, A., Shutthanandan, V., Zheng, J., Zhang, R., Gaffney, J., Marley, N. A., Paredes-Miranda, G., Arnott, W. P., Molina, L. T., Sosa, G., and Jimenez, J. L.: Mexico City aerosol analysis during MILAGRO using high resolution aerosol mass spectrometry at the urban supersite (T0) – Part 1: Fine particle composition and organic source apportionment, Atmos. Chem. Phys., 9, 6633-6653, 2009.

Crilley, L. R., Bloss, W. J., Yin, J., Beddows, D. C. S., Harrison, R. M., Allan, J. D., Young, D. E., Flynn, M., Williams, P., Zotter, P., Prevot, A. S. H., Heal, M. R., Barlow, J. F., Halios, C. H., Lee, J. D., Szidat, S., and Mohr, C.: Sources and contributions of wood smoke during winter in London: assessing local and regional influences, Atmos. Chem. Phys., 15, 3149–3171, 2015.

Crippa, M., El Haddad, I., Slowik, J. G., DeCarlo, P. F., Mohr, C., Heringa, M. F., Chirico, R., Marchand, N., Sciare, J., Baltensperger, U., and Prévôt A. S. H.: Identification of marine and continental aerosol sources in Paris using high resolution aerosol mass spectrometry, J. Geophys. Res., 118, 1950–1963, 2013.

Favez, O., El Haddad, I., Piot, C., Boréave, A., Abidi, E., Marchand, N., Jaffrezo, J.-L., Besombes, J.-L., Personnaz, M.-B., Sciare, J., Wortham, H., George, C., and D'Anna, B.: Inter-comparison of source apportionment models for the estimation of wood burning aerosols during wintertime in an Alpine city (Grenoble, France), Atmos. Chem. Phys., 10, 5295–5314, 2010.

Herich, H., Hueglin, C., and Buchmann, B.: A 2.5 year's source apportionment study of black carbon from wood burning and fossil fuel combustion at urban and rural sites in Switzerland, Atmos. Meas. Tech., 4, 1409–1420, 2011.

Mohr, C., DeCarlo, P. F., Heringa, M. F., Chirico, R., Slowik, J. G., Richter, R., Reche, C., Alastuey, A., Querol, X., Seco, R., Peñuelas, J., Jiménez, J. L., Crippa, M., Zimmermann, R., Baltensperger, U. and Prévôt, A. S. H.: Identification and quantification of organic aerosol from cooking and other sources in Barcelona using aerosol mass spectrometer data, Atmos. Chem. Phys., 12, 1649–1665, 2012.

Paatero, P., Eberly, S., Brown, S. G., and Norris, G. A.: Methods for estimating uncertainty in factor analytic solutions, Atmos. Meas. Tech., 7, 781–797, 2014.

Sciare, J., d' Argouges, O., Sarda-Estève, R., Gaimoz, C., Dolgorouky, C., Bonnaire, N., Favez, O., Bonsang, B., and Gros, V.: Large contribution of water-insoluble secondary organic aerosols in the region of Paris (France) during wintertime, J. Geophys. Res. Atmos., 116, D22203, 2011.

Setyan, A., Zhang, Q., Merkel, M., Knighton, W. B., Sun, Y., Song, C., Shilling, J. E., Onasch, T. B., Herndon, S. C., Worsnop, D. R., Fast, J. D., Zaveri, R. A., Berg, L. K., Wiedensohler, A., Flowers, B. A., Dubey, M. K., and Subramanian, R.: Characterization of submicron particles influenced by mixed biogenic and anthropogenic emissions using high-

resolution aerosol mass spectrometry: results from CARES, Atmos. Chem. Phys., 12, 8131-8156, 2012.

Zhang, Q. Q., Jimenez, J.L., Canagaratna, M.R., Ulbrich, I.M., Ng, N.L., Worsnop, D.R., and Sun, Y.: Understanding atmospheric organic aerosols via factor analysis of aerosol mass spectrometry: a review, Analyt. Bioanalyt. Chem., 401, 3045-3067, 2011.

Urban increments of gaseous and aerosol pollutants and their sources using mobile aerosol mass spectrometry measurements

M. Elser[1], C. Bozzetti[1], I. El-Haddad[1], M. Maasikmets[2], E. Teinemaa[2], R. Richter[1], R. Wolf[1], J.G. Slowik[1], U. Baltensperger[1] and A.S.H. Prévôt[1]

[1]{Laboratory of Atmospheric Chemistry, Paul Scherrer Institute, 5232, Villigen PSI, Switzerland}

[2]{Estonian Environmental Research Centre, 10617, Tallinn, Estonia}

Correspondence to: I. El-Haddad (imad.el-haddad@psi.ch) and A. S. H. Prévôt (andre.prevot@psi.ch)

Abstract

Air pollution is one of the main environmental concerns in urban areas, where anthropogenic emissions strongly affect air quality. This work presents the first spatially-resolved detailed characterization of the $PM_{2.5}$ in two major Estonian cities, ~~(~~Tallinn and Tartu~~.), using mobile measurements.~~ The measurements were performed in march 2014 using a mobile platform. In both cities, the non-refractory (NR)-$PM_{2.5}$ was characterized by a high-resolution time-of-flight aerosol mass spectrometer (HR-ToF-AMS) using a recently developed lens which increases the transmission of super-micron particles. Equivalent black carbon (eBC) and several trace gases including carbon monoxide (CO), carbon dioxide (CO_2) and methane (CH_4) were also measured. The chemical composition of the $PM_{2.5}$ was found to be very similar in the two cities. Organic aerosol (OA) constituted the largest fraction, explaining on average about 52 to 60 % of the $PM_{2.5}$ mass. Four sources of OA were identified using positive matrix factorization (PMF): hydrocarbon-like OA (HOA, from traffic emissions), biomass burning OA (BBOA, from biomass combustion), residential influenced OA (RIOA, probably mostly from cooking processes with possible contributions from waste and coal burning) and oxygenated OA (OOA, related to secondary aerosol formation). OOA was the major OA source during night-time, explaining on average half of the OA mass, while during day-time mobile measurements the OA was affected by point sources and dominated by the primary fraction. A strong increase in the secondary organic and inorganic components was

observed during periods with transport of air masses from ~~–~~northern Germany~~polluted continental areas~~, while the primary local emissions accumulated during periods with temperature inversions. Mobile measurements offered the identification of different source regions within the urban areas and the assessment of the extent to which pollutants concentrations exceeded regional background levels ~~and an accurate calculation of the (~~urban increments). HOA, eBC, CO_2 and CO showed stronger enhancements on busy roads during the morning and evening traffic rush hours; BBOA had its maximum enhancement in the residential areas during the evening hours and RIOA was enhanced in both the city center (emissions from restaurants) and in the residential areas (emissions from residential cooking). In contrast, secondary components (OOA, SO_4, NO_3, NH_4, and Cl) had very homogeneous distributions in time and space. We were able to determine a total $PM_{2.5}$ urban increment in Tartu of 6.0 µg m^{-3} over a regional background concentration of 4.0 µg m^{-3} (i.e., a factor of 2.5 increase). Traffic exhaust emissions were identified as the most important source of this increase, with eBC and HOA explaining on average 53.3 and 20.5 % of the total increment, respectively.

1 Introduction

Atmospheric particulate matter (PM) plays a central role in many environmental processes through its influence on climate (radiative forcing; Myhre et al., 2013), the hydrological cycle (Ramanathan, et al., 2001) and its adverse effects on health (Pope and Dockery, 2006). ~~Recently, m~~Major attention has been devoted to the study of the $PM_{2.5}$ fraction (particulate matter with an aerodynamic equivalent diameter $d_{aero} \leq 2.5$ µm), which has been linked to increased lung cancer rates (Hu and Jiang, 2014), acute bronchitis and asthma (Gao et al., 2015), and mortality (Dockery et al 1993; Laden et al., 2006). Atmospheric particles can be classified as primary or secondary aerosols according to their formation processes. Primary particles are directly emitted, while secondary aerosols are formed from gas-phase precursors following chemical transformation in the atmosphere. Aerosols can be further classified in terms of their emission sources as natural sources (e.g. volcanic eruptions, wildfires, sea salt, dust or biogenic emissions from plants) or anthropogenic sources (mostly from combustion processes, e.g. traffic and residential wood combustion).

Due to enhanced contributions of anthropogenic sources, air quality is commonly lower in urban areas compared to rural or suburban locations (Putaud et al., 2004). In Europe, annual

average $PM_{2.5}$ mass concentrations in urban areas commonly vary between a few μg m^{-3} up to 35 μg m^{-3} (Putaud et al., 2010). The predominance of specific aerosol sources (e.g. residential, traffic, industry) or the implementation of new technologies (e.g. car fleet, heating systems, etc.) may strongly influence the levels and physicochemical characteristics of the pollutants in these locations. Moreover, certain orographic features and stagnant meteorological conditions may induce the accumulation of local pollutants (Putaud et al., 2004; Carbone et al., 2010; Squizzato et al. 2012). Likewise, long-range transport of continental air masses has been shown to influence the PM in different urban areas in Europe (Niemi et al., 2009; Baker, 2010; Salvador et al., 2013; Beekmann et al., 2015; Di Gilioa et al., 2015; Ulevicius et al., 2015). While the PM levels and physicochemical properties of the particles are well characterized in Western Europe, data are scarce in Eastern European cities, especially in the Baltic region, hindering air quality assessment and quantification of the main aerosol sources.

In contrast to conventional stationary measurements, mobile measurements (including zeppelin, aircraft and ground measurements) are suited for pollutant mapping, chasing of mobile sources or measurements in emission plumes, etc. Ground-based measurements by mobile platforms have been successfully performed in the last years to measure particles and trace gases from real-world traffic emissions (Pirjola et al., 2004, 2006 and 2012; Kwak et al., 2014; Kyung Hwan et al., 2015) and from wood burning emissions (Pirjola et al., 2015). More recently, aerosol mass spectrometers (AMS) have been deployed in mobile laboratories in order to determine the physical and chemical properties of submicron aerosols (PM_1, particulate matter with aerodynamic equivalent diameter $d_{aero} \leq 1$ μm) in urban environments like Zurich (Mohr et al., 2011), Paris (Von der Weiden-Reinmueller et al., 2014a and 2014b) or Barcelona (Mohr et al., 2015). Moreover, a newly developed inlet for the AMS has been used to measure the chemical composition of the non-refractory (NR)-$PM_{2.5}$ fraction in Bologna (Wolf et al., 2015).

In this work we present the first detailed in-situ mass spectrometric measurements of air pollutants in the two biggest cities in Estonia (Tallinn and Tartu). The measurements were performed using the Paul Scherrer Institute (PSI) mobile laboratory (Bukowiecki et al., 2002; Mohr et al., 2011; Wolf et al., 2015). The use of a high-resolution time-of-flight aerosol mass spectrometer (HR-ToF-AMS) with a novel $PM_{2.5}$ lens allowed for a detailed characterization of the NR-$PM_{2.5}$ fraction in the measurement areas. The spatial distributions of the sources of organic aerosols (OA), inorganic aerosols (nitrate (NO_3), sulfate (SO_4), ammonium (NH_4),

and chloride (Cl)), equivalent black carbon (eBC) and some of the major gas-phase components (carbon monoxide (CO), carbon dioxide (CO_2) and methane (CH_4)) were determined in the urban areas. Such analyses allowed for the calculation of regional background and urban concentrations of the different gas- and particle-phase components and provided direct insights into the spatial resolution of local emissions and their impact on the air quality in different city areas. Long-range transport of pollutants and accumulation events as well as their effect on the particle- and gas-phase mass concentrations will also be discussed.

2 Methodologies

2.1 Measurement campaign

The measurements were performed in the two biggest cities in Estonia. Tallinn, the capital and the largest city of Estonia, has a population of 413,000 inhabitants (Statistical Database, 2015) and occupies an area of 158.3 km^2. Located on the northern coast of the country, Tallinn has some of the biggest ports in the Baltic Sea. Among them, the old city harbor is one of the busiest passenger harbors in the region. Tartu, with an area of 38.8 km^2 and more than 97,000 inhabitants in 2015 (Statistical Database, 2015), is the second largest city in Estonia. The city is situated in the center of southern Estonia, in the post-glacial valley of the Emajõgi River, which influences the local meteorological conditions and favors the accumulation of local pollutants under frequent temperature inversions. Previous studies identified traffic emissions and residential heating as the major sources of air pollution in these two cities (Urb et al., 2005; Orru et al., 2011). An older vehicle fleet, the limited network capacity of the city streets (which generates congestions during rush hours) and the extensive use of studded tires, have been reported to strongly enhance the ~~effect~~ signal of ~~the~~ traffic emissions in the city center and major roads (Urb et al., 2005; Orru et al., 2011). Residential heating includes extensive use of inefficient wood and coal stoves with low stacks in both cities. In this regard, a detailed modeling study performed in Tallinn and Tartu (Orru et al., 2011) revealed that the city centers and the neighborhoods with local heating are exposed to much higher average $PM_{2.5}$ concentrations compared to other areas of the cities.

The measurements took place from 10 to 17 March 2014 in Tartu and from 25 March to 1 April 2014 in Tallinn. ~~The GPS trace of the driving routes in the two cities is shown in Fig. 1.~~ Emission maps including residential wood combustion and industrial sources and the traffic

emission rates in the major streets of the two cities are reported in Fig. S1.The driving routes ~~paths~~ were chosen in order to cover heavily trafficked roads, residential areas ~~where different heating systems are used (wood/coal burning, central heating or mixed)~~ and background sites with little local emissions. In Tallinn, streets close to the old town harbor were also included in the route. To obtain statistically significant spatial distributions of the major pollutants, 25 loops were performed at each location throughout the measurement periods at different times of the day. The average loop duration was about 72 minutes in Tartu and 112 minutes in Tallinn. Stationary measurements were typically performed overnight at a gasoline station in Tartu (influenced by city center and residential emissions) and at the Estonian Environmental Research Centre (EERC) in Tallinn (a background site). Meteorological data were recorded on~~in~~ a meteorological ~~-~~tower in Külitse (around 10 km south-east from Tartu) and in the Tartu and Tallinn-Zoo meteorological stations. The most relevant parameters (including wind direction and speed, temperature and precipitation) are reported in Fig. S2.

2.2 Mobile laboratory set-up

A schematic of the instrumental set-up in the PSI mobile platform is shown in Fig. ~~S1~~S3. The main inlet of the mobile platform was kept at a constant ~~flow~~ velocity of ~11 m sec^{-1} for isokinetic sampling during driving conditions, assuming an average velocity in the city of ~ 40 km h^{-1}. Two different inlet lines connected the main inlet to the aerosol and gas-phase instrumentation. The size cut-off of the inlet system was estimated to be around 5 µm. The deployed instruments, measured parameters and their time resolution are listed in Table 1. All parameters were determined with high time resolution (between 1 and 25 seconds), critical for the identification of source regions using a mobile platform.

An HR-ToF-AMS (Aerodyne Research Inc.) was deployed to measure the chemical composition of the NR-$PM_{2.5}$ aerosol, including NO_3, SO_4, NH_4, Cl, and OA. For this work, the AMS was equipped with a recently developed aerodynamic lens which extends the measured particle size to the $PM_{2.5}$ fraction (in contrast to the conventional PM_1 lens). The $PM_{2.5}$ lens efficiently transmits particles between 80 nm and up to at least 3 µm and has been well characterized by Williams et al. (2013) and tested in previous chamber and ambient studies (Wolf et al., 2015; Elser et al., 2015). The operating principle of the instrument can be found elsewhere (DeCarlo et al., 2006). A nafion drier (Perma Pure MD-110) was set before the AMS inlet in order to dry the ambient particles and reduce uncertainties in the bounce-

related collection efficiency (CE_b) and possible transmission losses of large particles at high relative humidity (RH).

A 7-wavelength Aethalometer (Magee Scientific, model AE33) was used to measure the aerosol light absorption and to determine the ~~equivalent black carbon (~~eBC~~)~~ concentrations. The measurement at 7 different wavelengths (370, 470, 520, 590, 660, 880 and 950 nm) covers the range between ultraviolet and infrared and allows for the source apportionment of different eBC fractions (Sandradewi et al., 2008; Zotter et al., in prep). Moreover, the dual spot measurement method automatically corrects ~~automatically~~ for the loading effect and provides a real-time calculation of the loading compensation parameter (Drinovec et al., 2015).

The concentrations of trace gases were measured by a Picarro-G2301 $CO/CO_2/CH_4$ analyzer and a Licor-6262 CO monitor.~~, including CO, CO_2 and CH_4 were measured by two different analyzers (Picarro-G2301 and Licor-6262)~~. In addition, some important parameters for mobile measurements (GPS, temperature, relative humidity and solar radiation) were also measured continuously.

2.3 AMS data analysis

AMS data were analyzed in Igor Pro 6.3 (WaveMetrics) using the standard ToF-AMS Data Analysis toolkit (SQUIRREL version 1.53G and PIKA version 1.12G). Based on standard NH_4NO_3 calibrations, the ionization efficiency (IE, defined as ions detected per molecules vaporized) was determined to be $5.08 \cdot 10^{-8}$ (average of five calibrations during the full measurement period). Standard relative ionization efficiencies (RIE) were used for nitrate, chloride, and organics (RIE = 1.1, 1.3, and 1.4, respectively) and experimentally determined for sulfate and ammonium (RIE = 1.11 and 4.29, respectively). A composition dependent collection efficiency (CE) algorithm by Middlebrook et al. (2012) was used in the calculation of ~~to calculate the~~ ambient mass concentrations (Middlebrook et al., 2012).

2.4 Source apportionment techniques

2.4.1 OA source apportionment

To identify and quantify the major sources of OA in the different measurement areas, positive matrix factorization (PMF; Paatero and Tapper (1994)) was applied to the ~~highly~~ time resolved AMS data (see Table 1). The analysis were performed using the multilinear engine

tool (ME-2; Paatero, 1997) implemented in the Source Finder interface (SoFi; Canonaco et al., 2013) coded in Igor Wavemetrics.

PMF is a bilinear unmixing algorithm which, as defined in Eq. (1), allows the representation of ~~representing~~ a two-dimensional matrix of measured data (**X**) as a linear combination of a given number of static factors profiles (**F**) and their corresponding time series (**G**). The matrix **E** in Eq. (1) contains the model residuals. The model uses a least squares approach to iteratively minimize the object function Q described in Eq. (2):

$$\mathbf{X} = \mathbf{GF} + \mathbf{E} \quad (1)$$

$$Q = \sum_{i=1}^{m} \sum_{j=1}^{n} \left(\frac{e_{ij}}{\sigma_{ij}}\right)^2 \quad (2)$$

where e_{ij} are the elements from the error matrix (E) and σ_{ij} are the respective uncertainties of **X**.

In our case, the model input are the ~~consists of a~~ data and error matrices~~x~~ of OA mass spectra, where the rows represent the time series (62665 points, with steps of 25 seconds) and the columns contain the fits to the ~~ions fitted in~~ high-~~-~~resolution data (292 ions). The organic mass obtained from the high resolution fits (up to *m/z* 115) agrees with the mass calculated from the unit mass resolution ~~fits~~ integration (up to *m/z* 737) within ± 5 %. The initial error values were calculated with the HR-AMS data analysis software PIKA. A minimum error corresponding to the measurement of a single ion was applied (Ulbrich et al., 2009). All variables with signal-to-noise ratio (SNR) lower than 0.2 were removed and the variables with SNR between 0.2 and 2 were down-weighted by increasing their error by a factor of 3 (Paatero and Hopke, 2003). Moreover, all variables directly calculated from the CO_2^+ fragment using ~~in~~ the organic fragmentation table (i.e. O^+, HO^+, H_2O^+ and CO^+) (Allan et al., 2004) were excluded from~~for~~ the PMF analysis to appropriately weight the variability of the CO_2^+ ~~;in the algorithm and~~ these ions were reinserted post-analysis.

The possibility of local minima in the solution space and the uncertainty of the PMF solution were investigated by means of bootstrap analysis. This statistical method is based on the creation of replicate datasets resulting from the perturbation of ~~perturbing~~ the original data by resampling. In each replicate, some randomly chosen rows of the original matrix are present several times, while other rows are removed~~do not occur at all~~ (Paatero et al., 2014), such that the dimension of the data matrix is kept constant. This resulted in about 64 % of the original points being used in each replicate. PMF was applied to 100 different replicates and the variations among these results were used to estimate the uncertainty of the initial PMF

solution. Note that ~~as~~ each bootstrap run is started from a different initialization point; ~~and hence~~thus, this methodology inherently includes the investigation of the classic seed variability. All convergent solutions were found to be consistent, suggesting that the solution is robust.~~an indication of the robustness of the chosen solution.~~

The results presented in this section were obtained by merging the measurements from the two measurement locations, as no major changes were observed if the source apportionment was performed for the individual cities.

2.4.2 eBC source apportionment

The Aethalometer measurements can be used to separate eBC from wood burning (eBC_{wb}) and from traffic (eBC_{tr}), by taking advantage of the spectral dependence of absorption, as described by the Ångström exponent (Ångström, 1929). Specifically, the enhanced absorption of wood burning particles in the ultraviolet and visible wavelengths region (370–520 nm) relative to that of traffic particles is used to separate the contributions of the two fractions. This method is described in detail in Sandradewi et al. (2008) and has been successfully applied at many locations across Europe (Favez et al., 2010; Herich et al., 2011; Sciare et al., 2011; Crilley et al., 2015). For a proper separation of the eBC fractions, the Aethalometer data was averaged to 30 minutes in order to increase the signal to noise. Thus, the obtained fractions eBC_{wb} and eBC_{tr} could only be used for the correlations with the external tracers, but their spatial distributions couldn't be explored. The absorption Ångström exponent was calculated using the absorption measured at 470 and 950 nm and Ångström exponents of 0.9 and 1.7 were used for traffic and wood burning, respectively.~~,~~ These parameters were chosen following the suggestions in Zotter et al. (In prep.),~~,~~ where the comparison between radiocarbon (^{14}C) measurements of elemental carbon (EC) and the Aethalometer source apportionment results allowed the identification of the best wavelengths and Ångström exponents pairs.

3 Results and discussion

3.1 Pollutant concentrations and temporal variability

The temporal variation of all measured gas- and particle-phase components is shown in Fig. 12~~a~~. The type of measurement is indicated by different background colors (transparent for stationary measurements and orange for mobile measurements). The measurement period

included three distinct meteorological periods of transport of polluted air masses and accumulation of local emissions. These periods are referred to as special events (indicated by a red frame) and will be treated separately and discussed in detail in Section 3.4. While the AMS and Aethalometer were running almost continuously during the entire measurement period, there is a small gap in the CO_2, CO and CH_4 data due to an instrument malfunction. Over the full measurement period, the average mass concentration of $PM_{2.5}$ (NR-$PM_{2.5}$ plus eBC) was 12.3 µg m^{-3}. In the gas-phase, average concentrations of 414.1 ppm of CO_2, 0.24 ppm of CO and 1.92 ppm of CH_4 were measured. In contrast to these relatively low average values, extremely high concentrations were often recorded during the mobile measurements due to local emissions from point sources (around 50 spikes with $PM_{2.5}$ mass concentration exceeding 100 µg m^{-3}). Such intermittent pollution plumes (expected in some areas in a city) cannot be detected from stationary measurements at an urban background site, but ~~enhance~~ may be associated with negative health impacts. As shown in Fig. 1~~2~~b, neglecting the periods defined as special events, the $PM_{2.5}$ average concentrations and relative contributions of the particle phase species were very similar at the two locations. If we compare day-time (07:00 to 19:00, local time (LT)) and night-time (19:00 to 07:00, LT) measurements, in both cities the average $PM_{2.5}$ was higher during the day (11.0 µg m^{-3} in Tartu and 11.6 µg m^{-3} in Tallinn) than during the night (6.5 µg m^{-3} in Tartu and 7.1 µg m^{-3} in Tallinn), despite the development of the boundary layer and increased dilution during day-time. OA constituted in all cases the largest mass fraction, explaining on average 52.2 and 54.3 % of the $PM_{2.5}$ mass in Tartu (during night- and day-time, respectively) and 55.2 and 60.1 % in Tallinn (during day- and night-time, respectively). Primary emissions of eBC contributed on average 20.4 % and 33.7 % in Tartu (during night-time and day-time, respectively), and 13.4 and 26.9 % in Tallinn (during night-time and day-time, respectively), constituting a substantially higher fraction than at other European locations (Putaud et al., 2010). The remaining mass, 12 to 28 %, was related to secondary inorganic species, mostly ammonium sulfate and nitrate. These species were found to be neutralized within the uncertainties (ratio of NH_4 expected from an ion balance to NH_4 measured of 1.05, with R^2=0.95). During night-time a decrease in the relative contribution of eBC was observed in favor of an enhanced contribution of the inorganic species.

3.2 Sources of OA

To properly represent the temporal variations of the OA, four factors were required: hydrocarbon-like OA (HOA), biomass burning OA (BBOA), residential influenced OA (RIOA) and oxygenated OA (OOA). The mass spectra of these factors are reported in Fig. 2~~3~~. HOA is a primary source related to traffic emissions and its mass spectrum is characterized by the presence of alkyl fragment signatures (Ng et al., 2011), with prominent contributions of non-oxygenated species at *m/z* 43 ($C_3H_7^+$), *m/z* 55 ($C_4H_7^+$) and *m/z* 57 ($C_4H_9^+$). As shown in Fig. ~~S2~~S4, a fairly good correlation is found between HOA and eBC_{tr} (R^2 = 0.4). Moreover, the ratio of HOA to eBC_{tr} was 0.5, which is in good agreement with previous European studies (El Haddad et al., 2013 and references therein). BBOA is associated with domestic heating and/or agricultural biomass burning activities, and shows characteristic high contributions of the oxygenated hydrocarbons at *m/z* 60 ($C_2H_4O_2^+$) and *m/z* 73 ($C_3H_5O_2^+$), which are known fragments from anhydrous sugars (Alfarra et al., 2007). BBOA correlates fairly well with eBC_{wb} (R^2 = 0.4), and the ratio of BBOA to eBC_{wb} was 4.0 (Fig. ~~S2~~S4), which within the method uncertainties is consistent with previously reported values (Crippa et al., 2013a). The ratio BBOA to eBC_{wb} was found to be very sensitive to the chosen Ångström exponent for traffic, and it increased to 4.8 if a slightly higher Ångström exponent (i.e. 1.0 instead of 0.9) was considered for traffic. RIOA is a hydrocarbon-rich factor that was required for a reasonable explanation of the variability in the data. Due to its increase in the residential areas, this factor was associated with residential emissions. Given its strong correlation (R^2 = 0.9) with cooking markers such as the fragment ion $C_6H_{10}O^+$ at *m/z* 98 (Sun et al., 2011; Crippa et al., 2013b), we expect that a great part of this factor is related to cooking emissions (see Fig. ~~S2~~S4). Moreover, as in previously reported cooking spectra (Mohr et al., 2012), the RIOA mass spectrum shows a higher *m/z* 55 to *m/z* 57 ratio than HOA. However, in the absence of diurnal trends due to the driving conditions, the separation of cooking emissions from other residential emissions (such as domestic coal and waste burning) was not possible. OOA is associated with aged emissions and secondary organic aerosol formation, and its profile is characterized by a very high *m/z* 44 (CO_2^+). In general, OOA increases simultaneously with the secondary species (especially NO_3), but the ratio among these components changes during special events (Fig. ~~S2~~S4).

Some important diagnostic parameters of the source apportionment (including Q/Q_{exp}, factor-marker correlation, and time-series and profiles residuals for solutions with different number of factors) are reported in Fig. S5. The correlation coefficients (R^2) between factors and

markers significantly increase when a fourth factor is included, but are not improved when a fifth factor is added. The addition of the fourth factor, which enabled the extraction of RIOA, allows explaining additional structures in the residuals' time series and unsaturated fragments in the residuals mass spectrum. Including a fifth factor also improves the model mathematical quality, by additionally explaining $C_xH_yN_w$ and biomass burning (at *m/z* 60 and 73) related fragments. The additionally extracted factor in the five-factor solution, referred to as 'unknown', has elevated contributions from oxygenated fragments often related to SOA (*m/z* 44) and BBOA (*m/z* 60 and 73), but a time series that unambiguously relates this factor to a spatially variable primary emission source. In effect, the majority (62%) of this factor contribution arises from a split in the BBOA factor from the four-factor solution (the rest comes from the residuals and the OOA). Moreover, the sum of the contributions of the 'unknown' factor and the BBOA from the five-factor solution matches the BBOA contributions from the four-factor solution (R^2 = 0.97 and slope = 1.15 as shown in Fig. S6). This split in the BBOA is very likely a direct consequence of the variable nature of this combustion source, but the two BBOA-like factors extracted in the five-factor solution could not be related to different emission processes. Furthermore, the addition of this factor did not affect the spectral profiles and time series of the other factors and their correlations with their respective markers and did not aid the interpretation of the data. Therefore, we considered the four-factor solution as an optimal representation of our data. Table 2 contains the correlation coefficients (R^2) between the OA profiles from the four-factor solution and available literature profiles (Aiken et al., 2009; Mohr et al., 2012; Setyan et al., 2012; Crippa et al., 2013b). The high correlations obtained in all cases support the use of a four-factor solution and strengthen the link between the RIOA and cooking emissions (R^2 of about 0.8 between RIOA and cooking tracer). ~~If the number of factors is decreased, the RIOA factor is not resolved and the OOA time-series becomes contaminated by local spikes, which is unexpected for a regional component (see Fig. S3 and S4). In contrast, if a five-factor solution is considered an additional highly oxygenated factor is obtained ("unknown" factor in Fig. S3 and S4). The mass spectrum of this additional factor resembles a low-volatility OOA (LV-OOA), as resolved in many previous works (Jimenez et al., 2009), but its time series exhibits the typical characteristics of the primary factors, i.e. strong increases in emission areas. Therefore, this further increase in the number of factors doesn't seem to improve the interpretation of the data, as the new factor cannot be explicitly associated to distinct sources or processes. Accordingly, a four-factor solution was considered as optimal and is utilized below.~~

Figure 3~~4~~a represents the time series of the absolute mass (top panel) and relative contributions (bottom panel) of the retrieved OA sources for the two measurement locations. The variability of these time series over 100 bootstrap runs was relatively low, as shown in Fig. ~~S5~~S9. In both cities, the three primary sources (HOA, BBOA and RIOA) exhibit a very spiky temporal behavior, while the secondary source (OOA) is characterized by a relatively smooth time series. Figure 3~~4~~b reports the averaged total OA mass and relative contributions of the OA sources during the measurements in Tartu (top panel) and Tallinn (bottom panel). The reported errors (which correspond to the standard deviation among 100 bootstrap runs) are an indication of the high stability of the solution. Overall, the relative errors vary between 3 % and 7 %, except for the RIOA, which shows slightly higher variability during night-time (relative error of 11 % in Tartu and 13 % in Tallinn). Similarly to the total $PM_{2.5}$ mass and as reported in Fig. 3~~4~~b, neglecting the special events, a strong daily cycle can be observed in the total OA mass, with higher concentrations during day-time (6.0 µg m^{-3} and 6.3 µg m^{-3} in Tartu and Tallinn, respectively) than during night-time (3.4 µg m^{-3} and 4.2 µg m^{-3} in Tartu and Tallinn, respectively). This difference is mostly driven by the increase of primary aerosol emissions (HOA, BBOA and RIOA) during the day. This structure is observed independently of the nature of the measurements (stationary or mobile), indicating that except for the periods where emissions from point sources are sampled, the OA concentrations and sources are rather homogeneous across the sampling area. In terms of relative contribution, OOA is dominant during night-time, explaining on average between 42 and 44 % of the OA mass in Tartu and Tallinn, respectively. ~~HOA and RIOA relative contributions to the total OA are higher during day-time (the relative contribution of HOA increases from about 20 to 32% in Tartu and from 11 to 27% in Tallinn; the relative contribution of RIOA increases from 20 to 27 % in Tartu and from 20 to 22 % in Tallinn).~~ The relative contribution of HOA to total OA mass is higher during day-time (32% in Tartu and 27% in Tallinn) than during night-time (20% in Tartu and 11% in Tallinn). RIOA is also enhanced during day-time in Tartu (27% compared to 20% during night-time), and has similar relative contributions for day- and night-time in Tallinn (20 and 22%, respectively). In contrast, BBOA shows similar relative contributions for day- and night-time in Tartu (~~explaining~~ representing about 17 % of the OA mass), and slightly lower contributions during ~~the~~ day-time in Tallinn (20 % during day-time and 25 % at night-time).

3.3 Spatial distributions, regional background and urban increments

The average spatial distributions of the four OA sources, SO_4, NO_3, eBC, CO_2 and CO are represented in Fig. 45 and 56 for Tartu and Tallinn, respectively. The spatial distributions of the additionally measured gas and particle components are reported in Fig. S6 S10 and S7S11. All loops for which all the instruments were running (except CO_2, CO and CH_4 in Tallinn) were averaged on a grid with grid cells of 250 m^2. In order to get comparable distributions from different days of measurements, the 5th percentile (P05) of was subtracted from each single loop for all components. The subtraction of P05 was found to be optimal to decrease the variability among different loops enough to make them comparable. However, as it will be discussed in the following, P05 was not always sufficient to capture the regional background concentrations. The color scales in Fig. 45 and 56 represent the averaged enhancement over the background concentrations of each source/species. For a better visualization, the maximum of the color scale was set at the 75th percentile (P75) for SO_4, NO_3, eBC, CO_2 and CO. Moreover, the highest 75th percentile among all OA sources (i.e., 1.2 μg m^{-3} in Tartu and 2.4 μg m^{-3} in Tallinn) was used as a maximum for the four OA sources, in order to facilitate the comparison among them. Lastly, the sizes of the points represent the number of measurement points that were averaged in each case. The correlation coefficients (R^2) between the spatial distributions of all sources and components are reported in Table S1.

Longitude profiles of the enhancements of all considered components were obtained for Tartu by averaging the calculated enhancements in longitude bins (using the same grid of 250 m^2 as above). These results are shown in Fig. 67 (averages and standard deviation among all loops), Fig. S8 S12 (median and first and third quartiles) and Fig. S9 S13 (separation of all loops into time-bins of two hours). The longitude profiles in Fig. 67 and Fig. S8 S12 allowed for the calculation of regional background concentrations and urban increments, as defined by Lenschow et al. (2001) and reported in Table 23. The urban concentrations, which are given by the sum of the regional background and the urban increment, represent a mix between urban background and curbsidekerbside locations. While the averaged profiles take into account the effects of the measured point sources in the urban area (mostly traffic and residential emissions), the use of the median profiles is expected to represent more selectively exclude these effects, making the results more representative of the urban background concentrations. We note that the influence of curbside increments may not be completely removed when using median increments (e.g. accumulation of traffic emissions due to street canyon effects), and therefore these increments might be biased high and should be regarded

as our highest estimates of urban background concentrations. In the following we will present the results related to the average profiles, followed by the results from the median profiles reported in parenthesis. In all cases, the longitude profiles were fitted using sigmoid functions (black curves). In order to have a constant averaging city area, the fitting limits (indicated with blue and pink arrows) and the x-value of the sigmoid's midpoint (X_0) were determined from the fit of the total $PM_{2.5}$ mass (NR-$PM_{2.5}$ plus eBC) and imposed to all other components. In most ~~of the~~ cases the base of the sigmoid function~~s~~ is slightly above zero. This indicates that the ~~P05 previously~~ subtracted P05 didn't represent the full regional background, which is therefore given by the sum of the average P05 and the base of the sigmoid function. Note that the initial subtraction of P05 would not be necessary if the longitudinal profile of each single loop could be fitted. However, this is not possible due to the high concentration variability within each single loop. A sensitivity analysis was performed by using P10 instead of P05 and no major changes were observed in the final results. As shown by the wind rose in Fig. 4b, during the drives in Tartu the wind was predominantly from the west. However, the background concentrations measured at the east side of the loop don't seem to be affected by the transport of pollutants from the urban area, as the base values obtained for the east side are equal or lower than those from the west side (see Table 3). ~~Moreover, the fits on the west side of Tartu show always higher base values than those for the east, indicating the influence of local sources in the considered regional background area west of Tartu. However,~~ As the~~se~~ differences between the west and east fits are in most cases rather low, ~~and therefore~~ we use the west-east averages of the base values to calculate the urban increments concentrations in Table ~~2~~3.

In Tartu, the three primary OA sources (HOA, BBOA and RIOA) show a clear enhancement in the city center compared to the suburban areas (Fig. 6~~7~~ and S~~8~~12). Moreover, different source regions (see Fig. 4c-f~~5a-e~~) and emission times (see Fig. ~~S9~~S13) can be distinguished inside the urban area. For example, maximum HOA concentrations are observed on highly congested roads, especially at sites under stop-and-go conditions, and show a maximum enhancement in the morning and evening traffic rush hours (07:00 to 09:00 and 15:00 to 17:00, LT). The spatial distributions of the eBC, CO_2 and CO (Fig. 4i-k~~5g-i~~) are consistent with that of HOA (R^2 of 0.61, 0.59 and 0.58, respectively), which indicates that these species originate mostly from traffic. BBOA is ~~more~~ strongly enhanced in the residential areas, consistent with the distribution of residential wood combustion sources shown in Fig. S1. ~~and t~~The maximum BBOA enhancement is seen in the evening hours (15:00 to 21:00, LT) when

domestic heating is more active. RIOA shows enhanced contributions in both, the residential areas (probably related to domestic cooking emissions) and the major roads in the city center (probably related to cooking emissions from restaurants). The maximum enhancement of RIOA is also seen in the evening hours (15:00 to 19:00, LT), during and after the evening maximum of HOA. In contrast, OOA (Fig. 4f~~5d~~) and the other secondary species (SO_4, NO_3, NH_4 and Cl, see Fig. 4g-h~~5e-f~~ and Fig. ~~S6~~S10), show very homogeneous spatial distribution over the whole measurement area (as expected from their secondary nature), and no clear dependence on the time of the day can be seen for the OOA (Fig. ~~S8~~S13). Although slight enhancements are observed in these components close to residential areas (OOA enhancement of 0.8 µg m^{-3}), these increases are negligible within the measurement and source apportionment uncertainties.

As reported in Table ~~2~~3, the $PM_{2.5}$ mass concentration in Tartu shows an urban increment of 6.0 (4.6) µg m^{-3} over a regional background concentration of 4.0 (3.5) µg m^{-3}. This leads to urban $PM_{2.5}$ mass concentrations of up to 10 (8.1) µg m^{-3}, which represents an increase of a factor 2.5 (2.3) in the particle mass concentration in the urban area compared to the regional background. About half of this enhancement is related to the emissions of eBC, which shows an increase of 3.2 (2.3) µg m^{-3} over a regional background of 1.1 (0.58) µg m^{-3}. Thus, the urban concentration of eBC is 4.2 (2.9) µg m^{-3},~~-~~ which represents an enhancement of a factor 3.9 (5.0) of eBC in the urban area. The primary OA sources explain great part of the remaining increase in the $PM_{2.5}$ mass: HOA is increased by a factor 3.6 (3.0) in the urban area and has contribution of 1.7 (1.0) µg m^{-3} to the urban concentration; RIOA is enhanced by a factor 2.0 (2.3), contributing with 1.7 (1.0) µg m^{-3} to the urban concentration; and BBOA is enhanced by a factor 3.1 (2.4) and contributes with 1.0 (0.52) µg m^{-3} to the urban concentrations. On the other hand, OOA and the inorganic species (SO_4, NO_3, NH_4 and Cl) show very low increases in the urban area, resulting in a total urban increment below 0.21 µg m^{-3} (average and median). In the gas-phase, CO_2 shows an increase of 8.3 (5.3) ppm over a regional background of 403.5 ppm (both average and median); CO is increased by 0.15 (0.11) ppm over a regional background of 0.16 (0.14) ppm, which represents an increase of a factor 1.9 (1.7); while CH_4 shows very similar concentrations inside and outside the city, with average (and median) regional background of 1.90 ppm and urban concentrations of 1.91 ppm.

Similar results were obtained for Tallinn (see Fig. 5~~6~~ and Fig. ~~S7~~S11). However, given the larger extension of this city, it wasn't possible to include a real regional background site in

the route. Therefore, the longitude profiles and urban increments couldn't be properly explored for Tallinn. However, different source regions can still be distinguished within the examined area. Thus, the spatial distribution of HOA (Fig. 5c~~6a~~) is in agreement with those of eBC, CO_2 and CO (Fig. 5i-k~~6g-i~~) and shows substantial increases in areas with high traffic and on major streets in the city center with significant stop-and-go conditions. BBOA (Fig. 5d~~6b~~) has higher contributions in the ~~two~~ residential areas, especially in region 2 of the driving route, where there is a very high density of residential wood combustion sources (see Fig. S1). ~~while c~~Compared to Tartu, in Tallinn the spatial distribution of RIOA (Fig. 5e~~6c~~) is more homogeneous, with only slight enhancements in the residential area and in the city center. Finally, OOA (Fig. 5f~~6d~~) exhibits a small enhancement in the city center area, which again coincides with small increases in the secondary inorganic species concentrations (see Fig. 5g-h~~6e-f~~ and Fig. ~~S7~~S11) that are insignificant within the measurement and source apportionment uncertainties. Enhanced SO_4 levels are also found in the northern part of the route, likely from local ship emissions (Lack et al., 2009). Winds from west and east were observed during the mobile measurements in Tallinn (Fig. 5b). In order to identify possible processes influencing the spatial distributions of the measured pollutants for the two different wind patterns, the average spatial distributions were calculated for al loops with west wind (7 loops) and loops with east wind (16 loops, excluding drives during accumulation events). The results of these analyses are reported in the supplementary information (Fig. S14 and S15) and show that, in general, the wind direction didn't have an effect on the identified source areas and similar enhancements were found for both types of winds. A detailed analysis of these spatial distributions shows that BBOA, SO_4 and NO_3 are stronger enhanced during west winds, while HOA is more enhanced for east wind conditions. This difference is most probably related to the presence of west winds during the weekend (enhanced residential emissions) and east winds during the week-day measurements (enhanced traffic emissions).

3.4 Special events: transport and accumulation of pollutants

Enhanced concentrations of secondary species including OOA, SO_4, NO_3 and NH_4 were measured during the first measurement day in Tartu (see Fig. 1~~2~~a and Fig. 3~~4~~a). The analysis of the 24-hour back-trajectories reported in Fig. 7~~8~~a indicates that these mostly secondary components were probably transported from continental Europe, in particular from northern Germany. The later decrease in the concentrations of these species coincides with clean air masses originating from the Northern Atlantic at higher altitudes above ground level. As

reported in Fig. 7~~8~~b, during this transport event the average $PM_{2.5}$ mass concentration increased to 28.3 µg m^{-3} (compared to average concentrations of 11.0 µg m^{-3} measured during day-time and 6.5 µg m^{-3} during night-time). This increase in mass is mostly related to the increased concentrations of the secondary components, especially of NO_3 and OOA. Accordingly, the relative contributions of the inorganic species to the total NR-$PM_{2.5}$ increased to over 44 % during the transport event (compared to 12 % for day-time and around 28 % for night-time averages) and the relative contribution of the OOA to total OA increased to 56 % (compared to 25 % for day-time and 42 % for night-time averages). It is worth to note that source separation is more uncertain during the transport event due to lower statistics and increased mixing (if the transported air contains multiple sources). This is especially the case for RIOA, which has a relative error of 41 % (estimated by the bootstrapping procedure) during the transport event.

During the nights of 28 and 29 March, very high concentrations of organics (exceeding 200 µg m^{-3}), eBC (above 15 µg m^{-3}) and CO_2 (up to 500 ppm) were measured in Tallinn, as shown in Fig. 8~~9~~a. Relatively short back-trajectories originating from the Baltic Sea (North-West and West from the sampling site) and at high altitudes were obtained for these periods (not reported). Moreover, as shown in Fig. 8~~9~~a, during such accumulation events wind speed was close to zero and a strong near-ground temperature inversion (i.e. a positive temperature difference between the ground and 22 m above ground level (AGL)) was observed. Under such conditions, the vertical mixing is suppressed and the local pollutants are trapped at the surface. As reported in Fig. 8~~9~~b, during the accumulation periods the average $PM_{2.5}$ mass increased up to 41.7 µg m^{-3}, with OA explaining 73 % of the total mass. This increase was mostly related to the increase of the primary aerosols, mainly HOA and BBOA, which explained 33 and 37 % of the OA mass, respectively.

4 Conclusions

Mobile measurements allowed for the study of the spatial distributions of major gas- and particle-phase pollutants in two urban areas in Estonia, permitting the identification of particular source areas and the determination of regional background concentrations and urban increments for the individual components/sources. A comprehensive set of instruments including a HR-ToF-AMS (with a newly developed inlet to measure the NR-$PM_{2.5}$ fraction), a 7-wavelength Aethalometer and several gas-phase monitors were deployed in the mobile

laboratory to retrieve a detailed chemical characterization of the $PM_{2.5}$ fraction and the concentrations of several trace gases with high time resolution.

The measurements were performed in March ~~2013~~ 2014 in the two major cities of Estonia (Tallinn and Tartu) and no major differences were found in the chemical composition at the two sites. Higher mass concentrations were always measured during day-time, when point sources were sampled during mobile measurements. Under regular meteorological conditions, OA represented the largest mass fraction (on average 52.2 % to 60.1 % of $PM_{2.5}$), while the relative contribution of the inorganic species (mostly SO_4, NO_3 and NH_4) strongly increased during the transport of polluted air masses from northern Germany. Four sources of OA were identified by means of PMF: three primary sources (HOA, BBOA and RIOA) and a secondary OA (OOA). Although the RIOA is thought to be dominated by cooking emissions, contributions from other residential emissions to this factor cannot be excluded. For example, waste burning is known to be a common process in some cities in Estonia (Maasikmets et al., 2015). However, to properly separate the contribution of waste burning from other co-emitting sources, laboratory studies of direct emissions need to be performed in the future. While OOA dominated the OA mass during night-time (on average 42.3 % in Tartu and 43.8 % in Tallinn), the primary sources explained the major fraction of OA during day-time (75.2 % in Tartu and 68.3 % in Tallinn, with similar contributions from the three sources). During the period with transport of polluted air masses aforementioned, the OOA relative contribution was enhanced. In contrast, HOA, RIOA and BBOA were strongly enhanced during periods characterized by temperature inversions, which induced the accumulation of locally emitted primary pollutants (primary OA and eBC).

Different source regions were identified inside the two urban areas. All traffic related pollutants (including HOA, eBC, CO_2 and CO) where strongly enhanced on the major city roads, especially in areas with stop-and-go conditions during the morning and evening rush hours. BBOA showed a clear increase in the residential areas during the evening hours (due to domestic heating), while RIOA (believed to be strongly influenced by cooking emissions) was enhanced in both, the city center (from restaurant cooking emissions) and in the residential areas (from domestic cooking). In contrast, the secondary components (including OOA, SO_4, NO_3, NH_4 and Cl) had very homogeneous spatial distributions, with no clear enhancement in the urban areas (within the measurement uncertainties) or at certain times of the day. For Tartu, regional background concentrations and urban increments of all measured components/sources were also determined. On average, the $PM_{2.5}$ mass had an enhancement

inside the city of 6.0 μg m^{-3} over the regional background concentration of 4.0 μg m^{-3}. This urban increment was strongly related to the enhancement of eBC (3.2 μg m^{-3}) and the primary OA sources (on average 1.2 μg m^{-3} from HOA, 0.67 μg m^{-3} from BBOA and 0.72 μg m^{-3} from RIOA), while the secondary components (OOA, SO_4, NO_3, NH_4 and Cl) didn't contribute to a substantial enhancement. Moreover, the good correlation found between eBC with HOA indicates that up to 74 % of the enhancement in the $PM_{2.5}$ is related to traffic emissions in the urban area. CO_2 and CO, which were also found to be strongly correlated with HOA, had an average urban increment of 8.3 and 0.15 ppm over regional background concentrations of 403.5 and 0.15 ppm, respectively.

Our results show that mobile measurements are a very powerful technique for spatial characterization of the major pollutants in urban areas. The methodology presented in this work can be generalized to other cities, in order to determine the influence of human activity on the particle sources and levels in different areas of a city and the related health effects.

Acknowledgments

This work was carried out in the framework of the public procurement "Determination of Chemical Composition of Atmospheric Gases and Aerosols in Estonia" of the Estonian Environmental Research Centre (Reference number: 146623), funded by the Estonian-Swiss cooperation program "Enforcement of the surveillance network of the Estonian air quality: Determination of origin of fine particles in Estonia". JGS acknowledges the support of the Swiss National Science Foundation (Starting Grant No. BSSGI0 155846). IEH acknowledges the support of the Swiss National Science Foundation (IZERZ0 142146). The authors gratefully acknowledge the NOAA Air Resources Laboratory (ARL) for the provision of the HYSPLIT transport and dispersion model and READY website (http://www.ready.noaa.gov) used in this publication.

References

Aiken, A. C., Salcedo, D., Cubison, M. J., Huffman, J. A., DeCarlo, P. F., Ulbrich, I. M., Docherty, K. S., Sueper, D., Kimmel, J. R., Worsnop, D. R., Trimborn, A., Northway, M., Stone, E. A., Schauer, J. J., Volkamer, R. M., Fortner, E., de Foy, B., Wang, J., Laskin, A., Shutthanandan, V., Zheng, J., Zhang, R., Gaffney, J., Marley, N. A., Paredes-Miranda, G., Arnott, W. P., Molina, L. T., Sosa, G., and Jimenez, J. L.: Mexico City aerosol analysis during MILAGRO using high resolution aerosol mass spectrometry at the urban supersite (T0) – Part 1: Fine particle composition and organic source apportionment, Atmos. Chem. Phys., 9, 6633–6653, 2009.

Alfarra, M. R., Prévôt, A. S. H., Szidat, S., Sandradewi, J., Weimer, S., Lanz, V. A., Schreiber, D., Mohr, M., and Baltensperger, U.: Identification of the mass spectral signature of organic aerosols from wood burning emissions, Environ. Sci. Technol., 41, 5770–5777, 2007.

Allan, J. D., Delia, A. E., Coe, H., Bower, K. N., Alfarra, M. R., Jimenez, J. L., Middlebrook, A. M., Drewnick, F., Onasch, T. B., Canagaratna, M. R., Jayne, J. T., and Worsnopf, D. R.: A generalized method for the extraction of chemically resolved mass spectra from Aerodyne aerosol mass spectrometer data, J. Aerosol Sci., 35, 909–922, 2004.

Ångström, A.: On the atmospheric transmission of sun radiation and on dust in the air, Geogr. Ann., 11, 156–166, 1929.

Baker, J.: A cluster analysis of long range air transport pathways and associated pollutant concentrations within the UK, Atmos. Environ., 44, 563–571, 2010.

Beekmann, M., Prévôt, A. S. H., Drewnick, F., Sciare, J., Pandis, S. N., Denier van der Gon, H. A. C., Crippa, M., Freutel, F., Poulain, L., Ghersi, V., Rodriguez, E., Beirle, S., Zotter, P., von der Weiden-Reinmüller, S.-L., Bressi, M., Fountoukis, C., Petetin, H., Szidat, S., Schn, J., Borbon, A, Gros, V., Marchand, N., Jaffrezo, J. L., Schwarzenboeck, A., Colomb, A., Wiedensohler, A., Borrmann, S., Lawrence, M., Baklanov, A., and Baltensperger, U.: In-situ, satellite measurement and model evidence for a dominant regional contribution to fine particulate matter levels in the Paris Megacity, Atmos. Chem. Phys., 15, 9577–9591, 2015.

Bukowiecki, N., Dommen, J., Prévôt, A. S. H., Richter, R., Weingartner, E., and Baltensperger, U.: A mobile pollutant measurement laboratory: measuring gas phase and aerosol ambient concentrations with high spatial and temporal resolution, Atmos. Environ., 36, 5569–5579, 2002.

Canonaco, F., Crippa, M., Slowik, J. G., Baltensperger, U., and Prévôt, A. S. H.: SoFi, an IGOR-based interface for the efficient use of the generalized multilinear engine (ME-2) for the source apportionment: ME-2 application to aerosol mass spectrometer data, Atmos. Meas. Tech., 6, 3649–3661, 2013.

Carbone, C., Decesari, S., Mircea, M., Giulianelli, L., Finessi, E., Rinaldi, M., Fuzzi, S., Marinoni, A., Duchi, R., Perrino, C., Sargolini, T., Vardè, M., Sprovieri, F., Gobbi, G. P., Angelini, F., and Facchini, M. C.: Size-resolved aerosol chemical composition over the Italian Peninsula during typical summer and winter conditions, Atmos. Environ., 44, 5269–5278, 2010.

Crilley, L. R., Bloss, W. J., Yin, J., Beddows, D. C. S., Harrison, R. M., Allan, J. D., Young, D. E., Flynn, M., Williams, P., Zotter, P., Prevot, A. S. H., Heal, M. R., Barlow, J. F., Halios, C. H., Lee, J. D., Szidat, S., and Mohr, C.: Sources and contributions of wood smoke during winter in London: assessing local and regional influences, Atmos. Chem. Phys., 15, 3149–3171, 2015.

Crippa, M., DeCarlo, P. F., Slowik, J. G., Mohr, C., Heringa, M. F., Chirico, R., Poulain, L., Freutel, F., Sciare, J., Cozic, J., Di Marco, C. F., Elsasser, M., Nicolas, J. B., Marchand, N., Abidi, E., Wiedensohler, A., Drewnick, F., Schneider, J., Borrmann, S., Nemitz, E., Zimmermann, R., Jaffrezo, J.-L., Prévôt, A. S. H., and Baltensperger, U.: Wintertime aerosol chemical composition and source apportionment of the organic fraction in the metropolitan area of Paris, Atmos. Chem. Phys., 13, 961–981, 2013a.

Crippa, M., El Haddad, I., Slowik, J. G., DeCarlo, P. F., Mohr, C., Heringa, M. F., Chirico, R., Marchand, N., Sciare, J., Baltensperger, U., and Prévôt A. S. H.: Identification of marine and continental aerosol sources in Paris using high resolution aerosol mass spectrometry, J. Geophys. Res., 118, 1950–1963, 2013b.

DeCarlo, P. F., Kimmel, J. R., Trimborn, A., Northway, M. J., Jayne, J. T., Aiken, A. C., Gonin, M., Fuhrer, K., Horvath, T., Docherty, K. S., Worsnop, D. R., and Jimenez, J. L.: Field-deployable, high-resolution, time-of-flight aerosol mass spectrometer, Anal. Chem., 78, 8281–8289, 2006.

Di Gilioa, A., de Gennaroa, G., Dambruosoa, P., and Ventrellaa, G.: An integrated approach using high time-resolved tools to study the origin of aerosols, Sci. Total Environ., 530–531, 28–37, 2015.

Dockery, D. W., Pope, C. A., Xu, X., Spengler, J. D., Ware, J. H., Fay, M. E., Ferris, B. G. Jr, and Speizer, F. E.: An association between air pollution and mortality in six U.S. cities, N. Engl. J. Med., 329, 1753–1759, 1993.

Drinovec, L., Močnik, G., Zotter, P., Prévôt, A. S. H., Ruckstuhl, C., Coz, E., Rupakheti, M., Sciare, J., Müller, T., Wiedensohler, A., and Hansen, A. D. A.: The "dual-spot" Aethalometer: an improved measurement of aerosol black carbon with real-time loading compensation, Atmos. Meas. Tech., 8, 43–55, 2015.

El Haddad, I., D'Anna, B., Temime-Roussel, B., Nicolas, M., Boreave, A., Favez, O., Voisin, D., Sciare, J., George, C., Jaffrezo, J.-L., Wortham, H., and Marchand, N.: Towards a better understanding of the origins, chemical composition and aging of oxygenated organic aerosols: case study of a Mediterranean industrialized environment, Marseille, Atmos. Chem. Phys., 13, 7875–7894, doi:10.5194/acp-13-7875-2013, 2013.

Elser, M., Huang, R.-J., Wolf, R., Slowik, J. G., Wang, Q.-Y., Canonaco, F., Li, G. H., Bozzetti, C., Daellenbach, K. R., Huang, Y., Zhang, R.-J., Li, Z.-Q., Cao, J. J., Baltensperger, U., El-Haddad, I., and Prévôt, A. S. H.: New insights into $PM_{2.5}$ chemical composition and sources in two major cities in China during extreme haze events using aerosol mass spectrometry, Atmos. Chem. Phys. Discuss., 15, 30127–30174, 2015.

Favez, O., El Haddad, I., Piot, C., Boréave, A., Abidi, E., Marchand, N., Jaffrezo, J.-L., Besombes, J.-L., Personnaz, M.-B., Sciare, J., Wortham, H., George, C., and D'Anna, B.: Inter-comparison of source apportionment models for the estimation of wood burning aerosols during wintertime in an Alpine city (Grenoble, France), Atmos. Chem. Phys., 10, 5295–5314, 2010.

Gao, M., Guttikunda, S. K., Carmichael, G. R., Wang, Y., Liu, Z., Stanier, C. O., Saide, P. E., and Yu, M.: Health impacts and economic losses assessment of the 2013 severe haze event in Beijing area, Sci. Total Environ., 511, 553–561, 2015.

Herich, H., Hueglin, C., and Buchmann, B.: A 2.5 year's source apportionment study of black carbon from wood burning and fossil fuel combustion at urban and rural sites in Switzerland, Atmos. Meas. Tech., 4, 1409–1420, 2011.

Hu, D. and Jiang, J.: PM2.5 pollution and risk for lung cancer: A rising issue in China, J. Environ. Prot., 5, 731–738, 2014.

~~Jimenez, J. L., Canagaratna, M. R., Donahue, N. M., Prévôt, A. S. H., Zhang, Q., Kroll, J. H., DeCarlo, P. F., Allan, J. D., Coe, H., Ng, N. L., Aiken, A. C., Docherty, K. S., Ulbrich, I. M., Grieshop, A. P., Robinson, A. L., Duplissy, J., Smith, J. D., Wilson, K. R., Lanz, V. A., Hueglin, C., Sun, Y. L., Tian, J., Laaksonen, A., Raatikainen, T., Rautiainen, J., Vaattovaara, P., Ehn, M., Kulmala, M., Tomlinson, J. M., Collins, D. R., Cubison, M. J., Dunlea, E. J., Huffman, J. A., Onasch, T. B., Alfarra, M. R., Williams, P. I., Bower, K., Kondo, Y., Schneider, J., Drewnick, F., Borrmann, S., Weimer, S., Demerjian, K., Salcedo, D., Cottrell, L., Griffin, R., Takami, A., Miyoshi, T., Hatakeyama, S., Shimono, A., Sun, J. Y., Zhang, Y. M., Dzepina, K., Kimmel, J. R., Sueper, D., Jayne, J. T., Herndon, S. C., Trimborn, A. M., Williams, L. R., Wood, E. C., Middlebrook, A. M., Kolb, C. E., Baltensperger, U., and Worsnop, D. R.: Evolution of organic aerosols in the atmosphere, Science, 326, 1525–1529, 2009.~~

Kwak, J. H., Kim, H. S., Lee, J. H., and Lee, S. H.: On-road chasing measurement of exhaust of particle emissions from diesel, CNG LPG and DME-fueled vehicles using a mobile emission laboratory, Int. J. Vehicle Des., 15, 543–551, 2014.

Kyung Hwan, K., Daekwang, W., Seung-Bok, L., and Gwi-Nam, B.: On-road measurements of ultrafine particles and associated air pollutants in a densely populated area of Seoul, Korea, Aerosol Air Qual. Res., 15, 142–153, 2015.

Lack, D. A., Corbett, J. J., Onasch, T., Lerner, B., Massoli, P., Quinn, P. K., Bates, T. S., Covert, D. S., Coffman, D., Sierau, B., Herndon, S., Allan, J., Baynard, T., Lovejoy, E., Ravishankara, A. R., and Williams, E.: Particulate emissions from commercial shipping: Chemical, physical, and optical properties, J. Geophys. Res., 114, D00F04, doi: 10.1029/2008JD011300, 2009.

Laden, F., Schwartz, J., Speizer, F. E., and Dockery, D. W.: Reduction in fine particulate air pollution and mortality: Extended follow-up of the Harvard Six Cities study, Am. J. Respir. Crit. Care. Med., 173, 667–672, 2006.

Lenschow, P., Abraham, H. J., Kutzner, K., Lutz, M., Preuß, J. D., and Reichenbächer, W.: Some ideas about the sources of PM10, Atmos. Environ., 35, Supplement 1, S23–S33, 2001.

Maasikmets, M., Kupri, H-L., Teinemaa, E., Vainumäe, K., Arumäe, T., and Kimmel, V.: ACSM study to assess possible municipal solid waste burning in household stoves. Poster presented at: European Aerosol Conference 2015, Milan (Italy), September 6-11, 2015.

Middlebrook, A. M., Bahreini, R., Jimenez, J. L., and Canagaratna, M. R.: Evaluation of composition-dependent collection efficiencies for the Aerodyne aerosol mass spectrometer using field data, Aerosol Sci. Technol., 46, 258–271, 2012.

Mohr, C., Richter, R., DeCarlo, P. F., Prévôt, A. S. H., and Baltensperger, U.: Spatial variation of chemical composition and sources of submicron aerosol in Zurich during wintertime using mobile aerosol mass spectrometer data, Atmos. Chem. Phys., 11, 7465–7482, 2011.

Mohr, C., DeCarlo, P. F., Heringa, M. F., Chirico, R., Slowik, J. G., Richter, R., Reche, C., Alastuey, A., Querol, X., Seco, R., Peñuelas, J., Jiménez, J. L., Crippa, M., Zimmermann, R., Baltensperger, U., and Prévôt, A. S. H.: Identification and quantification of organic aerosol from cooking and other sources in Barcelona using aerosol mass spectrometer data, Atmos. Chem. Phys., 12, 1649–1665, 2012.

Mohr, C., DeCarlo, P. F., Heringa, M. F., Chirico, R., Richter, R., Crippa, M., Querol, X., Baltensperger, U., and Prévôt, A. S. H.: Spatial variation of aerosol chemical composition and organic components identified by positive matrix factorization in the Barcelona region, Environ. Sci. Technol., 49, 10421–10430, 2015.

Myhre, G., Shindell, D., Bréon, F.-M., Collins, W., Fuglestvedt, J., Huang, J., Koch, D., Lamarque, J.-F., Lee, D., Mendoza, B., Nakajima, T., Robock, A., Stephens, G., Takemura, T., and Zhang, H.: Anthropogenic and Natural Radiative Forcing. In: Climate Change 2013: The Physical Science Basis. Contribution of Working Group I to the Fifth Assessment Report of the Intergovernmental Panel on Climate Change [Stocker, T.F., Qin, D., Plattner, G.-K., Tignor, M., Allen, S. K., Boschung, J., Nauels, A., Xia, Y., Bex, V., and Midgley, P. M. (eds.)]. Cambridge University Press, Cambridge, United Kingdom and New York, NY, USA, 2013.

Ng, N. L., Canagaratna, M. R., Jimenez, J. L., Zhang, Q., Ulbrich, I. M., and Worsnop, D. R.: Real-time methods for estimating organic component mass concentrations from aerosol mass spectrometer data, Environ. Sci. Technol., 45, 910–916, 2011.

Niemi, J. V., Saarikoski, S., Aurela, M., Tervahattu, H., Hillamo, R., Westphal, D. L., Aarnio, P., Koskentalo, T., Makkonen, U.,Vehkamaki, H., and Kulmala, M.: Long-range transport episodes of fine particles in southern Finland during 1999–2007, Atmos. Environ., 43, 1255–1264, 2009.

Orru, H., Maasikmets, M., Lai, T., Tamm, T., Kaasik, M., Kimmel, V., Orru, K., Merisalu, E., and Forsberg, B.: Health impacts of particulate matter in five major Estonian towns: main sources of exposure and local differences, Air Qual. Atmos. Health, 4, 247–258, 2011.

Paatero, P. and Tapper, U.: Positive matrix factorization: a non-negative factor model with optimal utilization of error estimates of data values, Environmetrics, 5, 111–126, 1994.

Paatero, P.: Least squares formulation of robust non-negative factor analysis, Chemom. Intell. Lab. Syst., 37, 23–35, 1997.

Paatero, P. and Hopke, P. K.: Discarding or downweighting high-noise variables in factor analytic models, Anal. Chim. Acta, 490, 277–289, 2003.

Paatero, P., Eberly, S., Brown, S. G., and Norris G. A.: Methods for estimating uncertainty in factor analytic solutions, Atmos. Meas. Tech., 7, 781–797, 2014.

Pirjola, L., Parviainen, H., Hussein, T., Valli, A., Hämeri, K., Aalto, P., Virtanen, A., Keskinen, J., Pakkanen, T. A., Mäkelä, T., and Hillamo, R. E.: "Sniffer" - a novel tool for chasing vehicles and measuring traffic pollutants. Atmos. Environ., 38, 3625–3635, 2004.

Pirjola, L., Paasonen, P., Pfeiffer, D., Hussein, T., Hämeri, K., Koskentalo, T., Virtanen, A., Rönkkö, T., Keskinen, J., Pakkanen, T. A., and Hillamo, R. E.: Dispersion of particles and trace gases nearby a city highway: mobile laboratory measurements in Finland, Atmos. Environ., 40, 867–879, 2006.

Pirjola, L., Lähde, T., Niemi, J. V., Kousa, A., Rönkkö, T., Karjalainen, P., Keskinen, J., Frey, A.,and Hillamo, R. E.: Spatial and temporal characterization of traffic emission in urban microenvironments with a mobile laboratory, Atmos. Environ., 63, 156–167, 2012.

Pirjola, L., Virkkula, A., Petaja, T., Levula, J., Kukkonen, J., and Kulmala, M.: Mobile ground-based measurements of aerosol and trace gases during a prescribed burning experiment in boreal forest in Finland, Boreal Environ. Res., 20, 105–119, 2015.

Pope, C. A. and Dockery, D. W.: Health effects of fine particulate air pollution: lines that connect, J. Air Waste Manag. Assoc., 56, 709–742, 2006.

Putaud, J. P., Raes, F., Van Dingenen, R., Brüggemann, E., Facchini, M. C., Decesari, S., Fuzzi, S., Gehrig, R., Hüglin, C., Laj, P., Lorbeer, G., Maenhaut, W., Mihalopoulos, N., Müller, K., Querol, X., Rodriguez, S., Schneider, J., Spindler, G., ten Brink, H., Tørseth, K., and Wiedensohler, A.: A European aerosol phenomenology - 2: chemical characteristics of

particulate matter at kerbside, urban, rural and background sites in Europe, Atmos. Environ., 38, 2579–2595, 2004.

Putaud, J.-P., Van Dingenen, R., Alastuey, A., Bauer, H., Birmili, W., Cyrys, J., Flentje, H., Fuzzi, S., Gehrig, R., Hansson, H. C., Harrison, R. M., Herrmann, H., Hitzenberger, R., Hüglin, C., Jones, A. M., Kasper-Giebl, A., Kiss, G., Kousam, A., Kuhlbusch, T. A. J., Löschau, G., Maenhaut, W., Molnar, A., Moreno, T., Pekkanen, J., Perrino, C., Pitz, M., Puxbaum, H., Querol, X., Rodriguez, S., Salma, I., Schwarz, J., Smolik, J., Schneider, J., Spindler, G., ten Brink, H., Tursic, J., Viana, M., Wiedensohler, A., and Raes, F.: A European aerosol phenomenology - 3: Physical and chemical characteristics of particulate matter from 60 rural, urban, and kerbside sites across Europe, Atmos. Environ., 44, 1308–1320, 2010.

Ramanathan, V., Crutzen, P. J., Kiehl, J. T., and Rosenfeld, D.: Aerosols, climate, and the hydrological cycle, Science, 294, 2119–2124, 2001.

Salvador, P., Artinano, B., Molero, F., Viana, M., Pey, J., Alastuey, A., and Querol, X.: African dust contribution to ambient aerosol levels across central Spain: Characterization of long-range transport episodes of desert dust, Atmos. Res., 127, 117–129, 2013.

Sandradewi, J., Prévôt, A. S. H., Szidat, S., Perron, N., Alfarra, M. R., Lanz, V. A., Weingartner, E., and Baltensperger, U.: Using aerosol light absorption measurements for the quantitative determination of wood burning and traffic emission contributions to particulate matter, Environ. Sci. Technol., 42, 3316–3323, 2008.

Sciare, J., d' Argouges, O., Sarda-Estève, R., Gaimoz, C., Dolgorouky, C., Bonnaire, N., Favez, O., Bonsang, B., and Gros, V.: Large contribution of water-insoluble secondary organic aerosols in the region of Paris (France) during wintertime, J. Geophys. Res. Atmos., 116, D22203, 2011.

Setyan, A., Zhang, Q., Merkel, M., Knighton, W. B., Sun, Y., Song, C., Shilling, J. E., Onasch, T. B., Herndon, S. C., Worsnop, D. R., Fast, J. D., Zaveri, R. A., Berg, L. K., Wiedensohler, A., Flowers, B. A., Dubey, M. K., and Subramanian, R.: Characterization of submicron particles influenced by mixed biogenic and anthropogenic emissions using high-resolution aerosol mass spectrometry: results from CARES, Atmos. Chem. Phys., 12, 8131–8156, 2012.

Squizzato, S., Masiol, M., Innocente, E., Pecorari, E., Rampazzo, G., and Pavoni, B.: A procedure to assess local and long-range transport contributions to PM2.5 and secondary inorganic aerosol, J. Aerosol Sci., 46, 64–76, 2012.

Statistical database, Statistics Estonia: http://pub.stat.ee, last access: 09 November 2015.

Sun, Y. L., Zhang, Q., Schwab, J. J., Demerjian, K. L., Chen, W. N., Bae, M.-S., Hung, H.-M, Hogrefe, O., Frank, B., Rattigan, O.V., and Lin, Y.-C.: Characterization of the sources and processes of organic and inorganic aerosols in New York City with a high-resolution time-of-flight aerosol mass spectrometer, Atmos. Chem. Phys., 11, 1581–1602, 2011.

Ulbrich, I. M., Canagaratna, M. R., Zhang, Q., Worsnop, D. R., and Jimenez, J. L.: Interpretation of organic components from positive matrix factorization of aerosol mass spectrometric data, Atmos. Chem. Phys., 9, 2891–2918, 2009.

Ulevicius, V., Byčenkienė, S., Bozzetti, C., Vlachou, A., Plauškaitė, K., Mordas, G., Dudoitis, V., Abbaszade, G., Remeikis, V., Garbaras, A., Masalaite, A., Blees, J., Fröhlich, R., Dällenbach, K. R., Canonaco, F., Slowik, J. G., Dommen, J., Zimmermann, R., Schnelle-Kreis, J., Salazar, G. A., Agrios, K., Szidat, S., El Haddad, I., and Prévôt, A. S. H.: Fossil and non-fossil source contributions to atmospheric carbonaceous aerosols during extreme spring grassland fires in Eastern Europe, Atmos. Chem. Phys. Discuss., 15, 26315–26355, 2015.

Urb, G., Teinemaa, E., Kettrup A., Gebefügi, I., Laja, M., Reinik, J., Tamm, E., and Kirso, U.: Atmospheric pollution in Tallinn, levels of priority pollutants, Proc. Estonian Acad. Sci. Chem., 54, 123–133, 2005.

Von der Weiden-Reinmueller, S.-L, Drewnick, F., Crippa, M., Prévôt, A. S. H., Meleux, F., Baltensperger, U., Beekmann, M., and Borrmann, S.: Application of mobile aerosol and trace gas measurements for the investigation of megacity air pollution emissions: the Paris metropolitan area, Atmos. Meas. Tech., 7, 279–299, 2014a.

Von der Weiden-Reinmueller, S.-L., Drewnick, F., Zhang, Q. J., Freutel, F., Beekmann, M., and Borrmann, S.: Megacity emission plume characteristics in summer and winter investigated by mobile aerosol and trace gas measurements: the Paris metropolitan area, Atmos. Chem. Phys., 14, 12931–12950, 2014b.

Williams, L. R., Gonzalez, L. A., Peck, J., Trimborn, D., McInnis, J., Farrar, M. R., Moore, K. D., Jayne, J. T., Robinson, W. A., Lewis, D. K., Onasch, T. B., Canagaratna, M. R., Trimborn, A., Timko, M. T., Magoon, G., Deng, R., Tang, D., de la Rosa Blanco, E., Prévôt, A. S. H., Smith, K. A., and Worsnop, D. R.: Characterization of an aerodynamic lens for transmitting particles greater than 1 micrometer in diameter into the Aerodyne aerosol mass spectrometer, Atmos. Meas. Tech,, 6, 3271–3280, 2013.

Wolf, R., El Haddad, I., Crippa, M., Decesari, S., Slowik, J. G., Poulain, L., Gilardoni, S., Rinaldi, M., Carbone, S., Canonaco, F., Huang, R.-J., Baltensperger, U., and Prévôt, A. S. H.: Marine and urban influences on summertime PM2.5 aerosol in the Po basin using mobile measurements, Atmos. Environ., 120, 447–454, 2015.

Zotter, P., Herich, H., Gysel, M., El-Haddad, I., Zhang, Y. L., Močnik, G., Hüglin, C., Baltensperger, U., Szidat, S., and Prévôt, A. S. H.: Evaluation of the absorption Ångström exponents for traffic and wood burning in the Aethalometer based source apportionment using radiocarbon measurements of ambient aerosol, In preparation.

Table 1: Instrument list, measured components and time resolution of each measurement.

	Instrument list	Measured components	Time resolution
Aerosols	HR-ToF-AMS	Size resolved chemical composition of NR-PM2.5	25 sec
	Aethalometer	BC (7λ)	1 sec
Gas	CO_2 Picarro	CO_2, CO, CH_4, H_2O	1 sec
	CO_2 Licor	CO_2, H_2O	1 sec
Others	GPS, Temperature, Relative humidity & Solar radiation		2 sec

Table 2: Correlation coefficients (*R2*) between the OA profiles from the four-factor solution and literature profiles. Note: The different nomenclatures used in the literature for the OOA factors have been homogenized to a semi-volatile OOA (SV-OOA) and a low-volatility OOA (LV-OOA).

R^2	Aiken et al., 2009	Mohr et al., 2012	Setyan et al., 2012	Crippa et al., 2013b
HOA-HOA	0.82	0.96	0.72	0.78
BBOA-BBOA	0.86	0.68	---	---
RIOA-COA	---	0.83	---	0.81
OOA-SVOOA	0.96	0.72	0.90	0.71
OOA-LVOOA	0.91	0.93	0.94	0.96

Table ~~2~~3: Results obtained from the average (~~A~~a) and median (~~B~~b) longitude profiles for each measured component/source. P05 represents the averaged 5th percentile subtracted for the calculation of the enhancements; base and increment values were obtained from the sigmoid fits; the regional background is given as the sum of P05 and the average base value; urban concentrations are the sum of the regional background and the average urban increment; the factor increase represents the ratio between the urban and the regional backgrounds.

(~~A~~a) Average longitude profiles:

	P05[1]	Base			Urban increment			Regional background	Urban concentration	Factor increase
		West	East	Average	West	East	Average			
$PM_{2.5}$ (µg m^{-3})	1.8	2.6	1.8	2.2	5.6	6.3	6.0	**4.0**	**10.0**	**2.5**
HOA (µg m^{-3})	0.18	0.34	0.24	0.29	1.2	1.3	1.2	**0.47**	**1.7**	**3.6**
BBOA[2] (µg m^{-3})	0.11	0.24 (0.16)	0.19	0.21	0.60 (0.64)	0.75	0.67	**0.32**	**1.0**	**3.1**
RIOA (µg m^{-3})	0.27	0.44	-0.30	0.44	0.72	1.9	0.72	**0.71**	**1.4**	**2.0**
OOA (µg m^{-3})	0.44	0.42	0.32	0.37	0.024	0.11	0.069	**0.81**	**0.87**	**1.1**
SO_4 (µg m^{-3})	0.29	0.075	0.055	0.065	0.032	0.051	0.042	**0.35**	**0.39**	**1.1**
NO_3 (µg m^{-3})	0.095	0.075	0.076	0.075	0.042	0.038	0.040	**0.17**	**0.21**	**1.2**
NH_4 (µg m^{-3})	0.079	0.032	0.028	0.030	0.012	0.016	0.014	**0.11**	**0.12**	**1.1**
Cl (µg m^{-3})	0.012	0.036	0.035	0.035	0.022	0.022	0.022	**0.047**	**0.069**	**1.5**
eBC (µg m^{-3})	0.34	0.96	0.54	0.75	3.0	3.3	3.2	**1.1**	**4.2**	**3.9**
CO_2 (ppm)	403.0	0.99	0.04	0.52	7.8	8.9	8.3	**403.5**	**411.9**	**1.0**
CO (ppm)	0.14	0.028	0.012	0.020	0.14	0.15	0.15	**0.16**	**0.31**	**1.9**
CH_4[3] (ppm)	1.90	0.0060 (0.0052)	<0.001	0.001 2	0.0047 (0.0064)	0.012	0.0083	**1.90**	**1.91**	**1.0**

(~~B~~b) Median longitude profiles:

	P05[1]	Base			Urban increment			Regional background	Urban concentration	Factor increase
		West	East	Average	West	East	Average			
$PM_{2.5}$ (µg m^{-3})	1.8	1.8	1.6	1.7	4.6	4.6	4.6	**3.5**	**8.1**	**2.3**
HOA (µg m^{-3})	0.18	0.16	0.13	0.14	0.66	0.66	0.66	**0.33**	**1.0**	**3.0**
BBOA (µg m^{-3})	0.11	0.088	0.12	0.11	0.35	0.27	0.31	**0.22**	**0.52**	**2.4**
RIOA (µg m^{-3})	0.27	0.20	0.15	0.17	0.58	0.60	0.59	**0.45**	**1.0**	**2.3**
OOA (µg m^{-3})	0.44	0.28	0.26	0.27	0.084	0.096	0.090	**0.71**	**0.80**	**1.1**
SO_4 (µg m^{-3})	0.29	0.064	0.053	0.059	0.029	0.039	0.034	**0.35**	**0.38**	**1.1**
NO_3 (µg m^{-3})	0.095	0.043	0.053	0.048	0.056	0.039	0.047	**0.14**	**0.19**	**1.3**
NH_4 (µg m^{-3})	0.079	0.028	0.026	0.027	0.0094	0.011	0.010	**0.11**	**0.12**	**1.1**
Cl (µg m^{-3})	0.012	0.022	0.025	0.024	0.024	0.019	0.021	**0.035**	**0.06**	**1.6**
eBC (µg m^{-3})	0.34	0.45	0.027	0.24	2.0	2.5	2.3	**0.58**	**2.9**	**5.0**
CO_2 (ppm)	403.0	0.95	0.051	0.50	5.0	5.6	5.3	**403.5**	**408.8**	**1.0**
CO (ppm)	0.14	0.011	<0.001	0.0052	0.096	0.12	0.11	**0.14**	**0.25**	**1.7**
CH_4[3] (ppm)	1.90	0.0032 (0.0028)	<0.001	<0.001	0.0051 (0.0055)	0.011	0.0079	**1.90**	**1.91**	**1.0**

(1) Excluding special events (2) (X_0 not fixed) (3) Excluding spike

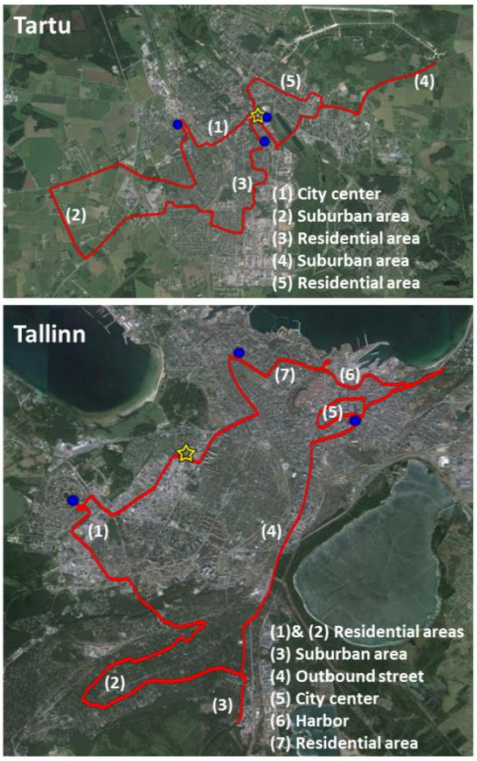

Figure 1: Driving routes in Tartu (top) and Tallinn (bottom). Red line represents: GPS data; Yellow star: stationary measurements location; Blue dots: monitoring stations of the Estonian Environmental Research Institute (EERC).

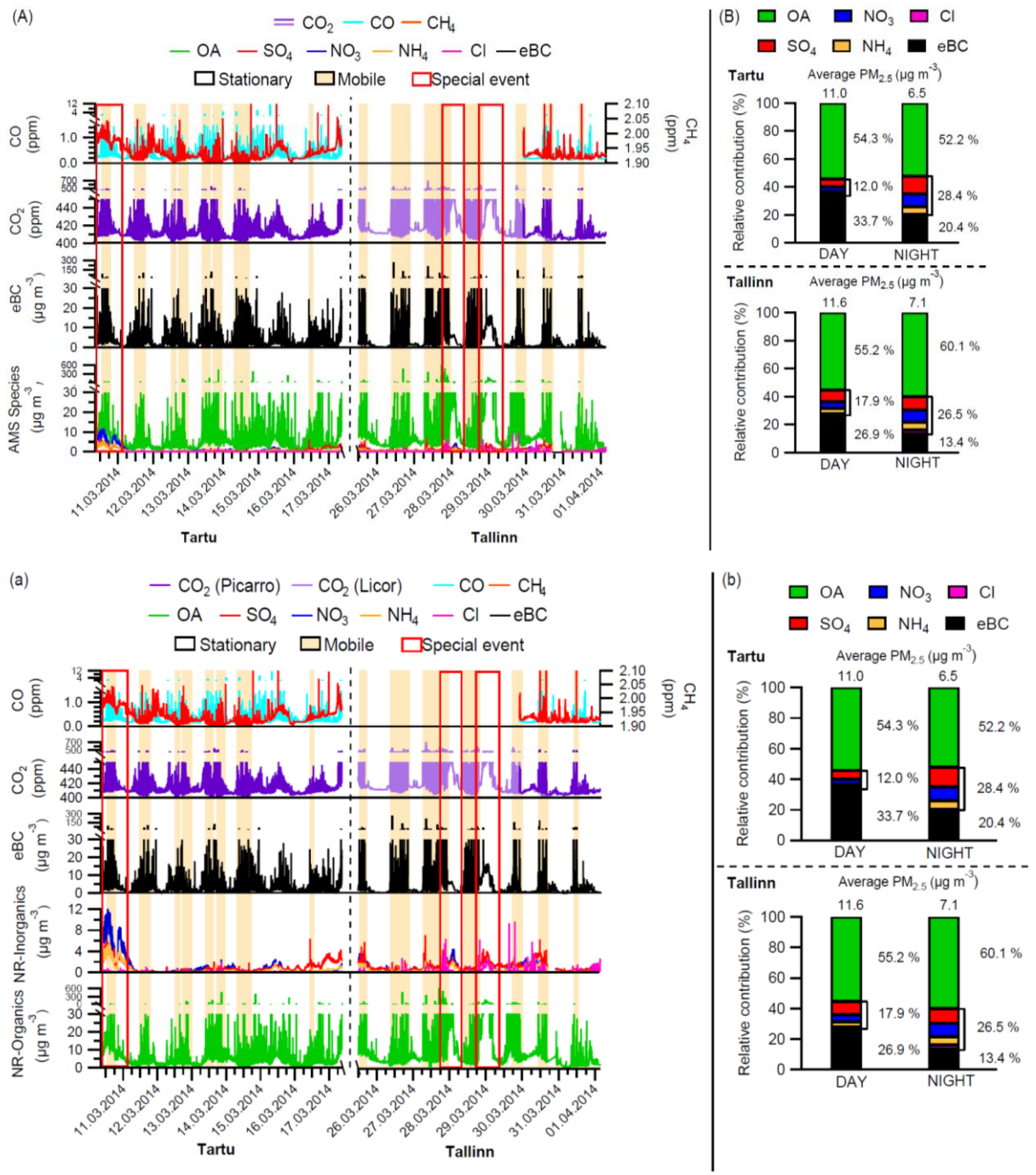

Figure ~~2~~1: (a) Temporal evolution of all gas- and particle-phase measured components over the full measurement period; (b) Average $PM_{2.5}$ (NR-$PM_{2.5}$ plus eBC) mass concentration and chemical composition for the measurements in Tartu (top panel) and Tallinn (bottom panel), with day- and night-time distinction. Note: Special events were excluded.

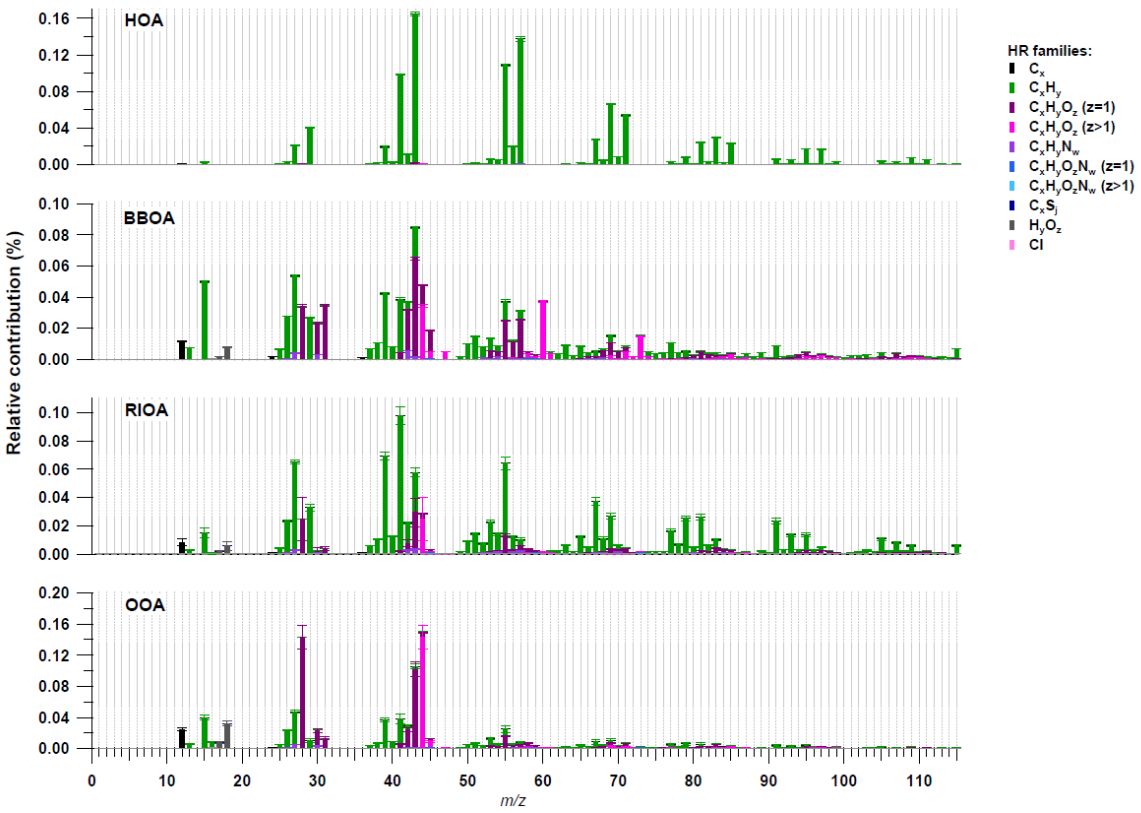
HOA
BBOA
RIOA
OOA
Relative contribution (%)
m/z
HR families:
C_x
C_xH_y
$C_xH_yO_z$ (z=1)
$C_xH_yO_z$ (z>1)
$C_xH_yN_w$
$C_xH_yO_zN_w$ (z=1)
$C_xH_yO_zN_w$ (z>1)
C_xS_j
H_yO_z
Cl

1

2

3

4

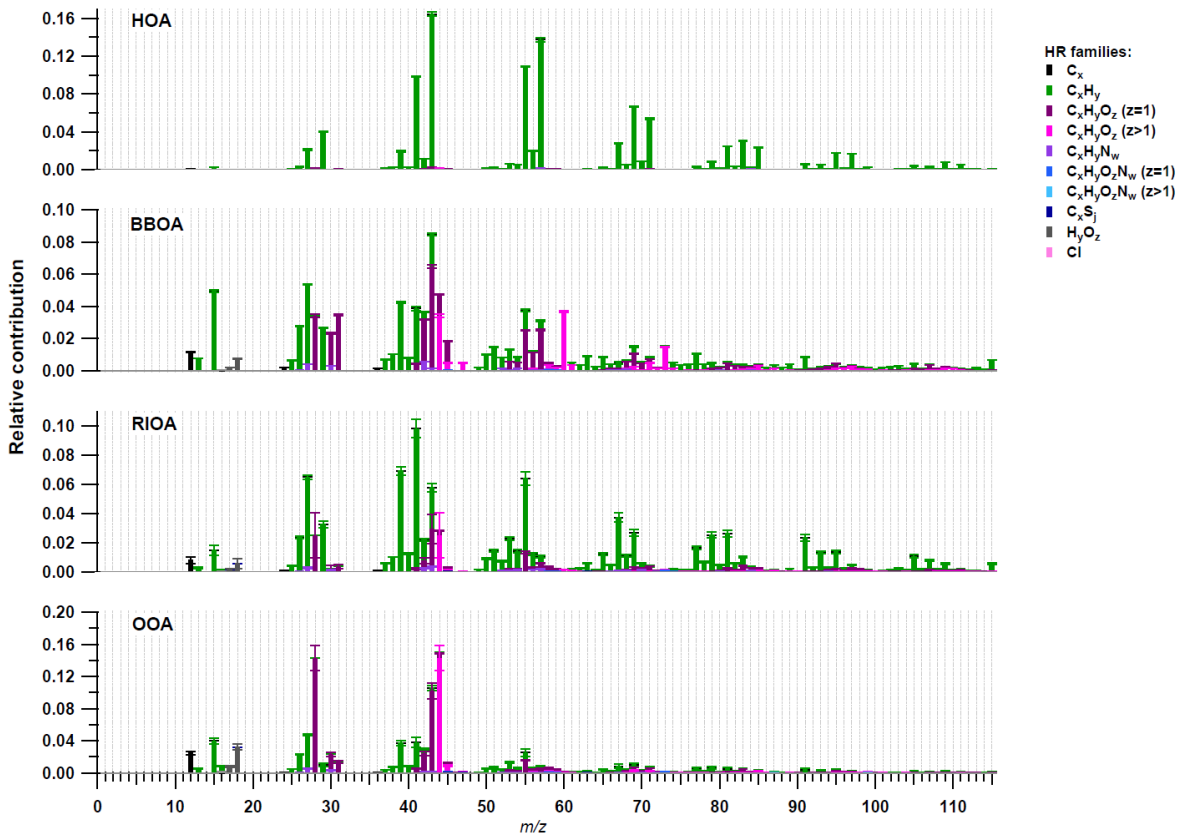

Figure ~~3~~2: Mass spectra of the four OA sources identified with PMF. From top to bottom: HOA, BBOA, RIOA and OOA. Error bars indicate the standard deviation among 100 bootstrap runs.

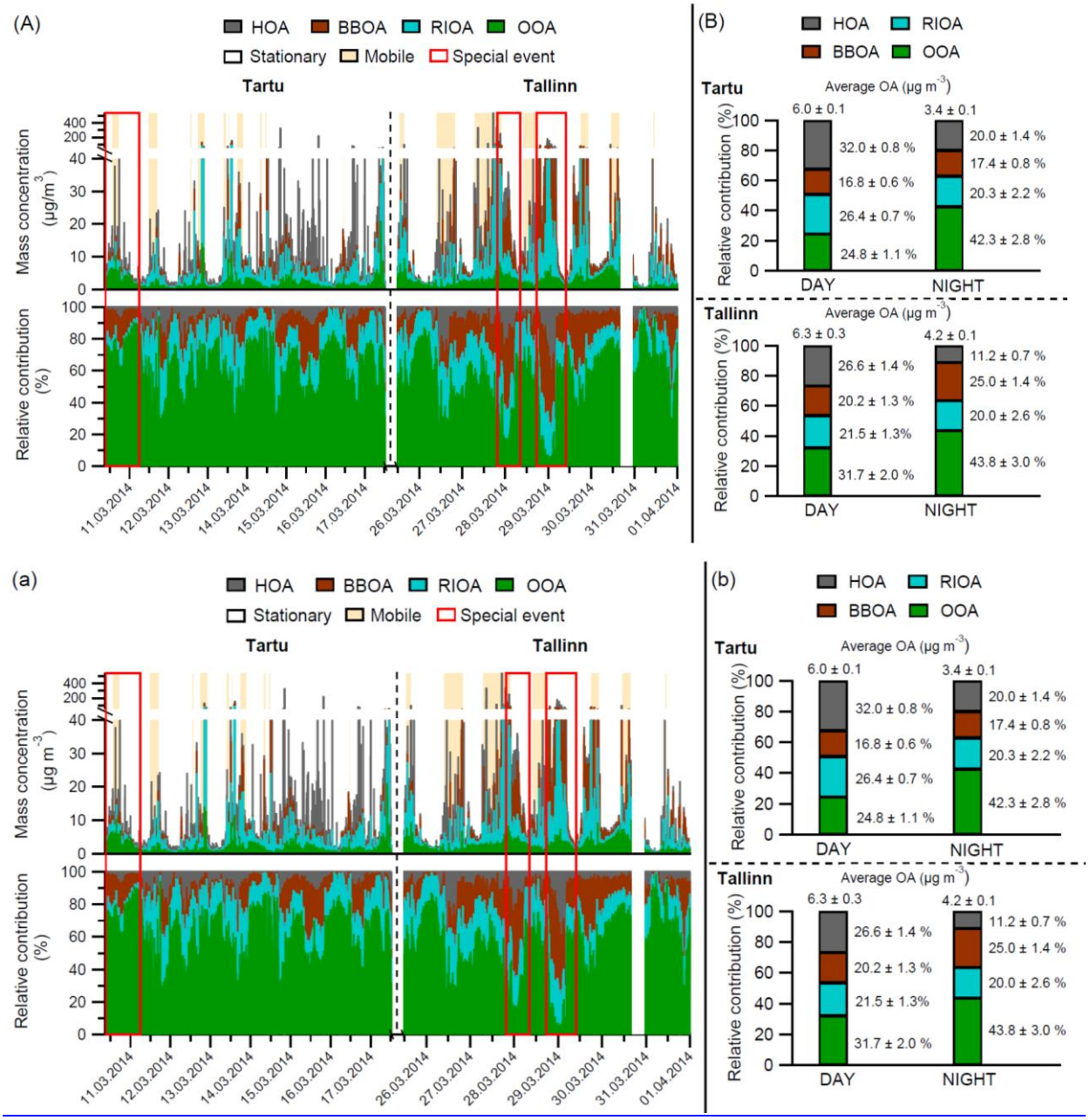

Figure 43: (a) Temporal evolution of the absolute mass (top panel) and relative contributions (bottom panel) of the four OA sources over the full measurement period; (b) Average OA mass concentrations and relative contributions of the OA sources for the measurements in Tartu (top panel) and Tallinn (bottom panel), with day- and night-time distinction. Errors indicate the standard deviation among 100 bootstrap runs. Note: Special events were excluded.

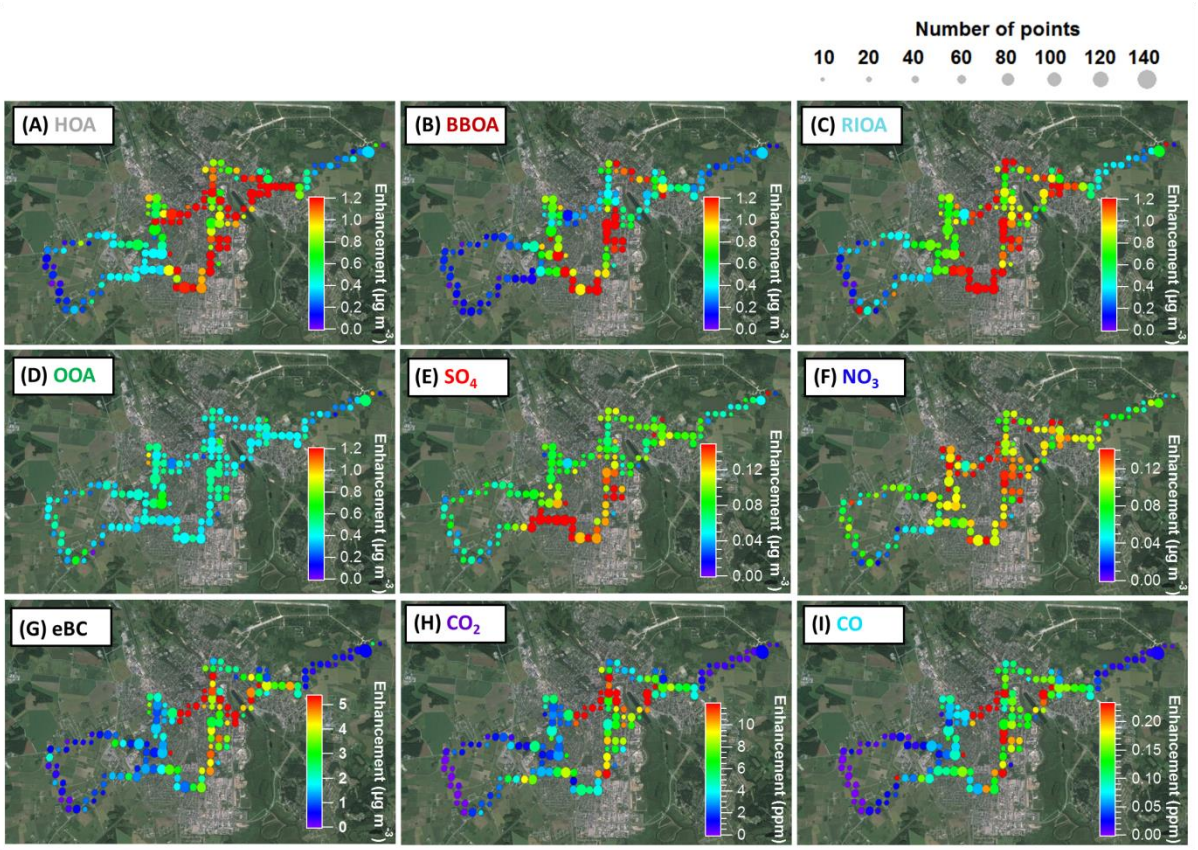
Number of points
10 20 40 60 80 100 120 140
(A) HOA
(B) BBOA
(C) RIOA
(D) OOA
(E) SO_4
(F) NO_3
(G) eBC
(H) CO_2
(I) CO
Enhancement (μg m^{-3})
Enhancement (ppm)

1

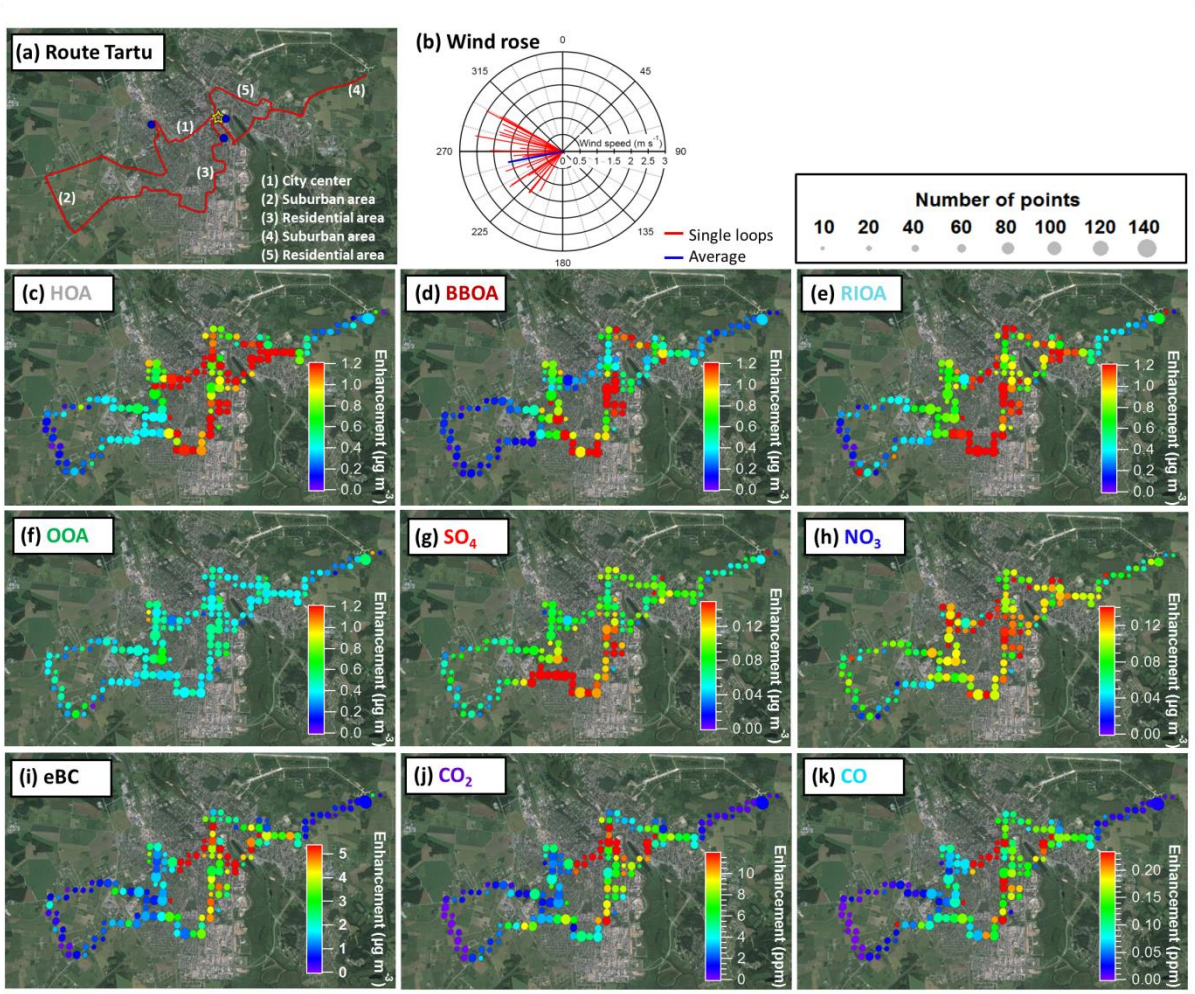

Figure ~~5~~4: (a) Driving route in Tartu: the red trace represents the GPS data, the yellow star the stationary measurements location and the blue dots the monitoring stations of the Estonian Environmental Research Institute (EERC); (b) Wind conditions during the mobile measurements in Tartu: red traces represent the wind direction and speed for the single loops and the average of all loops is represented in blue; (c to k) Average spatial distributions of all identified OA sources (panels c to f~~a-d~~) and other measured components (panels g to k~~e-i~~) in Tartu. The color scales represent enhancement over the background concentrations; the maximum of the color scales is~~have been~~ fixed to the 75th percentile of the average enhancement of each component in panels g to k~~e-i~~ and to the highest 75th percentile among all OA sources in panels c to f~~a-d~~. The sizes of the points represent the number of points that were~~have been~~ averaged in each case.

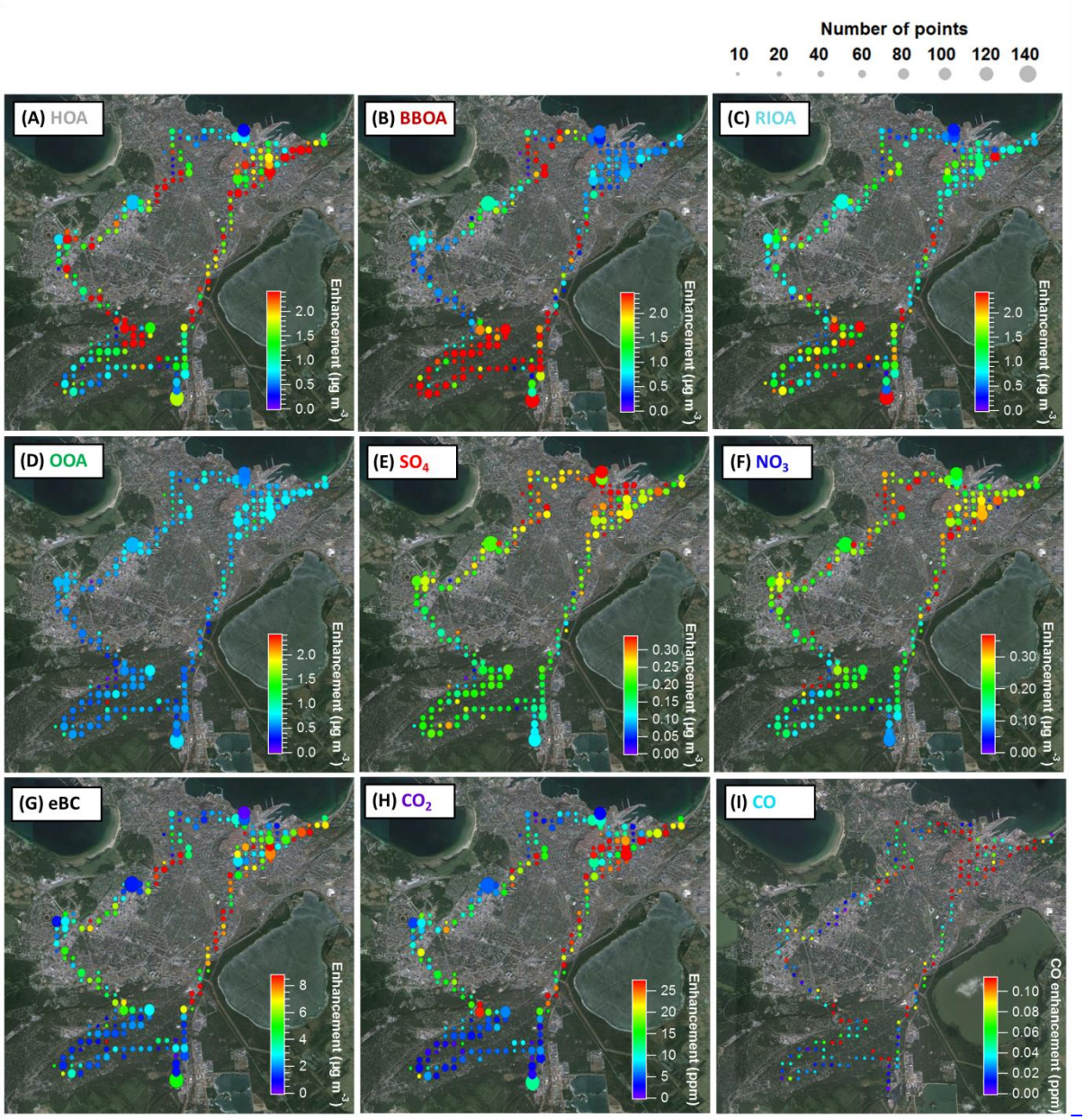
Number of points
10 20 40 60 80 100 120 140
(A) HOA
(B) BBOA
(C) RIOA
(D) OOA
(E) SO4
(F) NO3
(G) eBC
(H) CO2
(I) CO
Enhancement (μg m-3)
CO enhancement (ppm)

1

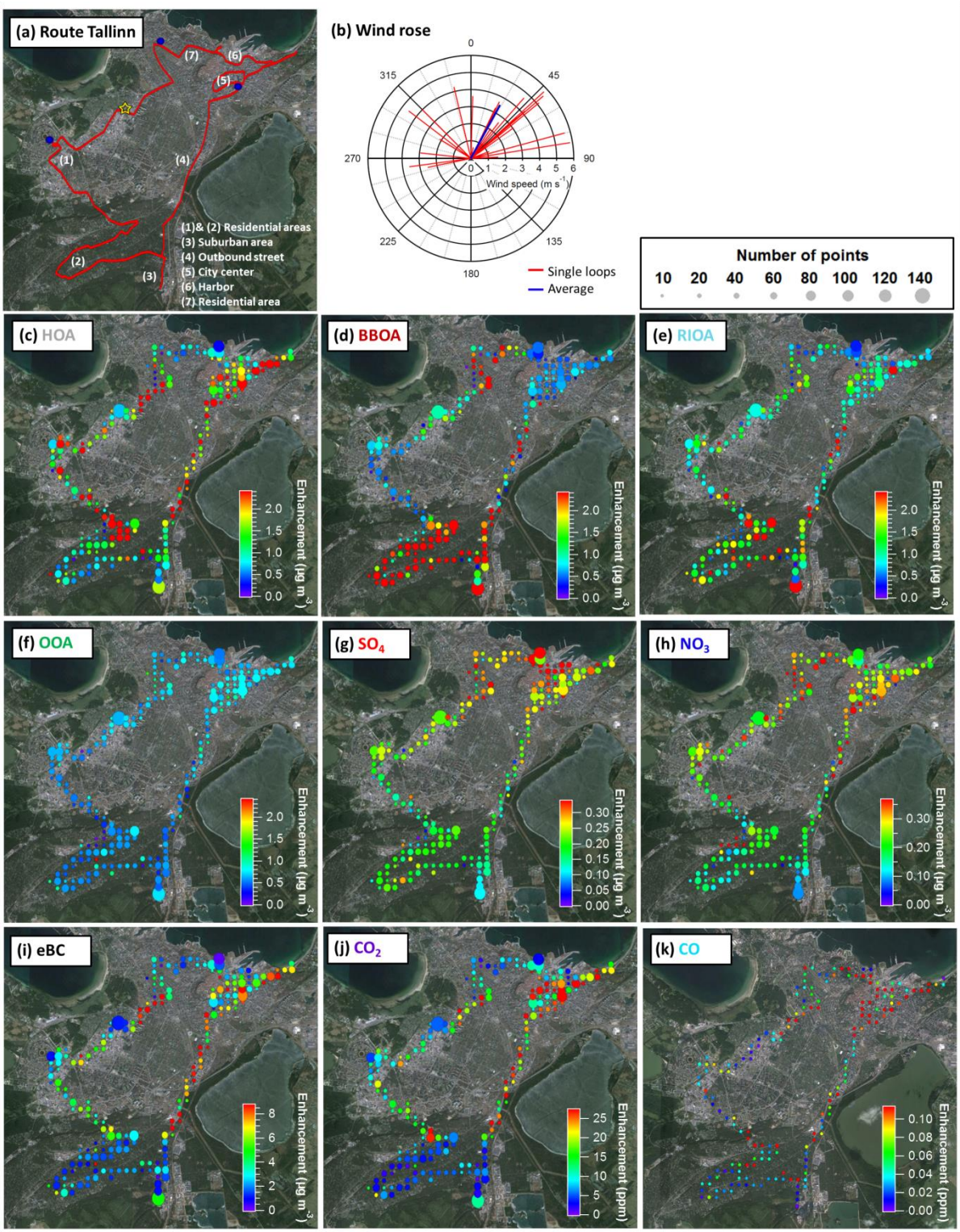

Figure ~~6~~5: (a) Driving route in Tartu: the red trace represents the GPS data, the yellow star the stationary measurements location and the blue dots the monitoring stations of the Estonian Environmental Research Institute (EERC); (b) Wind conditions during the mobile measurements in Tartu: red traces represent the wind direction and speed for the single loops and the average of all loops is represented in blue; (c to k) Average spatial distributions of all

identified OA sources (panels c to f~~a–d~~) and other measured components (panels g to k~~e–i~~) in Tallinn. The color scales represent enhancement over the background concentrations; the ~~maximum~~ maxima of the color scales have been fixed to the 75th percentile of the average enhancement of each component in panels g to k~~e–i~~ and to the highest 75th percentile among all OA sources in panels c to f~~a–d~~. The sizes of the points represent the number of points that have been averaged in each case (Note: less data available for CO).

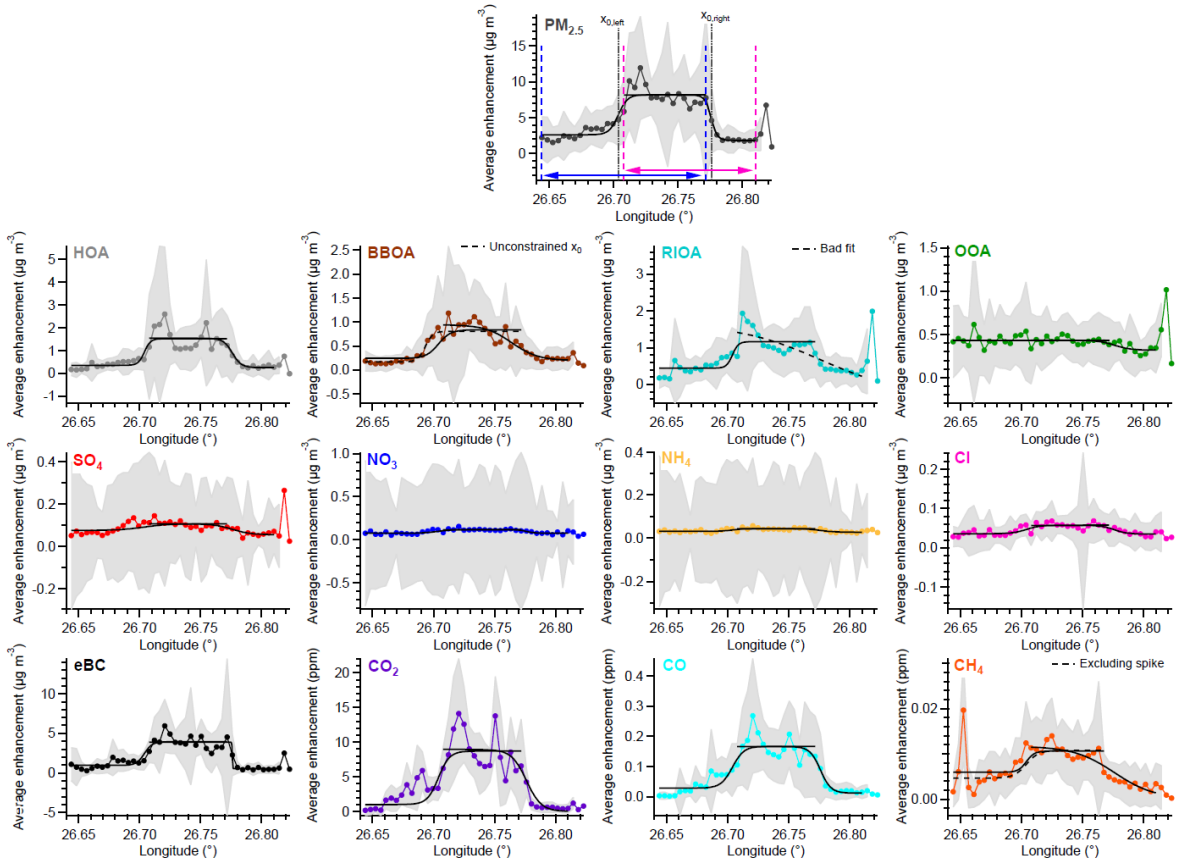

Figure ~~7~~6: Average longitude profiles of the enhancements of all measured components and sources in Tartu. Colored curves represent the average enhancement of each source/components over 26 loops and the grey shaded area is the standard deviation among them. The average enhancements were fitted with sigmoid functions (black curves). The fitting limits (pink and blue arrows in top panel) and the sigmoid's midpoint (X_0) were determined from the fit of the total $PM_{2.5}$ mass (NR-$PM_{2.5}$ plus eBC) and then imposed to the other components/sources. Dashed black lines indicate a non-standard fit (described in each case in the plot) and the results of these fits are represented in parenthesis and grey color in Table 2. Notes: The spike found in the east for RIOA, OOA and SO_4 is not representative, as it is related to one single measurement point. The spike in CH_4 in the west side is related to consistent increases of this component nearby a cowshed and will be further investigated in a future publication.

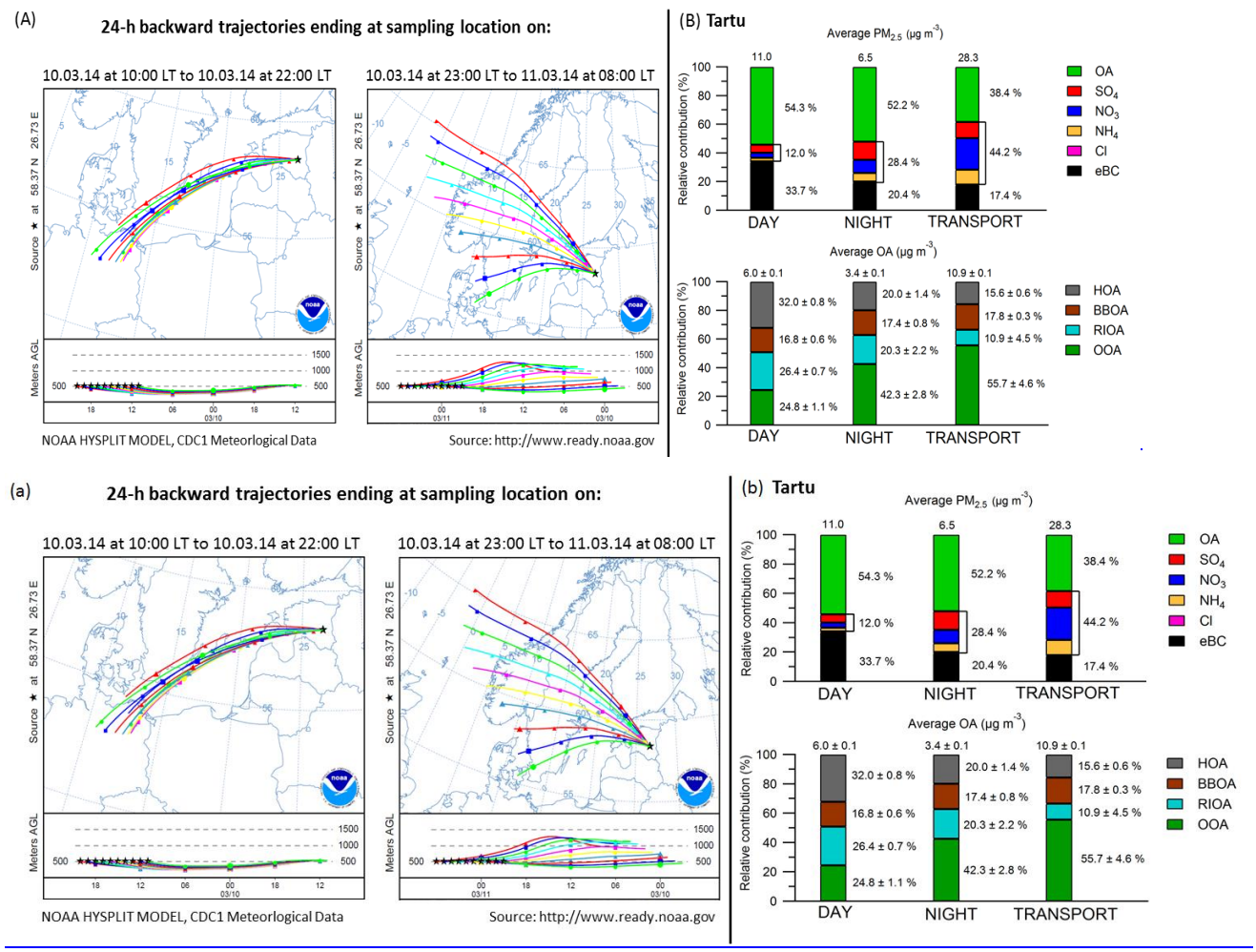

(a)
24-h backward trajectories ending at sampling location on:
10.03.14 at 10:00 LT to 10.03.14 at 22:00 LT
10.03.14 at 23:00 LT to 11.03.14 at 08:00 LT
NOAA HYSPLIT MODEL, CDC1 Meteorlogical Data
Source: http://www.ready.noaa.gov
(b) Tartu

Figure 87: (a) 24-hour back-trajectories (NOAA HYSPLIT MODEL) of the air masses ending at the sampling location (Tartu) during the transport event (10th of March between 10:00 and 22:00 LT, left panel) and the successive hours (from 10th of March at 23:00 LT until 11th of March at 08:00 LT, right panel). (b) $PM_{2.5}$ mass concentration and chemical composition (top panel) and OA mass concentration and relative contributions of the OA sources (bottom panel) during the measurements in Tartu during day-time, night-time and transport event. Errors indicate the standard deviation among 100 bootstrap runs.

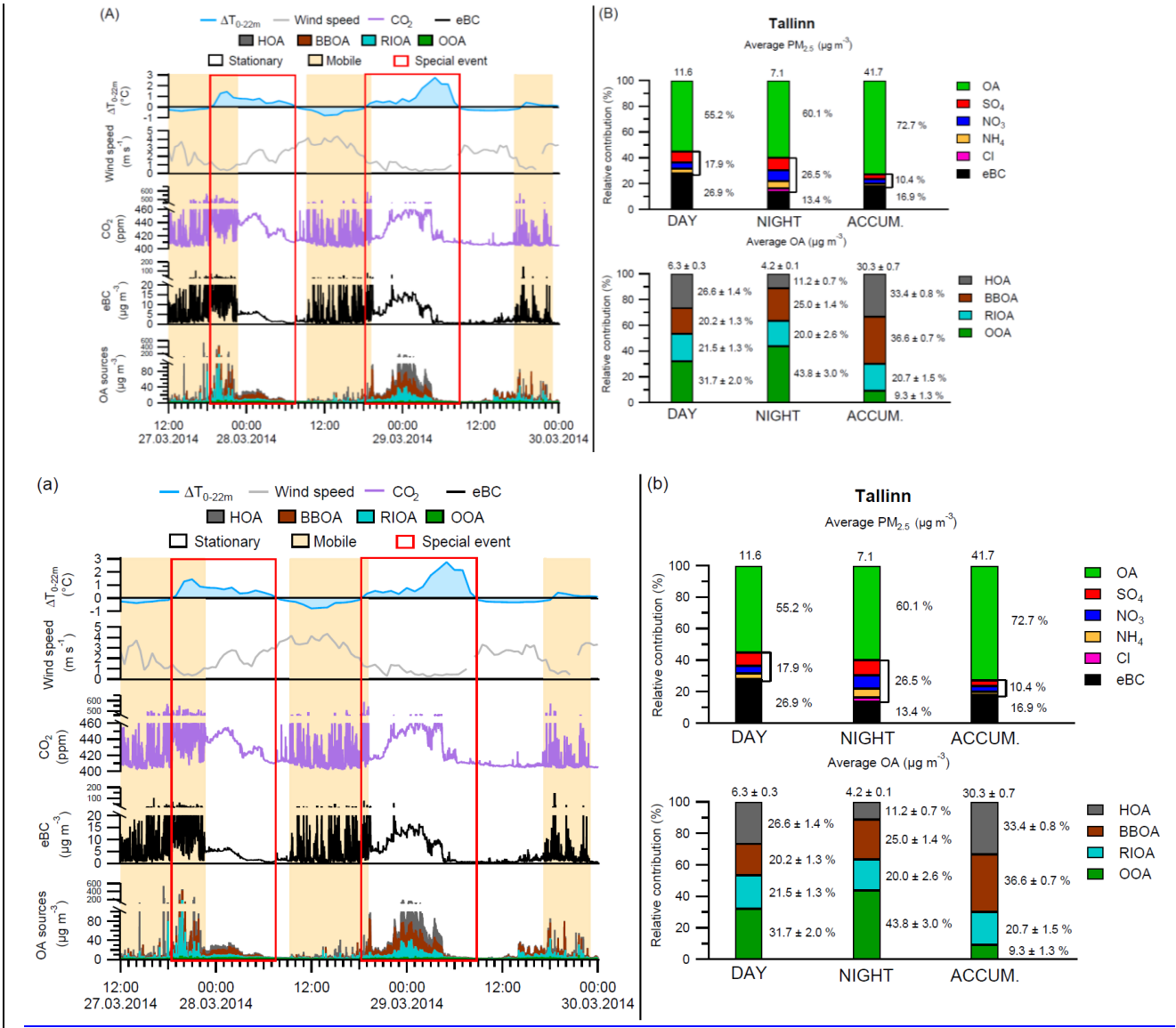

Figure 98: (a) Temporal evolution of the OA sources, eBC and CO_2, wind speed and $\Delta T_{0\text{-}22m}$ (temperature difference between ground level and at 22 meters above ground level) during the accumulation events in Tallinn. (b) $PM_{2.5}$ mass concentration and chemical composition (top panel) and OA mass concentration and relative contributions of the OA sources (bottom panel) during the measurements in Tallinn during day-time, night-time and accumulation events. Errors indicate the standard deviation among 100 bootstrap runs.